Université de Montréal

Étude de la plasticité du cortex strié par l'entremise de la kétamine et de l'adaptation visuelle

Par

Afef Ouelhazi

Département de Sciences Biologiques, Faculté des Arts et Sciences

Thèse présentée en vue de l'obtention du grade de Philosophiae Doctor (Ph. D.) en Sciences Biologique

Décembre 2022

Université de Montréal
Département de Sciences Biologiques, Faculté des Arts et Sciences

Cette thèse intitulée

Étude de la plasticité du cortex strié par l'entremise de la kétamine et de l'adaptation visuelle

Présentée par

Afef Ouelhazi

A été évaluée par un jury composé des personnes suivantes

Dre Frédérique Dubois

Présidente-rapporteure

Dr Stéphane Molotchnikoff

Directeur de recherche

Dre Annie Angers

Membre du jury

Dr Éric Plourde

Examinateur externe

Résumé

Le cortex cérébral est impliqué dans plusieurs fonctions entre autres le traitement des informations sensorielles. Il inclut des zones recevant directement une entrée sensorielle telle que le cortex visuel primaire (V1) qui traite les informations visuelles. Au niveau du V1 des mammifères, chaque neurone présente une combinaison préférentielle de stimuli pour lesquels sa réponse est optimale. Cela dit, chaque attribut de stimulus tel que les fréquences temporelle et spatiale, l'orientation et la direction du mouvement induit une réponse maximale du neurone. Le neurone du V1 est donc sélectif. Cependant, cette sélectivité n'est pas le résultat de l'activité du neurone en question seul, mais plutôt du réseau neuronal dans lequel il est impliqué. L'ensemble des préférences d'un neurone ainsi que le réseau neuronal auquel il appartient demeurent sensiblement inchangés, tant que les facteurs contextuels ne varient que peu ou pas. Toutefois, si les composantes de l'environnement changent de manière imposante, la sélectivité neuronale et l'organisation du réseau original seront modifiées pour induire un nouvel état d'équilibre. C'est la plasticité neuronale.

Le but ultime de cette thèse est de comprendre et d'approfondir les connaissances relatives aux mécanismes régissant la sélectivité à l'orientation ainsi que la plasticité dans V1, et ce, par différentes études qui sont organisées, dans cette thèse en trois sections.

Les sections (3) et (4) se basent sur une étude pharmacologique qui vise à examiner l'effet de la kétamine sur la sélectivité à l'orientation (section 3) et sur l'adaptation visuelle tout en traitant la connectivité neuronale (section 4). La section (5) vise à examiner l'effet de l'adaptation sur l'affinité des courbes d'accord des neurones.

Ce travail a permis d'étudier l'effet de la kétamine et de l'adaptation visuelle sur les propriétés sélectives à l'orientation des neurones ainsi que sur la dynamique des relations fonctionnelles au sein du microcircuit.

Méthodes

Nos expériences ont été effectuées sur V1 de la souris et du chat adulte. Une anesthésie générale suivie d'une craniotomie étaient des préalables aux enregistrements électrophysiologiques. L'activité spontanée des neurones a été enregistrée en utilisant un écran

noir. Cependant, pour enregistrer l'activité évoquée, des barres équidistantes et en palissade orientées en huit différentes orientations ont été aléatoirement présentées. Ainsi, les activités multiunitaires ont été enregistrées dans de différentes conditions (contrôle, après adaptation visuelle et après l'application locale de la kétamine) selon les objectifs de l'étude. Les potentiels d'action des cellules ont été triés par la méthode du « *Spike Sorting* ». Les courbes de syntonisation à l'orientation dans les différentes conditions ont été construites et ajustées en utilisant la fonction gaussienne von Mises. La mesure de l'indice de sélectivité à l'orientation (OSI), les déplacements des pics de courbes d'accord (Shifts) entre les conditions de contrôle et après manipulation ainsi que la bande passante d'accord à la moitié de la magnitude (FWHM) ont été calculés à partir des ajustements gaussiens. Les relations fonctionnelles entre les neurones sont dévoilées par les calculs de corrélations croisées.

Résultats et conclusions

Dans la section (3), nous démontrons que les pics des courbes de syntonisation à l'orientation se déplacent sous l'effet de la kétamine. De plus, une corrélation significative a été dénotée entre l'orientation initialement préférée et celle qui est nouvelle. Aussi, les résultats ont montré que la kétamine induit une baisse de l'OSI et une stabilité du taux de décharge évoqué des neurones.

Nous rapportons dans la section (4) l'abolition des effets de l'adaptation sur la sélectivité neuronale par la kétamine qui démontre une dualité d'effet. De plus, nous démontrons une réorganisation des cartes de connectivité après l'adaptation et l'application de la kétamine. Seulement chez le chat, la kétamine a provoqué une augmentation significative du nombre moyen et de la force moyenne des connexions ainsi qu'une amélioration de l'activité synchrone des cellules.

Dans la section (5), les résultats ont montré, chez la souris, une augmentation significative de l'OSI moyen, et ce, uniquement chez les cellules réceptrices de nouvelles connexions après adaptation. Un modèle est présenté pour expliquer comment l'émergence des nouvelles connexions après adaptation pourrait améliorer l'OSI.

Mots-clés : Adaptation visuelle, Connectivité, Corrélation, Cortex visuel primaire, Kétamine, Plasticité corticale, Sélectivité à l'orientation

Abstract

The cerebral cortex plays a key role in several functions including the processing of sensory information. It contains areas that receive direct sensory input such as the primary visual cortex (V1) which processes visual information. V1 neurons of mammals are selective for several attributes, such as spatial and temporal frequencies, orientation, and direction of motion. Thus, V1 neurons exhibit selectivities. This neuronal selectivity rests in the convergence of clusters of synapses involved in the network. Neural selectivity and networks are formed during the sensitive period of brain development and is present throughout the animal's life. However, in V1 during postnatal life, the neuronal selectivity and the neural circuitry are further shaped by experience, thus, rendering it plastic.

The main objective of the current thesis is to understand the mechanisms involved in the orientation selectivity as well as the neuroplasticity in V1. To this aim, different investigations, organized in this thesis, in three sections, were carried out.

The sections (3) and (4) are based on a pharmacological study that aim to examine the effect of ketamine on orientation selectivity (section 3) and on visual adaptation in relation with neural connectivity (section 4). The study presented in the third section (section 5) investigated the effect of adaptation on the cell's tuning.

Here, we disclose the effects of ketamine and visual adaptation on the cell's tuning properties as well as on the dynamics of functional relationships between neurons in the microcircuit.

Methodology

The animal procedures were performed on the primary visual cortex of adult mouse and adult domestic cat. General anesthesia and craniotomy were achieved before the electrophysiological recordings. Spontaneous activity was recorded using a blank black screen. However, the evoked responses were carried out using drifting sine wave gratings. Thus, eight orientations were applied. in a random order. The V1 multi-unit activity (MUA) was recorded in different conditions (control, after visual adaptation, after local application of ketamine) depending on the objectives of the study. For cat and mouse, action potentials were sorted from the MUA using the off-line spike sorting. Orientation tuning curves were fitted by using the Gaussian

function with the von Mises function. The orientation selectivity index (OSI), the distance between peak positions of the fitted tuning curves pre- and post-manipulation (shifts) and the tuning bandwidth at half magnitude (FWHM) were calculated from the Gaussian fits. Crosscorrelograms (CCGs) were performed to disclose the functional relationships between simultaneously recorded cells.

Results and conclusions

The major finding reported in the first study (section 3) is that ketamine leads to shifts in the optimal orientation of neurons with a significant correlation between the initial preferred orientation and the new one. In addition, ketamine induces a significant decrease of the mean OSI of tuned cells and more regularity of neurons' firing rate.

In the second study (section 4), we note that ketamine abolishes the adaptation effects and imposes a new intrinsic property of individual neurons. In fact, ketamine shows a dual effect. In addition, adaptation activates dedicated networks and ketamine reorganizes them. Only in cat, the mean connectivity strength and counts increases after ketamine application which enhances neuronal synchrony.

Adaptation and ketamine lead both to tuning properties changes and the network recalibration, but it seems that their pathways involved in plasticity are different.

In the third study (section 5), we showed that adaptation failed to modify the mean OSI of cells. However, the emergence of new connections in a microcircuit, following adaptation, enhanced the cell's tuning.

Keywords: Visual adaptation, Connectivity, Correlation, Primary visual cortex, Ketamine, Cortical plasticity, Orientation selectivity

TABLE DES MATIERES

Liste des figures et des abréviations

Liste des figures

Liste des abréviations

ACG : Autocorrelograms

AMPA : α-amino-3-hydroxy-5-methyl-4-isoxazolepropionic acid receptor

BDNF: Brain derived neurotrophic factor

CCGs: Cross-correlograms

CGL : Corps genouillé latéral

CGR : Cellules ganglionnaires de la rétine

CS : Collicule supérieur

Cs: Cumulative sum

E: Synaptic excitation

EEF2: Eukaryotic elongation factor 2

EEG: Electroencephalograms

F : Fano factor

FR : Firing rate

FR_m : Minimum firing rate

FR_{PO} : Firing rate for the preferred orientation

FWHM : Bande passante d'accord à la moitié de la magnitude

GABA : γ-aminobutyric acid

GAD : Glutamic acid decarboxylase

GAD67 : Glutamic acid decarboxylase type 67

GSK3: Glycogen synthase kinase 3

I: Synaptic inhibition

(K) : Voie koniocellulaire

LTP : Long-term plastictity

(M) : Voie magnocellulaire

mTOR: Mammalian target of rapamycin

MUA: Multi-unit activity

MUR : Multi-unit recording

NMDA : N-methyl-D-aspartate

NMDAR : N-methyl-D-aspartate receptor

NRG1: Neuregulin-1

OSI : Orientation selectivity index

OSIpre : Orientation selectivity index in control condition

OSIpost : Orientation selectivity index after adaptation

P : Probabilité de connexion

(P) : Voie parvocellulaire

PA : Potentiel d'action

PCA : First principal components analysis

PO : Preferred orientation

PSTH : Peri-stimulus time histograms

PV cells: Parvalbumin-expressing inhibitory cells

SRP: Stimulus-selective response potentiation

SSRI : Selective serotonin reuptake inhibitor

RP : Raster plots

T : Tuned cells

U : Untuned cells

V1: Primary visual cortex

À MES ENFANTS RAYEN ET ADAM.

Remerciements

Je voudrais remercier ceux, qui par leur aide, leur patience, leur sympathie et leur soutien, m'ont permis d'arriver au bout de ce chemin fastidieux.

- Dr Stéphane Molotchnikoff, mon directeur de thèse, pour sa bienveillance, sa bonne conduite du laboratoire et sa parfaite direction de mes travaux de recherche commençant par la conceptualisation de mon projet et allant jusqu'aux publications scientifiques. Je voudrais aussi le remercier de s'être toujours montré disponible. Un merci tout spécial pour le bon climat et les croissants lors des réunions du laboratoire.

- Dr Steve Itaya pour toute la correction d'articles qui m'a fait et sa précieuse collaboration à mes publications.

- Mon équipe de laboratoire : surtout Vishal, Lyes et Nayan avec qui j'ai fait mon stage de CRSNG et qui m'ont transmis l'amour des neurosciences à ma première visite du labo. Ces personnes m'ont appris la collaboration et le travail avec un esprit d'équipe. Ils m'ont également aidé à bâtir et enrichir ma compréhension sur le cerveau et son fonctionnement. Ils étaient tous partants à régler un tas de problèmes logistiques dans le labo notamment lors de mes premières expériences sur la souris et lors de mes premières analyses de données avec des logiciels tous nouveaux pour moi.

Le groupe de recherche NECOTIS, étudiants et professeurs, qui a favorisé un bel échange de connaissances en neurosciences computationnelles lors des colloques annuels qui se sont maintenus même durant la grande crise de la Covid 19.

- Les étudiants que je les ai supervisés lors des stages de recherches et qui ont contribués d'une façon ou d'une autre à l'avancement de mes travaux.

Il y a également d'autres personnes de l'extérieur du labo que je tiens à les remercier chaleureusement.

-Dr Maurice Ptito dont l'enseignement, l'accueil dans son laboratoire lors de mon stage, et les conseils étaient précieux. Une mention spéciale pour l'acceptation d'appuyer ma demande de bourse.

-Dre Sophie Breton qui, entre autres, grâce à elle j'ai bénéficié de ma bourse de CRSNG.

- Louise Pelletier pour sa cordialité, son sourire radieux, ses propos apaisants, ses délicieux brownies et ses cadeaux de Noël. À la merci de Louise que l'uréthane (anesthésiant utilisé lors des expériences sur la souris) ne manquait pas dans notre laboratoire. J'étais aussi très heureuse quand elle s'est ajoutée à notre équipe d'auxiliaires d'enseignement de Bio 3674. Elle a montré beaucoup de pertinence et d'efficacité du travail.

- Les auxiliaires d'enseignement avec qui j'ai travaillé lors des séances de travaux pratiques.

- Les membres du jury qui ont accepté d'évaluer ma thèse et de siéger à ma défense et qui sont:

Dre Frédérique Dubois, présidente;
Dre Annie Anger, membre du jury; et
Dr Eric Plourde, examinateur externe.

- Mes deux fils, mon mari Aziz et mes parents Ali et Halima pour leur patience et leur soutien inébranlable. J'ai pris beaucoup de leur temps pour en donner à la recherche.

Enfin, peut-être j'ai oublié de mentionner le nom de certains ou certaines. C'est pour ça que je veux remercier toute personne qui m'a aidé à la réalisation de ce travail. Ces personnes se retrouvent dans ma liste de remerciements même si leurs noms ne figurent pas.

1. Introduction

Les premières étapes de construction des circuits cérébraux au cours de la vie fœtale dépendent des processus cellulaires et moléculaires intrinsèques (Purves et al., 2019). Une fois la connectivité cérébrale mise en place dans ses grandes lignes, les profils d'activités nerveuses résultant des interactions avec le monde extérieur au cours de la vie postnatale modifient le câblage synaptique du cerveau et par le fait même, les fondations fœtales de l'architecture cérébrale. Ce potentiel de remodeler les connexions et par conséquent, de modifier le code neural en fonction de l'environnement et des expériences vécues par l'individu est qualifié de plasticité cérébrale (Tropea et al., 2009). Ce concept est l'une des découvertes assez récentes et parmi les plus importantes en neurosciences. Ainsi ce concept met l'emphase sur le fait que le cortex cérébral est un système dynamique en perpétuelle reconfiguration (McCoy et al., 2009). Plusieurs études ont démontré que le cerveau se « reprogramme » selon les stimulations et que son organisation à l'âge adulte n'est pas figée. En effet, l'équipe de Livingstone a suggéré que le cortex est un prototype qui aboutit à un cerveau sur mesure (Srihasam et al., 2014). Duffy & Mitchell, ont manipulé l'organisation du cerveau en imposant une période d'obscurité (Duffy et Mitchell, 2013). Avec d'autres (Sharma et al., 2000), il était aussi possible de démontrer que les limites de la cartographie cérébrale ne sont pas immuables.

Il serait légitime de se demander en quoi la plasticité, un processus dynamique et continu de renforcement, d'élimination et de création de connexions synaptiques**,** est fondamentale? En fait, la plasticité cérébrale est à l'œuvre lors de l'apprentissage et dans certains cas d'autoréparation. En effet, les systèmes sensoriels encodent l'information de notre environnement dans un langage de potentiels d'action qui se propagent dans des réseaux de neurones. Le remaniement de ces circuits nerveux permet l'expression de nouveaux comportements probablement plus appropriés aux exigences environnementales et contextuelles, de façon à être plus susceptible de préserver la structure de l'espèce et d'améliorer son « *fitness* ». Ceci est particulièrement vrai pour l'aire visuelle primaire (V1) à laquelle s'intéresse ce projet de recherche. Effectivement, bien que la maturation des circuits du système visuel débute avant la perception visuelle en soi, et que le ciblage des connexions thalamocorticales se produise à des stades de développement précoces, il était démontré que le bon développement du système visuel nécessite l'entrée (*input*) sensorielle (Crowley et Katz, 1999). Le cortex visuel a longtemps été un terrain d'essai pour l'étude de la

plasticité, car l'expérience visuelle peut être facilement manipulée et les conséquences de ces manipulations peuvent être facilement mesurées à des niveaux anatomique, physiologique et moléculaire (Tropea et al., 2009). Les travaux de notre laboratoire (Ghisovan et al., 2008) ont démontré que chez le chat, l'imposition d'une orientation non préférée déplace le pic de la courbe d'accord à l'orientation, et ce, surtout en direction de l'orientation imposée. Des résultats analogues ont été décrits pour la direction, la vitesse du déplacement de la cible (Kohn et Movshon, 2004; Krekelberg et al., 2006), et la fréquence spatiale (Bouchard et al., 2008; Marshansky et al., 2011). Ces données signifient que les neurones du cortex visuel d'un cerveau adulte sont susceptibles d'acquérir de nouvelles propriétés et de changer leur sélectivité sensorielle selon la stimulation la plus active. Il semble donc qu'il y a une réorganisation du cortex et que les cartes corticales du V1 se retracent selon les conditions de stimulation adaptante. Il s'agit d'une réorganisation corticale. De plus, il était démontré que certains antidépresseurs qui sont souvent utilisés pour traiter les troubles mentaux et affectifs tels que la fluoxétine facilitent la plasticité induite par l'adaptation (Bachatene et al., 2013). Bien que les mécanismes d'action des antidépresseurs soient différents, les modifications des taux de monoamines telles que la sérotonine, la noradrénaline et la dopamine (hypothèse monoaminergique) sont communément acceptées pour souligner leurs effets. La plupart des antidépresseurs augmentent la disponibilité des monoamines en inhibant leur recapture ou leur dégradation ; ou en augmentant leur recapture ou leur libération (X. Li et al., 2012). Certains, comme la kétamine, agissent directement sur les récepteurs (Leong, 2002). Puisque les antidépresseurs affectent la neurotransmission, et vu le rôle évident de cette dernière dans l'induction de la plasticité corticale (par la régulation de la dépolarisation membranaire et les niveaux de calcium intracellulaire) (Tropea et al., 2009), il devient probable qu'ils influencent la plasticité visuelle. Dans cette thèse nous nous interrogeons sur plusieurs aspects de la plasticité ainsi que les voies empruntées. Les questions que nous avons posées étaient : est-il possible que des antidépresseurs, tels que la kétamine, induisent aussi la plasticité (qui est dans le cadre de cette étude l'acquisition d'une nouvelle sélectivité et des nouvelles relations fonctionnelles entre les cellules) au niveau de V1? Si tel est le cas, par quel(s) mécanisme(s) potentiel(s)? Est-ce que l'adaptation pourrait être un inducteur de la plasticité chez la souris qui a une organisation corticale en sel et poivre? Est-ce que les effets de l'adaptation sur les propriétés sélectives et les connexions entre les neurones persistent- ils après l'application de la kétamine ou un nouvel état d'équilibre prend naissance? Est-ce que l'adaptation affecte-t-elle le

degré de sélectivité des cellules à l'orientation? Si oui par quel(s) mécanisme(s) hypothétique(s)? Dans cette thèse, nous avons essayé de fournir des réponses à ces interrogations dans le but de mieux comprendre la façon avec laquelle le code neural ainsi que ses bases fonctionnelles sont élucidés. En effet, les mécanismes physiologiques responsables des changements incessants du cerveau adulte demeurent largement méconnus et restent une question fondamentale en neurosciences. En somme, la thèse se divise en 3 principales sections :

Section 3 : Effet de la kétamine sur la sélectivité à l'orientation et la variabilité des réponses neuronales dans V1 (Article connexe : voir page suivante).
Section 4 : Effet de la kétamine sur la plasticité induite par l'adaptation (Article connexe : voir page suivante).
Section 5 : L'adaptation affine les propriétés sélectives des cellules du V1 (Article connexe : voir page suivante).
Dans la **Section 3**, nous fournissons une réponse à la première question posée : est-il possible que des antidépresseurs, tels que la kétamine, induisent la plasticité au niveau de V1?
Dans la **Section 4**, nous répondons aux deux suivantes questions : est-ce que l'adaptation pourrait être un inducteur de la plasticité chez la souris qui a une organisation corticale en sel et poivre? Est-ce que les effets de l'adaptation sur les propriétés sélectives et les connexions entre les neurones persistent- ils après l'application de la kétamine ou un nouvel état d'équilibre prend naissance?
Dans la **Section 5**, l'exploration de l'effet de l'adaptation sur les réseaux neuronaux permet de répondre aux deux dernières questions posées qui sont : est-ce que l'adaptation affecte-t-elle le degré de sélectivité des cellules à l'orientation? Si oui par quel(s) mécanisme(s) hypothétique(s)? Les études décrites dans les sections 3 et 4 étaient conduites chez la souris et le chat ce qui a permis de comparer les résultats obtenus entre les deux espèces. Cependant, l'étude décrite dans la section 5 portait seulement sur la souris.

1.1. Le système visuel: une merveilleuse ingénierie

Puisque notre terrain d'essai pour l'étude de la plasticité est le cortex visuel, voyons comment se fait le traitement de la scène visuelle depuis la rétine jusqu'au niveau cortical. Le système visuel permet la perception presque instantanée de l'information visuelle du monde extérieur et par le fait même l'interaction avec ce dernier. L'analyse de l'image visuelle s'avère complexe, car celle-

ci est très diversifiée dans notre environnement. En effet, pour que l'image d'un oiseau par exemple se construise, il faut qu'il y ait une perception de sa forme, de sa ou ses couleurs, sa texture, sa position dans l'espace, son mouvement ainsi que d'autres attributs. Une combinaison des mécanismes complexes allant de la rétine jusqu'au cortex visuel, sont impliqués dans le processus de traitement de l'information visuelle. Malgré la variété des aspects anatomiques et fonctionnels du système visuel selon les différentes espèces, ce dernier répond bien à l'exigence de vie de chacune d'entre elles en leur permettant une interaction assez réussie avec l'environnement extérieur (chasse, fuite, organisation d'une attaque chez les animaux sociaux…). On s'intéresse dans les prochaines sections à une étude comparative des régions impliquées dans la vision essentiellement chez les primates (mammifères supérieurs) et la souris (notre modèle expérimental).

1.1.1. Rétine : pellicule photographique où s'impriment les images

Rétine du chat et des primates

On est capable de reconnaitre quelque 10 000 odeurs grâce aux 400 différents types de protéines de récepteurs olfactifs (Bushdid et al., 2014), mais avec l'œil, la machinerie est plus géniale puisque c'est seulement avec 4 types de photorécepteurs (cellules sensibles à la lumière), qu'on est capable de détecter la quantité et la diversité des stimuli rencontrés dans notre milieu. En effet, tout commence au niveau de la rétine (fine membrane qui tapisse le fond de l'œil) qui porte, tout au fond, trois sortes de cônes permettant la vision photopique trichromatique, et des bâtonnets, qui eux permettent la vision scotopique en noir et blanc. Au niveau des cônes et des bâtonnets, la lumière est transformée par des cascades biochimiques en signal électrique (Purves et al., 2019).

Chez le chat, la densité des bâtonnets est plus grande que celle des cônes. Une étude récente a montré que la vision du chat est, tout comme les primates, trichomatique. En effet, la rétine du chat comporte des photorécepteurs sensibles aux longueurs d'onde proches de 560 nm, d'autres sont sensibles à 460 nm et un troisième type sensible aux longueurs d'onde entre 500 nm et 520 nm (Clark et Clark, 2016). Dans l'épaisseur de la rétine (figure 1), les cellules horizontales et amacrines commencent à préparer le traitement de l'information. En établissant des connexions latérales, elles pré-arrangent les trains d'impulsions émises par les cellules voisines en espèce de bouquet et créent ce qu'on appelle des champs récepteurs. En plus de ces cellules, il existe aussi les cellules bipolaires et les cellules ganglionnaires ayant des champs récepteurs concentriques

avec une organisation centre-pourtour (ON/OFF ou OFF/ON). Le traitement de l'image visuelle (paquets d'informations préarrangées données par les champs récepteurs) reste à ce stade parcellaire, l'image se déconstruit (une barre ayant une certaine orientation est détectée sous forme de points dans la même orientation). Les potentiels d'action générés par les cellules ganglionnaires vont, par le nerf optique, être acheminés majoritairement vers l'étage suivant: les corps genouillés latéraux (Purves et al., 2004).

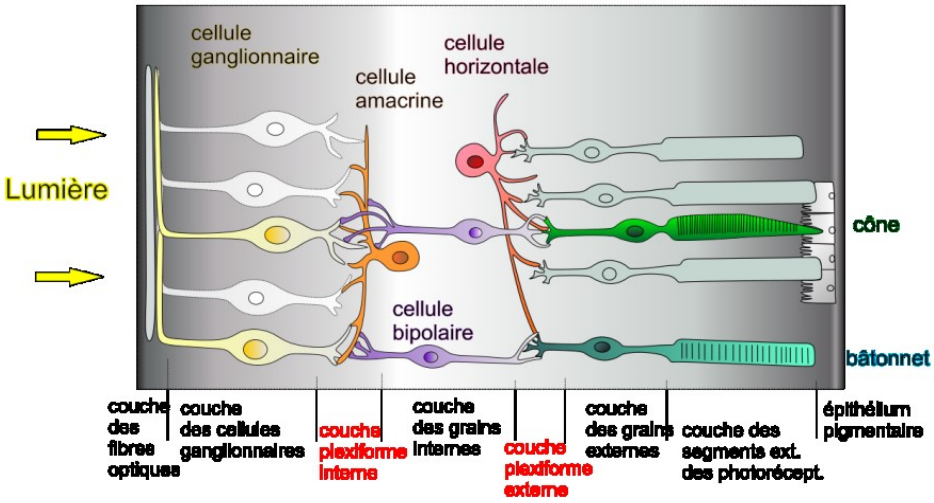

Figure 1.1: Les couches de la rétine et organisation des cellules ganglionnaires, des cellules bipolaires et des photorécepteurs (Purves et al., 2004).

Rétine de la souris

De la même manière que les attributs des pixels dans un appareil photo numérique (c.-à-d. le nombre de pixels, les propriétés d'encodage de couleur, etc.) déterminent la qualité des photos prises, les attributs des photorécepteurs rétiniens contraignent les aspects de traitement de la scène visuelle par le cerveau et donc la qualité visuelle selon les espèces (Huberman et Niell, 2011). La rétine des souris est spécialisée à la vision dans des conditions de faible luminosité (scotopie) et par conséquent, elle est dominée par les bâtonnets (Jeon et al., 1998). Seulement environ 3% des photorécepteurs sont des cônes. Ces derniers expriment un seul photopigment ou une combinaison de deux photopigments dont l'un est sensible aux petites longueurs d'onde (centré à 360 nm - ultraviolet) et l'autre sensible aux longueurs d'onde moyennes (centré à 511nm - vert) (Calderone et Jacobs, 1995). Comme les souris (de même que les chats) ne possèdent pas le cône à photopigment rouge, que l'on trouve chez de nombreux primates, ils sont donc dichromates (ne

peuvent pas différencier le rouge des teintes vertes). Remarquablement, l'expression de cônes à photopigment rouge chez des souris transgéniques s'est avérée suffisante pour discriminer les couleurs rouge-vert (Jacobs et al., 2007), ce qui souligne à quel point les photorécepteurs constituent le principal obstacle à la perception visuelle. De plus, cela indique que le reste du système visuel de la souris est équipé pour traiter des combinaisons sophistiquées d'informations visuelles, même lorsque ces informations ne sont pas normalement fournies par la rétine. Bien que la rétine des souris soit dominée par les bâtonnets, la sensibilité des cônes s'est révélée similaire à celle des humains (Stiles, 1949). En outre, la sensibilité des bâtonnets est si puissante que les souris pourraient détecter et signaler l'arrivée de moins de 30 photons à l'œil (Naarendorp et al., 2010). En raison de la différence globale dans la taille de leurs yeux, le nombre total de photorécepteurs chez les souris est beaucoup plus petit comparé à celui des primates. Cependant, par unité de surface rétinienne, la souris a plus de photorécepteurs que le macaque (Jeon et al., 1998). Pourquoi alors la vision des primates est-elle plus nette que celle de la souris ? Premièrement, comme l'œil de la souris est beaucoup plus petit que celui d'un primate, et malgré le fait que la densité de photorécepteurs est plus élevée dans la rétine de la souris, par zone il y a moins de photorécepteurs couvrant la scène visuelle. De plus, chez les primates, 99% des cônes résident dans la fovéa, une région occupant environ 1% de la surface de la rétine et où l'acuité visuelle est à son maximum (Perry et Cowey, 1985). La fovéa est utilisée pour les tâches nécessitant une forte acuité telles que la lecture ou la détection de petits objets à distance, contrairement à la vision périphérique qui est de faible acuité et qui permet de détecter de gros objets à distance ou de petits objets plus proches, en particulier des objets en mouvement. La souris n'a pas de fovéa et toute sa rétine ressemble donc à la rétine périphérique du primate; en effet, la densité de cônes dans la rétine de souris (par mm^2) est similaire à celle retrouvée dans l'œil du primate à environ 3 mm de la fovéa (Jeon et al., 1998). La distribution des bâtonnets à travers la rétine de la souris est relativement uniforme, alors que les cônes présentent une variation régionale marquée avec des cônes- ultraviolet qui sont dominants dans la rétine ventrale (Haverkamp et al., 2005). Ainsi, le modèle de photorécepteurs en mosaïque chez la souris semble très efficace pour l'échantillonnage de la scène visuelle, et compense les contraintes d'un œil qui est petit (Huberman et Niell, 2011).

Une fois que les photorécepteurs convertissent la lumière en impulsions électriques, ces informations sont filtrées par les trois classes principales d'interneurones rétiniens dont les principaux types retrouvés chez les primates (1 40: 1 à 2 types d'interneurones horizontaux; 10 à

15 types d'interneurones bipolaires et 40 types de cellules amacrines), sont également présents chez la souris (Masland, 2001). Ces interneurones filtrent et transmettent les informations visuelles aux cellules ganglionnaires de la rétine (CGR). Il existe trois principaux types de CGR. Chez les carnivores, ces types sont couramment appelés des CGR : X (ou bêta), Y (ou alpha) et W (gamma); et chez les singes, ils sont appelés respectivement des CGR nain, parasol et koniocellulaire (Nassi et Callaway, 2009). En réalité, le nombre de types de CGR (souvent appelés sous-types) est beaucoup plus complexe. En effet, on a répertorié plus de 20 sous-types différents de CGR chez les différentes espèces (Field et Chichilnisky, 2007). Chez la souris, les CGR sont très diversifiés et comprennent au moins 22 sous-types anatomiquement distincts (Völgyi et al., 2009) (Figure 2). En plus d'avoir trois sous-types de CGR de type Y (Huberman et al., 2008), la rétine de la souris héberge au moins huit sous-types différents de CGR sélectives à la direction (CGSD) (Ecker et al., 2010). Ces CGSD sont particulièrement nombreux et représentent au moins la moitié du nombre total de CGR (Jeon et al., 1998). En outre, une étude a montré que certaines CGR de la souris sont sensibles aux stimuli qui sont de la même famille tels que les différentes catégories de mouvement : ces cellules répondent aux différents mouvements d'un objet et non pas à un seul type (Münch et al., 2009). Récemment, des CGR intrinsèquement photosensibles ont été découvertes chez de nombreuses espèces, notamment chez la souris (avec 4 à 5 sous-types), le macaque et l'Homme. L'existence de CGR qui expriment le photopigment mélanopsine leur permet de transduire directement les photons, indépendamment des photorécepteurs (Berson et al., 2002).

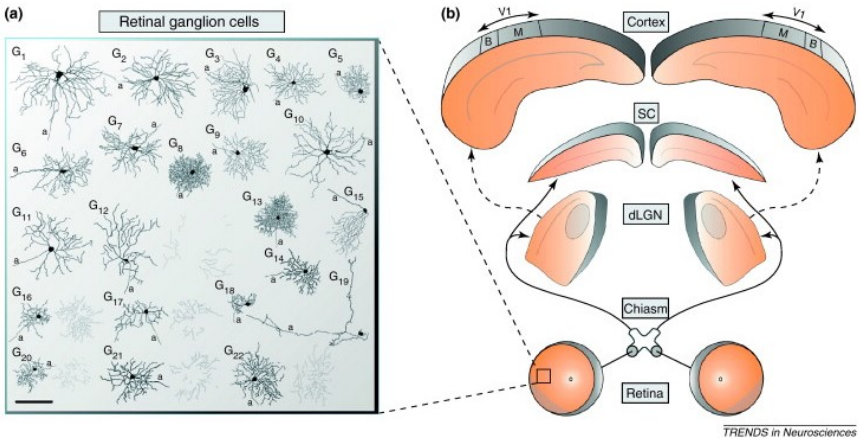

Figure 1.2 : Les différentes CGR ainsi que les voies visuelles chez la souris. **À gauche** : Les 22 sous-types anatomiquement distincts de CGR « G1-G22 » chez la souris. Des exemples de chaque

sous-type (basés sur des injections de colorant) sont représentés. Les lignes sombres représentent les somas et les dendrites de CGR. Les lignes plus claires représentent l'arborisation dendritique dans des couches plus profondes. Chaque patch de rétine comprend une partie ou la totalité de ces 22 sous-types et tous ces axones s'étendent au cerveau (Völgyi et al., 2009).
À droite : Diagramme des voies visuelles chez la souris, montrant les projections directes de la rétine (flèches en trait plein) vers le corps genouillé latéral dorsal (CGL) et le colliculus supérieur (CS), ainsi que les voies géniculo-corticales allant du CGL au cortex visuel (flèches pointillées). Les parties ombrées de la rétine indiquent l'emplacement des CGR dont les axones se projettent de manière ipsilatérale. Les ovales dans le CGL correspondent aux zones de terminaison des axones ipsilatéraux. Les champs binoculaire (« B ») et monoculaire (« M ») situés dans la zone V1 du cortex sont représentés. Les lignes plus claires dans les CGL et CS représentent les limites approximatives où se terminent les axones de différentes catégories fonctionnelles de CGR (Huberman et al., 2008).

1.1.2. Corps genouillé latéral : Arrangement plus élaboré des informations

Corps genouillé latéral du chat et des primates

Les CGR du chat projettent directement ou indirectement sur plusieurs structures sous-corticales. Cependant, les plus importantes connexions sont celles qui relient directement les CGR au collicule supérieur et au corps genouillé latéral (CGL) (Garey et Powell, 1968). Le CGL est un relais thalamique de l'information rétinienne et qui projette au cortex visuel primaire, ainsi que sur de nombreuses autres régions médiatrices de comportements allant des mouvements oculaires réflex à la dilatation des pupilles. Sur l'ensemble des aires visuelles sous-corticales, l'attention est de loin portée sur le CGL, en raison de son rôle dans le traitement et la transmission d'informations visuelles au cortex (Huberman et Niell, 2011). Bien que chez les primates, les CGR projettent sur plus de 20 cibles sous-corticales, la projection rétine-CGL est aussi considérée la plus importante et la mieux étudiée (Ling et al., 1998). Chez le chat et les primates, les bouquets de la rétine (mentionnés dans 1.1.1) qui envoient un même type d'information tel que "ligne d'orientation verticale" se retrouvent tous sur un même feuillet du CGL, ceux qui détectent un autre type d'information seront sur un autre feuillet. Ces feuillets se construisent au cours de la vie fœtale. Les projections rétiniennes se divisent en trois voies dans le CGL dont les cellules ont des champs récepteurs concentriques avec un centre ON ou OFF: parvocellulaire (P), magnocellulaire (M), et koniocellulaire (K) ou (X, Y et W chez le chat) (figure 3). La voie parvocellulaire-interblobe de (P) avec des cellules ayant les propriétés de X (X- like) permet surtout la détection et l'analyse des formes, alors que la voie parvocellulaire-blobe de (P), avec des cellules ayant les propriétés de Y (Y- like), détectent et analyse les couleurs (De Monasterio et Gouras, 1975). Les neurones de cette voie ont des champs récepteurs plus petits que les autres (M et K), et sont sensibles à des

contrastes élevés, à des fréquences spatiales hautes et à des cibles qui bougent lentement (Troy et Enroth-Cugell, 1993). Ces cellules déchargent en tout temps lors d'une stimulation répétée dans leur champ récepteur contrairement à la réponse de la voie M qui est généralement en phase avec le stimulus présenté (Enroth-Cugell et Robson, 1966). La voie (M) est plutôt impliquée dans la détection du mouvement, l'établissement des relations spatiales et la perception de la profondeur (Poggio et Fischer, 1977). Les champs récepteurs des cellules de cette voie sont habituellement grands et répondent surtout à des contrastes faibles ainsi qu'à des fréquences spatiales basses et à des cibles visuelles qui se déplacent rapidement. Les cellules de la voie (K) ont des champs récepteurs très grands. Il était démontré que les neurones du CGL sont syntonisés à certaines caractéristiques visuelles et donc plus sophistiqués que des simples cellules à centre ON/ OFF. En effet, des cellules de CGL sélectives à la direction ont été décrites chez le lapin (Levick et al., 1969), et des neurones sélectifs à l'orientation et à la direction sont présents chez le chat (Thompson et al., 1994). Chez les primates comme chez le chat, on observe des projections réciproques entre le CGL et le V1, avec des fibres cortico-thalamiques plus nombreuses que les fibres thalamo-corticales (Darian-Smith et Gilbert, 1995).

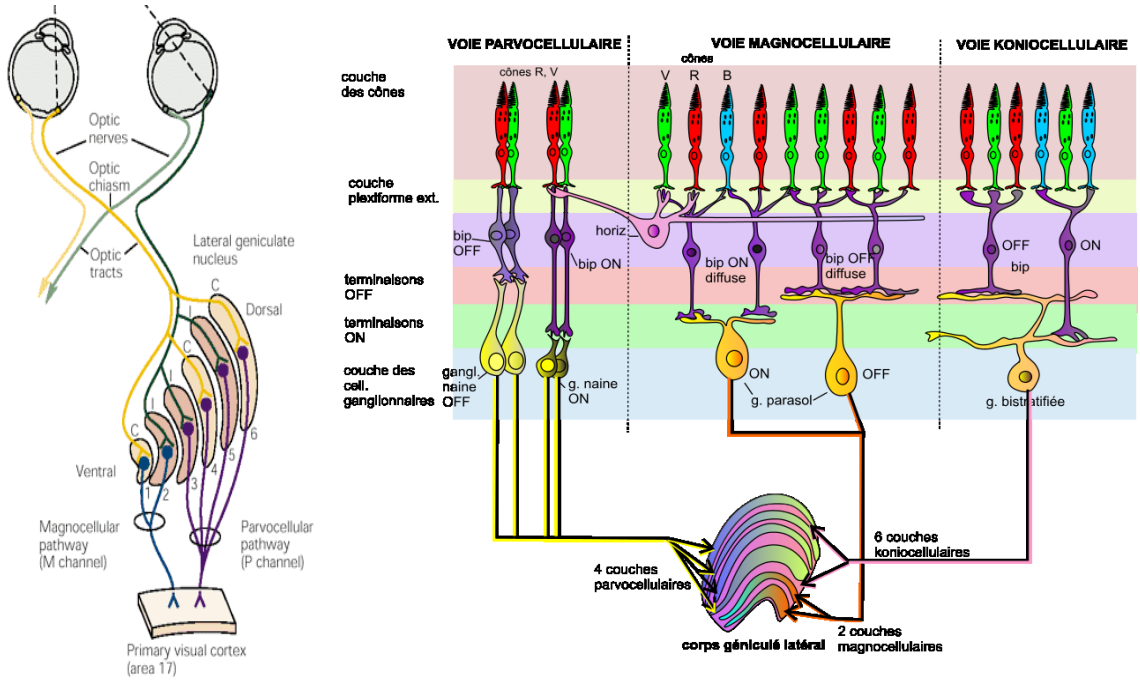

Figure 1.3. Schéma des projections rétiniennes sur le CGL. **À gauche** : projections controlatérale (œil gauche) et ipsilatérale (œil droit) sur le CGL droit. Le CGL est constitué de 6 couches avec la voie magnocellulaire (couches 1 et 2) et la voie parvocellulaire (couches 3 et 6) (Kandel et al., 2000). **À droite**: La rétine des primates avec les connexions au corps géniculé latéral (schéma modifié de Nieuwenhuys et als, The Human CNS, Springer, 2008).

Le thalamus visuel de la souris

Tout comme chez le chat et les primates, les neurones du CGL de la souris ont des champs récepteurs à centre ON et OFF, et des réponses transitoires et prolongées similaires à celles des CGR (Grubb et Thompson, 2003). Ils ont également des modes de déclenchement en rafale et en tonique (Niell et Stryker, 2010). Ainsi, mis à part le manque apparent de cellules de type Y-like, les comptes rendus physiologiques des neurones de CGL chez la souris indiquent qu'ils ont les mêmes propriétés fondamentales que celles de leurs correspondants de chats ou de primates. Les différentes catégories fonctionnelles de CGR se connectent aux neurones CGL en une série de couches parallèles spatialement distinctes, mais qui semblent inclure des territoires "sélectifs à la direction" (Huberman et al., 2008).

1.1.3. Le cortex visuel primaire :

Chez le chat et les primates

Chez les primates, de même que chez les chats, les voies parvocellulaires et magnocellulaires aboutissent toutes dans la couche IV. La voie K projette sur les couches I, II, III et V de V1. Au niveau cortical, l'image qui était déconstruite par la rétine se reconstruit (et donc la barre est perçu comme une barre et pas comme des points) grâce au moins à deux types cellulaires: les cellules simples et les cellules complexes (Hubel et Wiesel, 1962). Les cellules simples permettent l'analyse des détails d'une image visuelle, elles préfèrent des fréquences spatiales hautes et elles sont sélectives à l'orientation d'une barre lumineuse de forme allongée (champ récepteur petit longiligne résultat de la sommation de plusieurs champs récepteurs circulaires des cellules du CGL où leurs centres sont alignés (Movshon et al., 1978)). Le patron de décharge de ces cellules est en phase avec le stimulus présenté. Les cellules complexes préfèrent des fréquences spatiales basses (Skottun et al., 1991), elles sont sélectives à la direction des stimuli visuels, au mouvement d'une barre lumineuse présentée (Hubel et Wiesel, 1962), à son orientation, mais pas à sa localisation précise dans l'espace. Pour les cellules complexes, et contrairement aux cellules simples, le champ récepteur est grand et ne possède pas des régions excitatrices et d'autres inhibitrices distinctes. En plus, elles ne modulent pas leur réponse lors de l'apparition, dans leurs champs récepteurs, d'un stimulus en mouvement périodique (Hubel et Wiesel, 1962).

La sélectivité à l'orientation chez les chats et les primates

Au niveau du V1, les informations arrivent sur des espèces de colonnes verticales de traitement constituées par des cellules ayant des propriétés fonctionnelles similaires (Mountcastle, 1997). En effet, les cellules d'une même colonne répondent préférentiellement à une orientation particulière (Freeman, 2003). Les colonnes montrent une dominance oculaire (droite ou gauche). C'est ainsi, les informations reçues d'un point précis de l'œil gauche arrivent sur une colonne située juste à côté de celle qui reçoit les informations du point homologue de l'œil droit. L'intégration de ces deux types d'informations donnera le relief (et aussi la profondeur). L'imagerie optique (figure 1.4), a permis de construire des cartes d'orientations appelées "pinwheels" due à leur organisation semblable aux rayons d'une roue de bicyclette, puisque les colonnes d'orientation convergent en certains points corticaux où toutes les orientations se rencontrent (Bonhoeffer et Grinvald, 1991). Sur une surface corticale d'environ 2 mm^2, les colonnes d'orientation qui constituent des modules corticaux s'organisent en hypercolonne qui regroupe une représentation de toutes les orientations possibles de 0 à 180° d'un stimulus pour une certaine portion du champ visuel (Hubel et Wiesel, 1974) . En plus d'être sélectifs à l'orientation, les neurones de V1, tout comme ceux des aires visuelles extrastriées, sont sensibles à la vitesse, au contraste, et à la fréquence spatiale (Mountcastle, 1997).

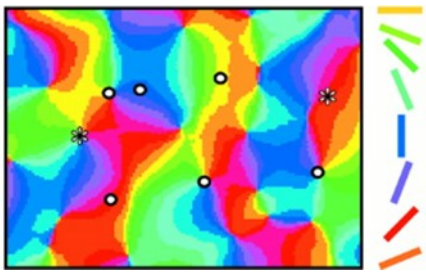

Figure 1.4 : Carte des préférences d'orientation codées par des couleurs pour une région corticale obtenue par imagerie intrinsèque. Les cercles dans les panneaux indiquent les emplacements des pénétrations de tétrode. Ces pénétrations visaient des domaines d'iso-orientation. Barre d'échelle, 1 mm. L'orientation préférée pour chaque point est codée par une couleur, comme indiquée à droite. Cette carte d'orientation révèle l'organisation typique des cartes de préférences d'orientation en centres de moulinet (où différentes préférences d'orientation convergent, par exemple en un point cortical représenté par l'astérisque gauche) et des domaines iso-d'orientation (où des neurones de préférence d'orientation similaires sont regroupés : astérisque droit).

Chez la souris

Le cortex visuel de la souris présente de nombreuses similitudes avec celui d'autres espèces, avec la structure typique à six couches, l'organisation rétinotopique (deux cellules voisines de la rétine sont stimulées par deux points contigus du champ visuel et projettent sur deux neurones corticaux adjacents) et une variété de sous-types de neurones excitateurs et inhibiteurs (Huberman et Niell, 2011).

La sélectivité à l'orientation chez la souris

La sélectivité à l'orientation des cellules de V1, décrite par Hubel et Wiesel (Hubel et Wiesel, 1962), est retrouvée chez la souris (Dräger, 1975). En effet, beaucoup de neurones montrent une sélectivité robuste à l''orientation, sans qu'il y ait de structure locale discernable en colonne. Il s'agit d'une organisation en sel et poivre où des neurones voisins répondent souvent à des orientations différentes. Bien que V1 de la souris ait une carte topographique claire de l'espace visuel, d'autres types d'organisation à grande échelle sont absents, en particulier, une carte d'orientation ordonnée, qui varie à travers la surface corticale selon un schéma stéréotypé de «roues à aubes» (Bonhoeffer et Grinvald, 1991). L'absence d'une telle carte d'orientation pourrait expliquer en partie pourquoi de nombreux chercheurs ont supposé que les souris auraient une sélectivité d'orientation réduite (Sompolinsky et Shapley, 1997). Cependant, les cartes d'orientation semblent être absentes chez tous les rongeurs, même ceux avec une acuité relativement élevée, tels que les rats (Ohki et al., 2005) et les écureuils (Van Hooser et al., 2005). Bien que ces cartes ne jouent peut-être pas un rôle direct dans la fonction corticale (Horton et Adams, 2005), elles pourraient être importantes pour l'efficacité du câblage (Koulakov et Chklovskii, 2001). Plusieurs études ont montré que, malgré l'absence d'une carte d'orientation discernable dans le cortex visuel de souris (Wang et Burkhalter, 2007), les cellules nerveuses sœurs issues d'un même clone radial présentaient des préférences d'orientation similaires. En utilisant un vecteur rétroviral codant pour une protéine fluorescente verte qui marque les clones radiaux de neurones excitateurs, et l' imagerie calcique in vivo à deux photons qui mesure les propriétés de la réponse neuronale, il était montré que les cellules sœurs préféraient des orientations similaires, alors que les non-sœurs voisines ne présentaient pas cette relation (Y. Li et al., 2012).

Chez la souris, la gamme d'orientations à laquelle répondra une cellule donnée est assez similaire à celle observée chez les chats ou les singes (Niell et Stryker, 2008), malgré le fait que l'acuité

visuelle varie de près de deux ordres de magnitude entre ces espèces (Van Hooser, 2007), ce qui suggère qu'il pourrait s'agir d'un aspect fondamental d'analyse corticale (Van Hooser, 2007). Une étude électrophysiologique des propriétés de la réponse dans les couches de V1 de la souris a confirmé que presque tous les aspects du traitement visuel cortical sont présents (Niell et Stryker, 2008), y compris la syntonisation à la fréquence spatiale, la sélectivité à la direction, les réponses linéaires et non linéaires (correspondant respectivement aux réponses des cellules simples et celles des cellules complexes décrites par Hubel et Wiesel), ainsi que le contrôle du gain dû au contraste. En effet, une fois que la taille relative des champs récepteurs des cellules corticales V1 de la souris et du singe a été compensée comme l'a montré une analyse quantitative sans échelle (Niell et Stryker, 2008), la sous-structure spatiale des champs récepteurs individuels se montre similaire entre la souris et le singe. Ensemble, ces résultats suggèrent que le cortex de la souris effectue effectivement des analyses similaires à celles d'autres espèces, mais avec une résolution spatiale inférieure.

Parmi les neurones corticaux, la diversité morphologique la plus frappante réside aussi bien chez la souris que chez le chat et les primates dans la classe des neurones inhibiteurs (les cellules chandelier, de panier et de double bouquet) (Markram et al., 2004). Chez la souris, une grande classe de neurones inhibiteurs exprimant la parvalbumine, et ayant des potentiels d'action à hautes fréquences, présente une sélectivité beaucoup moins grande que les neurones excitateurs. Cette importante population de cellules non syntonisées est une caractéristique observée chez la souris, mais qui n'est peut-être pas présente chez d'autres espèces, bien que des études récentes portant sur des chats et des singes aient montré une plus grande diversité de degré de sélectivité à l'orientation entre les neurones et qu'on l'avait couramment sous-estimée (Ringach et al., 2002).

1.1.4. Le cortex extrastrié: plusieurs niveaux pour un traitement visuel d'ordre supérieur

Chez le chat et les primates

Chez les chats, les primates et l'homme, le cortex visuel primaire envoie sa sortie à une série hiérarchique d'aires visuelles extrastriées (Felleman et Van Essen, 1991), qui assurent le traitement d'une gamme de caractéristiques visuelles d'ordre supérieur, notamment le mouvement, la perception de la profondeur, la segmentation de l'image et la reconnaissance d'objets (Orban, 2008). Un principe organisateur de ces zones est la notion d'un flux ventral portant des informations sur l'identité de l'objet (la voie « quoi ») et d'un flux dorsal portant des informations

sur la localisation de l'objet (la voie « où ») (Ungerleider et Haxby, 1994). Cependant, au-delà de cet organigramme approximatif, on en sait beaucoup moins sur la façon dont les caractéristiques visuelles particulières sont calculées par les circuits neuronaux à l'intérieur et entre ces régions.

Le cortex extrastrié de la souris

Des études anatomiques (Wang et Burkhalter, 2007) et d'autres études de cartographie (Kalatsky et Stryker, 2003; Wagor et al., 1980) ont révélé la présence de plusieurs aires de vision extrastriées dans le cortex de la souris, et jusqu'à neuf recevant une entrée directe de V1. De plus, leurs modèles de connectivité sont cohérents avec un flux dorsal et ventral, comme chez d'autres espèces (Wang et al., 2011), cependant les propriétés fonctionnelles de ces zones chez la souris sont très mal connues.

1.1.5. Collicule supérieur : un centre médian pour les comportements visuellement guidés

Une étude électrophysiologique du collicule supérieur (CS) de la souris confirme que la plupart des champs récepteurs sont semblables à ceux d'autres mammifères (Wang et al., 2010), mais ils sont plus grands en raison de la résolution inférieure de la rétine de la souris. Cette étude a également montré l'existence des cellules du CS sélectives à la direction et même à l'orientation. Cette sélectivité ne dépendant pas de l'apport du cortex, ce qui suggère qu'elle est héritée directement de CGR sélectives à l'orientation ou qu'elle immerge au niveau du CS. La présence de ces différentes réponses visuelles dans le CS pourrait être due à la position intermédiaire de la souris dans la hiérarchie évolutionnaire, avec CS et cortex jouant un rôle partagé dans le traitement visuel. En effet, les souris peuvent encore effectuer des tâches simples de détection des cibles même après des lésions du cortex visuel (Prusky et Douglas, 2004), ce qui suggère que certaines des fonctions attribuées chez les chats et les primates au cortex visuel sont médiées par le CS chez la souris. En revanche, le rôle du CS dans l'analyse de la scène visuelle et la direction de comportements guidés visuellement pourrait être sous-estimé chez les espèces supérieures, où la plus grande partie de l'attention a été accordée au rôle du CS dans les mouvements oculaires saccadiques (Lovejoy et Krauzlis, 2010).

1.2. La syntonisation des courbes d'accord à l'orientation dans V1: un modèle de la plasticité

Chez les mammifères, une fois que la période critique est dépassée, la préférence des cellules du V1 à une orientation donnée reste inchangée, et ce, tout au long de la vie de l'animal (Purves et

al., 2019). Cela dit, la carte des préférences des cellules de V1 à l'orientation est une empreinte physiologique du fonctionnement cortical. Puisque la sélectivité à l'orientation est une propriété intrinsèque immuable, tout changement de l'orientation préférée (OP) est une marque du potentiel plastique des cellules du V1. Par conséquent, dans le cadre de cette thèse, la syntonisation des courbes d'accord était notre modèle de la plasticité corticale. Plusieurs études ont montré qu'à la suite des différentes manipulations, les cellules corticales déplacent le pic de leurs courbes d'accord à l'orientation. En effet, l'imposition d'une orientation non préférée pendant quelques minutes (adaptation) fait modifier dans une fenêtre spatiale et temporelle relativement étroite la carte des préférences des cellules de V1 à l'orientation (Bachatene, Bharmauria, Cattan, Rouat, et al., 2015). Chez le chat et la souris, l'adaptation induit plus de déplacements attractifs (déplacement des pics des courbes d'accord à l'orientation vers l'orientation adaptante) que de déplacements répulsifs (déplacement des pics des courbes d'accord à l'orientation en s'éloignant de l'orientation adaptante) (Ghisovan et al., 2009; Jeyabalaratnam et al., 2013b). Le modèle de « push-pull » était proposé pour expliquer les effets de l'adaptation sur les préférences cellulaires à l'orientation (Ferster, 1988, 1992; Palmer et Davis, 1981; Shapley et al., 2003; Tolhurst et Dean, 1990; Troyer et al., 1998). En effet, lors de l'adaptation, il y aurait une inhibition de l'OP initiale et une facilitation de l'orientation imposée ; la somme de ces deux forces induit une nouvelle OP (Ferster, 1988, 1992; Palmer et Davis, 1981; Shapley et al., 2003; Tolhurst et Dean, 1990; Troyer et al., 1998). De plus, le renforcement de l'entrée de l'orientation adaptante sur les autres entrées explique les déplacements attractifs alors que leur affaiblissement favorise un biais d'une orientation sur le côté opposé de la courbe d'accord et induit donc de déplacements répulsifs. L'avantage tiré de ces changements est une amélioration des performances pour la discrimination d'orientation adaptante (Krekelberg et al., 2006; Teich et Qian, 2003) ou une augmentation de la détectabilité (Clifford et al., 2001). En outre, la formation des réseaux neuronaux fonctionnels est requise pour le traitement visuel. Ceci implique que le changement des préférences cellulaires est lié au changement au niveau des connexions entre les cellules appartenant à un même assemblé fonctionnel. Par conséquent, la plasticité synaptique qui désigne l'apparition de nouvelles synapses, la disparition d'autres ou le changement du poids synaptique entre les cellules connectées est une représentation de la plasticité qui affecte la sélectivité cellulaire à l'orientation. Puisqu'il a été suggéré que l'adaptation est un apprentissage de court terme (Bachatene, Bharmauria, Cattan, Chanauria, et al., 2015; Bachatene et al., 2013; Dragoi et al., 2000), il était

proposé que cet apprentissage implique une réorganisation des forces de connexions entre les neurones sélectifs à l'orientation et par le fait même l'implication des récepteurs, notamment les récepteurs glutaminergiques (Bachatene, Bharmauria, Cattan, Chanauria, et al., 2015; Gilbert et Li, 2012). Certains antidépresseurs en affectant la neurotransmission peuvent être inducteurs de la neuroplasticité. Une étude récente a révélé que la fluoxétine qui est un inhibiteur de la recapture de la sérotonine affecte l'OP acquise et facilite l'adaptation des cellules (Bachatene et al., 2013). Il a été suggéré que la fluoxétine potentialise la réponse cellulaire acquise après adaptation en facilitant le mécanisme SRP (stimulus-selective response potentiation) où les réponses cellulaires se trouvent améliorées quand les cellules sont exposées d'une façon répétitive au même stimulus (Frenkel et al., 2006). De plus, il était montré que la sérotonine améliore les réponses médiées par les récepteurs NMDA (Reynolds et al., 1988). À l'encontre, la kétamine, en se liant aux NMDAR, bloque leur canal lorsqu'il est ouvert, induisant ainsi une modification de l'état conformationnel du canal. Le canal bouché empêche le passage des ions Ca2+ et Na +. Il semble que les effets anesthésiques, antalgiques et antidépresseurs de la kétamine soient dus, entre autres, à ce blocage (Dinis-Oliveira, 2017; Zanos et Gould, 2018). Le blocage de l'ion Ca2+ perturbe la transmission synaptique et par le fait même affecterait les connexions neuronales et modulerait ainsi l'encodage des stimuli : les réponses cellulaires (OP) peuvent se trouver modifiées. La kétamine pourrait aussi induire la plasticité au niveau du V1 par altération de l'équilibre entre l'excitation et l'inhibition. En effet,), il a été démontré que l'application chronique de la kétamine à des souris mène à des altérations des interneurones dans le cortex prélimbique (McNally et al., 2013. Sur la même voie, Zhou et son groupe ont publié que, en tant qu'antagoniste des récepteurs NMDA, la kétamine a le potentiel d'induire la perte du phénotype inhibiteur des interneurones (FS: fast spike) (Zhou et al., 2012). La conséquence fonctionnelle de cette baisse de l'inhibition est une augmentation de l'excitation et par le fait même une modification au niveau de la balance excitation-inhibition. Cet effet était démontré par une autre étude qui a annoncé que le blocage des récepteurs NMDAR modifie l'équilibre entre l'excitation et l'inhibition dans les circuits corticaux (Homayoun et Moghaddam, 2007). Une autre étude a révélé que l'application de la kétamine sur le cortex préfrontal a induit la formation de nouvelles synapses et donc des nouvelles connexions entre les cellules (Moda-Sava et al., 2019). Cette plasticité synaptique aurait des incidences sur la réponse cellulaire à l'orientation dont les courbes de syntonisation peuvent être vues comme un reflet de cette plasticité.

Conclusion

Les études ont montré que, comme le chat et les primates, la souris est capable de discriminer des formes complexes (Bussey et al., 2001). Malgré les évidentes différences de comportement visuel et d'acuité entre la souris, le chat et les primates, les preuves qui montrent que les similitudes surpassent les différences deviennent de plus en plus nombreuses. En outre, le potentiel plastique du V1 chez les mammifères est démontré par plusieurs études. En partant du V1 comme modèle d'étude de la plasticité chez la souris et le chat, l'effet de certaines manipulations telles que l'application locale des antidépresseurs ou l'adaptation sur la sélectivité à l'orientation ainsi que sur les connexions entre les cellules peuvent être testé. Ceci nous mène à présenter nos objectifs de recherche dans la section suivante.

2. Objectif et hypothèses de recherche

2.1. Objectif 1

Les travaux fondateurs de David Hubel et Torsten Wisel ont démontré que les cellules de l'aire visuelle primaire des mammifères sont sélectives à l'orientation; (Chapman et Stryker, 1993; Hubel et Wiesel, 1968; Niell et Stryker, 2008). En effet, les neurones du V1 répondent à des stimuli contenant des bordures claires/sombres présentées à des angles particuliers dans le champ visuel. Alors que ces neurones sélectifs montrent une organisation en sel et poivre chez les rongeurs (Bonin et al., 2011), ils sont organisés en colonne d'orientation chez les mammifères plus évolués tels que le chat ou les primates (Mountcastle, 1997). La sélectivité à l'orientation est le résultat de la convergence spatiale d'un groupe de synapses ayant des sélectivités spécifiques sur un neurone récipient. Ce groupe de synapse crée un biais par rapport à une orientation bien déterminée chez ledit neurone. La préférence d'un neurone pour une orientation donnée est établie pendant la période critique et reste inchangeable tout le long de la vie de l'animal (Mountcastle, 1997). Cependant, les expériences ont mis en évidence une plasticité au niveau du V1 de l'animal adulte, donc, en dehors de la période critique. Cette plasticité est révélée par de différentes interventions. À titre d'exemple, la privation oculaire entraine chez plusieurs mammifères tels que le chat et la souris la dominance de l'œil restant (Sato et Stryker, 2008; Wang et al., 2019). Ce mécanisme compensatoire, qui contrebalance la perte des afférences due à la privation oculaire, est le résultat de l'augmentation de l'activation des récepteurs NMDA et AMPA d'une part, et de la baisse du niveau d'activation des récepteurs $GABA_A$ d'autre part (Hofer et al., 2006). D'autres

études ont montré l'efficacité de certains antidépresseurs, tels que la fluoxétine à restaurer la fonction visuelle chez des rats atteints d'amblyopie, et ce, par la réduction de l'inhibition intracorticale (Maya Vetencourt et al., 2008). Par imagerie optique, il s'est révélé que l'administration de fluoxétine permet de rétablir et réactiver la plasticité observée lors de la période critique (Steinzeig et al., 2019). Chez l'humain, l'altération de la LTP (long-term plastictity) lors du traitement des réponses visuelles évoquées se trouve restaurer par l'utilisation des antidépresseurs de la classe SSRI (selective serotonin reuptake inhibitor) (Normann et al., 2007). Les effets des antidépresseurs sur la plasticité corticale nous ont poussés à s'interroger si la kétamine pouvait affecter les propriétés intrinsèques des neurones et si elle induisait un certain aspect de plasticité au niveau du V1.

La kétamine, un antagoniste non compétitif du récepteur NMDA (N-methyl-D-aspartate), est un anesthésique à action rapide principalement utilisé lors d'interventions chirurgicales; cependant, il est également utilisé comme sédatif, un analgésique, et même comme antidépresseur (Berman et al., 2000; Leong, 2002; Priebe et Ferster, 2008; Zanos et al., 2016). En se liant à un site de fixation sur la sous-unité NR1, la kétamine bloque le canal préalablement ouvert, ce qui empêche l'afflux du calcium et par le fait même la LTP et donc la plasticité médiée par cette voie. L'effet bloqueur de la kétamine des récepteurs AMPA des cellules pyramidales est aussi démontré par les travaux de Darell A L., 2002 faits sur des tranches de cortex auditif de la gerbille (Leong, 2002). Mis ensemble, ces faits prédisent qu'en absence de l'activation des récepteurs glutamatérgiques (par exemple par la kétamine), le potentiel plastique des neurones serait affecté partiellement ou totalement à la suite du blocage des microcircuits. Cependant de nombreuses études ont montré que l'application chronique de la kétamine améliore la plasticité corticale (Lepack et al., 2015) et permet la restauration des circuits altérés au niveau du cortex préfrontal grâce à l'induction de la formation des nouvelles épines remplaçant celles qui étaient perdues (Moda-Sava et al., 2019). Ces résultats suggèrent que la voie glutamatergique n'est pas le seul mécanisme menant aux changements de l'activité des neurones et des réseaux dans lesquels ils sont impliqués directement ou indirectement. Bien que l'effet inducteur de la plasticité à la suite de l'application chronique de la kétamine fût montré par plusieurs études sur de différentes régions du cerveau, l'effet de son application locale sur les réponses cellulaires au niveau du V1 est inconnu.

Le premier objectif était donc d'examiner, chez le chat et la souris, l'effet de la kétamine sur la sélectivité à l'orientation et sur la variabilité des activités spontanées et évoquées par un protocole de stimulation visuelle dans V1 des souris et du chat adultes. L'hypothèse de ce travail était que les cellules corticales de V1 déplaçaient leurs pics de courbes de syntonisation à l'orientation après l'application locale de kétamine. Cela dit, la kétamine interfère avec le mécanisme de la sélectivité neuronale à l'orientation en termes d'OSI et de variabilité des réponses cellulaires. Cette hypothèse est fondée par les résultats de plusieurs travaux. En effet, il était démontré que la signalisation synaptogénique de mTOR (mechanistic target of rapamycin), de BDNF (brain-derived neurotrophic factor), et de EEF2 (Eukaryotic Translation Elongation Factor 2) augmente en réponse à l'application de la kétamine (Lepack et al., 2015; Zanos et Gould, 2018; Zanos et al., 2016). La mTOR régule la synthèse protéique et la transcription des gènes. Le BDNF est un facteur de croissance. Il active aussi la synthèse des protéines par la déphosphorylation du facteur d'élongation EEF2. Compte tenu de leurs rôles, l'activation de ces différentes classes de molécules par la kétamine pourrait altérer la force synaptique et donc la connectivité entre les cellules (Aleksandrova et al., 2017; Autry et al., 2011). Cela dit, la sélectivité des cellules pourrait être altérée puisque celles-ci, sous l'effet de la kétamine, reçoivent des nouvelles afférences (entrées synaptiques) différentes de celles de la condition de contrôle. Les résultats de cette première étude vont nous permettre de divulguer si la kétamine affecterait les propriétés sélectives intrinsèques des neurones. Cependant, il est aussi intéressant de voir si cette drogue impacterait les propriétés sélectives acquises après adaptation, et ce, chez le chat et la souris. Ceci est le sujet de la deuxième étude dont l'objectif est présenté plus en détail dans la section suivante.

2.2. Objectif 2

La plasticité corticale est une fonction cérébrale fondamentale au développement, à la mémoire, à l'apprentissage et à la récupération après une blessure par exemple. Des recherches sur la plasticité au niveau du V1 ont montré que les neurones peuvent modifier leurs préférences sélectives après certaines interventions expérimentales appropriées comme l'adaptation visuelle qui consiste en une imposition d'un stimulus non préféré pendant plusieurs minutes (Bachatene et al., 2013; Dragoi, Rivadulla, et al., 2001; Dragoi et al., 2000; Dragoi, Turcu, et al., 2001; Jin et al., 2005; Nemri et al., 2009) ou l'application de la kétamine (Ouelhazi et al., 2019). Cependant, l'effet de la kétamine sur l'adaptation visuelle n'est pas encore élucidé. En plus, le neurone du V1 est actif, mais pas d'une façon isolée du réseau auquel il appartient. Autrement dit, la réponse cellulaire telle que la

préférence d'une orientation donnée est la conséquence de l'établissement d'un état particulier des connexions locales entre les neurones (Lindquist et Barrett, 2012; Shen et al., 2012). L'ensemble de ces connexions demeure sensiblement inchangé après la naissance. Toutefois, un changement contextuel peut mener à des changements des patrons de connexions entre les cellules (Bachatene, Bharmauria, Cattan, Chanauria, et al., 2015). Nous cherchons, par conséquent à examiner en un premier temps, si la kétamine affecte les effets de l'adaptation visuelle et en un deuxième temps si l'adaptation suivie par l'application locale de la kétamine au niveau de V1 conduisait à un changement majeur des connexions préétablies, ce qui pourrait expliquer le glissement des pics des courbes de syntonisation observé lors de la première étude (chapitre 1). Nous supposons que des changements de la connectivité entre les neurones peuvent éventuellement soutenir la réorganisation de la carte corticale (Alloway et Roy, 2002; Wise et al., 2010). Les cross-corrélogrammes (CCG) entre les trains de potentiels d'action sont un outil révélant les relations fonctionnelles entre les paires neuronales dans un microcircuit (Denman et Contreras, 2014; Fujisawa et al., 2008; Perkel et al., 1967). Après avoir fixé comme objectif l'étude de l'effet de la kétamine sur les propriétés sélectives intrinsèques (objectif 1) et post-adaptatives des neurones (objectif 2), lors de la dernière étude, on s'intéressait à préciser l'effet de l'adaptation sur la syntonisation des courbes d'accord à l'orientation. Ce dernier objectif est expliqué plus en détail dans la section suivante.

2.3. Objectif 3

La sélectivité à l'orientation est l'une des propriétés clefs du cortex visuel primaire que la souris partage avec les mammifères supérieurs comme les chats et les primates. C'est la signature fonctionnelle du V1(Niell et Stryker, 2008). Elle est le résultat d'un biais pour une orientation particulière dans les entrées synaptiques qu'un neurone reçoit. En effet, la sélectivité est attribuée à un biais dans la distribution des préférences au niveau des épines dendritiques ou à un biais dans les forces synaptiques qui peuvent être plus fortes pour les entrées d'une orientation particulière (Bachatene et al., 2013; Jia et al., 2010). Il était montré que l'adaptation induit chez la souris des changements transitoires des propriétés de la réponse neuronale par une modification des relations interneuronales (Afef et al., 2022). Cependant, l'effet de l'adaptation sur le degré de sélectivité, mesuré par l'OSI, n'est pas encore connu. Le but de cette étude est d'examiner si l'adaptation visuelle affecte l'OSI des cellules et si cet effet est relié aux changements de la connectivité

fonctionnelle entre les cellules. Les propriétés sélectives dépendent non seulement de la dynamique des réseaux neuronaux, mais aussi de l'équilibre entre l'excitation (E) et l'inhibition (I) intracorticale (Dragoi, Turcu, et al., 2001). Or l'adaptation induit un changement de l'orientation préférée et une réorganisation des relations fonctionnelles entre les cellules. Ceci pourrait suggérer une abolition de cet équilibre entre E et I. Par conséquent, nous supposons que l'adaptation pourrait affecter l'OSI des cellules et spécifiquement celles qui ont modifié leurs connexions après adaptation.

En somme, on cherche, en premier temps, à divulguer si la kétamine affecte les propriétés sélectives des neurones (objectif 1) et en un second temps, si elle altère les réponses post-adaptatives (objectif 2) chez la souris et le chat. Finalement, on veut étudier, chez la souris, si l'affinité de ces réponses post-adaptatives est le résultat des changements qui se produisent au niveau des relations fonctionnelles entre les cellules du microcircuit (objectif 3). Donc, les trois études vont permettre d'étudier certaines manipulations (l'application de la kétamine et adaptation) sur la plasticité au niveau du V1.

3. Effects of ketamine on orientation selectivity and variability of neuronal responses in primary visual cortex

Ouelhazi A, Bharmauria V, Chanauria N, Bachatene L, Lussiez R, Molotchnikoff S

Publié dans : Brain Research, Volume 1725, 15 December 2019, 146462

Numéro CDEA : **20-068**

Rôles des auteurs :
Conceptualization, A.O., and L.B; Methodology, A.O., and V. B.; Software, O.A. and N.C.; Validation, A.O.; Formal Analysis, A.O.; Investigation, A.O.; Resources, A.O; Data Curation, A.O.; Writing – Original Draft, A.O.; Writing – Review & Editing, A.O., and M.S; Visualization, A.O.; Supervision, S.M. and A.O.; Project, S.M.; Funding Acquisition, S.M., and NSERC Canada.

https://doi.org/10.1016/j.brainres.2019.146462

Highlights

• Acute ketamine changes the orientation selectivity in V1 of adult mouse and cat.

• Ketamine application decreases the variability of evoked responses.

• Evoked firing, but not spontaneous, are affected by acute exposure to ketamine.

Abstract

The plasticity of the adult brain is one of the most highly evolving areas of recent neuroscience research. It has been acknowledged that the visual cortex in adulthood can adapt and restructure the neuronal connections in response to a sensory experience or to an imposed input such as in adaptation or ocular deprivation protocols. In order to understand the basic cellular mechanisms of plasticity in the primary visual cortex (V1), we examined the effects of ketamine, a non-competitive, glutamatergic NMDAR (N-methyl-D-aspartate receptor) antagonist, on the orientation of cortical cells by measuring their response variability and the Gaussian tuning curves in adult anesthetised mouse and cat. Neurons were recorded extracellularly using glass electrodes. The ketamine was applied locally by placing a custom-cut filter paper (1x1mm) soaked in ketamine solution (10 mg/ml) on the cortical surface next the site of the recording tip, in both species. Our results show that the local and acute exposure of ketamine on V1 changes the preferred orientation of the visual neurons established during the critical period of development. Furthermore, ketamine also leads to a decrease in the orientation selectivity (measured by orientation selectivity index, OSI) and the variability of neuronal evoked responses (measured by Fano factor) but does not affect spontaneous activity. These results suggest that ketamine induces plasticity in V1 neurons that might be operated by a different pathway than that of NMDARs.

3.1. Introduction

Neurons in the primary visual cortex (V1) of mammals are selective for a number of attributes, such as spatial and temporal frequencies, and direction of motion and orientation (Hubel et Wiesel, 1968; Mountcastle, 1997). In mouse (Niell et Stryker, 2008), and in other mammals (Chapman et Stryker, 1993), V1 neurons respond best to stimuli containing light/dark borders presented at particular angles in the visual field (Chapman et Stryker, 1993; Hubel et Wiesel, 1968; Niell et Stryker, 2008), thus exhibiting orientation selectivity. Importantly, orientation selective V1 neurons are arranged in a salt-and-pepper fashion in mouse (Bonin et al., 2011), whereas they are arranged systematically into orientation columns in higher vertebrates (Mountcastle, 1997).

Orientation selectivity rests in the convergence of spatially grouped synapses driven by a specific orientation. Such clusters of synapses create a bias in favor of a specific orientation. It is formed during the sensitive period of brain development and is present throughout the animal's life (Hubel et Wiesel, 1974). However, in the neocortex during postnatal life, the form and function of neural circuitry are further shaped by experience, thus, rendering it plastic (Hensch, 2005; Ko et al., 2013) . Often, this plasticity in the adult cortex lies dormant but its subsequent activation may be possible (Hensch, 2005). In fact, processes that trigger neuroplasticity can be reactivated by experimentally manipulating sensory inputs through adaptation (Bachatene, Bharmauria, Rouat, et al., 2012; Jeyabalaratnam et al., 2013b), or ocular deprivation (Goel et Lee, 2007), or through the application of drug (Bachatene et al., 2013). Such interventions, potentially targeting the molecular pathways, can alter the level and pattern of activity in the cortical circuits, thus leading to neural plasticity (Hofer et al., 2006; Hübener et Bonhoeffer, 2014).

Ketamine, an NMDAR antagonist, is a fast-acting anesthetic mainly used during surgical procedures; however, it is also used as a sedative, a pain-reliever, and even as an antidepressant (Berman et al., 2000; Leong, 2002; Priebe et Ferster, 2008; Zanos et al., 2016). Studies have shown that ketamine impairs the activity (neuronal response decline) in dorsal horn neurons which are centrally involved in pain transmission (Conseiller et al., 1972). Other investigations revealed that ketamine disrupts synaptic transmission by interacting with AMPA/Kainite receptors in neocortical neurons (Leong, 2002). It has also been shown that chronic ketamine treatments engender behavioral effects and structural modifications in cortical interneurons (Hamm et al., 2017). Ketamine may also modify cortical circuitry in the prelimbic cortex resulting in circuit dysfunction (J. McNally et al., 2013). Interestingly, it was shown that ketamine interferes with top-down processes (reducing feedback to the early visual cortex), thereby influencing the neuronal object representations and distorting the image recognition processes (van Loon et al., 2013). Indeed, there are many other studies that suggest that ketamine enhances cortical plasticity (Lepack et al., 2015). However, the local effects of ketamine on V1 responses are unknown. Here, we examine the effects of ketamine on neuronal firing and orientation tuning curves (cortical orientation selectivity) in V1 of anesthetised mouse and cat. We show that local application of ketamine induces shifts of orientation selectivity, a decrease of neuronal orientation selectivity, and a decrease of the variability of evoked responses. These results suggest that ketamine induces orientation plasticity in V1 neurons, and this robust and transient orientation plasticity might be

driven via a different pathway than that of NMDAR, since ketamine is an NMDAR-channel blocker by impeding Ca++ entry (Guo et al., 2017).

3.2. Results

The aim of the present study was to examine the effect of ketamine (a dissociative anesthetic) on evoked and spontaneous activities of orientation-selective neurons in V1 of adult mouse. In mouse, a total of 105 neurons were further explored, hence all statistical analyses were solely on these cells. A few cells were eliminated because their firing activities were lost during the experiment, and as a consequence they could not be traced. The general set-up is displayed in Fig. 3.1. Further, to verify if ketamine affects the orientation selectivity in cat (where V1 is organized into orientation domains); we extended our experiments to cat. From three recordings, we sorted 20 neurons that could be tracked pre- and post-ketamine application.

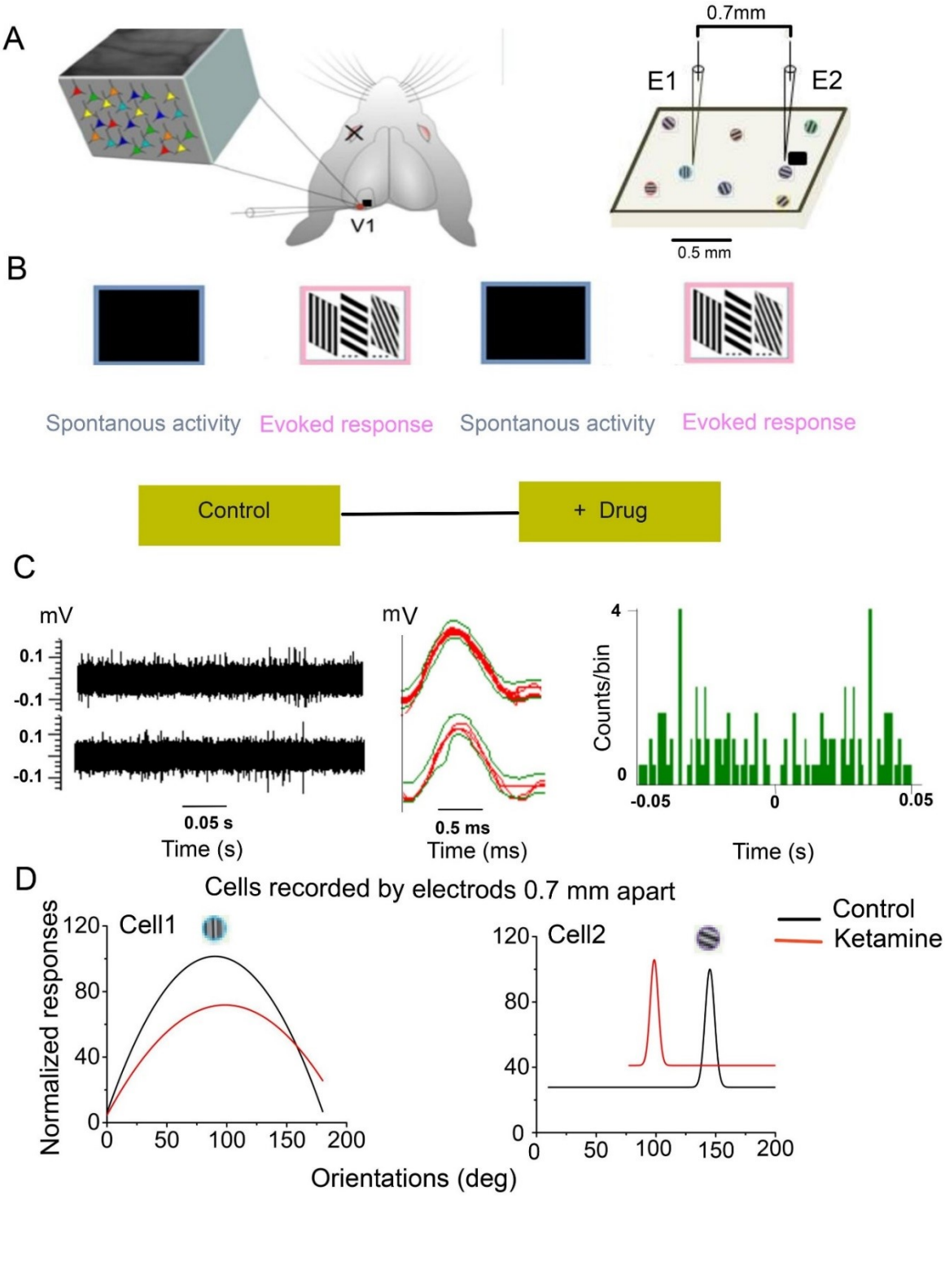
A
0.7mm
E1
E2
V1
0.5 mm
B
Spontanous activity
Evoked response
Spontanous activity
Evoked response
Control
+ Drug
C
mV
0.1
-0.1
0.1
-0.1
0.05 s
Time (s)
mV
0.5 ms
Time (ms)
4
Counts/bin
0
-0.05
0
0.05
Time (s)
D
Cells recorded by electrods 0.7 mm apart
Cell1
Cell2
Control
Ketamine
Normalized responses
120
80
40
0
0
50
100
150
200
Orientations (deg)

Fig.3.1. Experimental protocol showing ketamine's effect on spontaneous and evoked activity of V1 neurons in adult mouse. 1A. On the left shows the site of electrophysiological recording (red plot); two electrodes were implanted, and the salt and pepper pattern of V1 organisation in mouse. Black square shows the deposit site of a custom-cut filter paper soaked in ketamine solution. On the right, two electrodes, E1 and E2, positioned laterally (inter-electrode distance 0.7 mm). The filter paper soaked with the drug (black square) is beside electrode E2. Small colored circles represent a putative pattern of cells' preferred orientations. 1B. Experimental time course: Black screen was used to record spontaneous activity before and following drug administration. A range of orientations are randomly presented on the screen in 25 trials with arbitrary intervals for evoked cells' responses in control and post-ketamine conditions. 1C. left: typical example of multi-unit recordings of evoked activities for control (above) and drug diffusion (below). Middle, waveforms of a sorted cell spike before and after ketamine application. Right, the auto correlogram of the same sorted cell. 1D. Ketamine diffusion was assessed by recording responses from both electrodes. Gaussian fits of normalized responses of two mouse cells recorded from two sites separated by 0.7 mm. On the bottom left (cell #1), a non-significant shift after ketamine application, while on the bottom right (cell #2, closer to ketamine deposit site), the shift is 48.08°. (For interpretation of the references to color in this figure legend, the reader is referred to the web version of this article.

3.2.1. Ketamine changes orientation selectivity

In mouse and cat, the shift amplitude of preferred orientation was determined from the Gaussian fits. Results in mouse (Fig. 3.2A) show that in a total of 103 cells, only 6 neurons (7.77%) displayed a shift smaller than 5° in preferred orientation, which was statistically not significant (paired sample two tailed t-test, $P < 0.01$), that is, they retained their original preferred orientation. On the other hand, following ketamine administration, most cells (92.23%) shifted their peaks of orientation tuning curves. One typical example is illustrated in Fig. 3.2C (raw data on left, Gaussian on right). The mean shift is 40.03° ± 2.601°. In Fig. 3.2D, an unaffected typical example is illustrated. Fig. 3.2B displays the distribution of shift magnitudes. This distribution does not show a particular bias since shifts are distributed in all classes but mostly between 10°–20° and 60°–70°. Fig. 3.2E shows that ketamine affects cortical orientation selectivity in cat in a manner similar to mouse, since it induces shifts of the tuning curve peaks, as shown in the two examples (left: first cell shifts by 26.83°, right: second cell shifts by 23.04°). Recovery curves are shown in blue. More importantly, this recovery indicates that the observed ketamine effects are reversible.

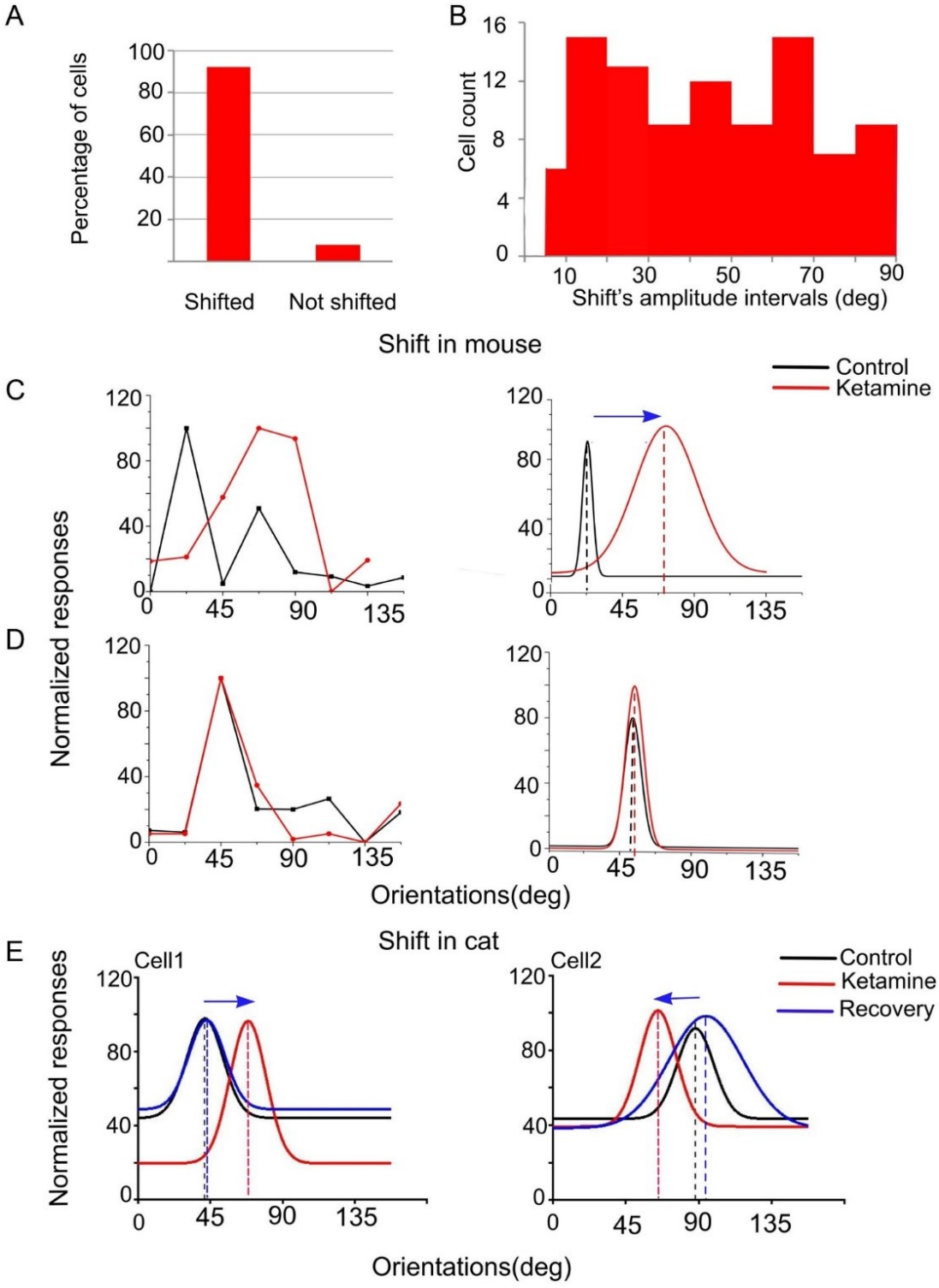

Fig. 3.2. Data from mouse. Modification of orientation selectivity of neurons and percentages of cells shifting (or not) their peak of tuning curves after ketamine application. (A) Percentages of cells depending on their behavior. (B) Distribution of shift amplitudes. (C) Typical example of

optimal orientation shift. Values normalized, 100% corresponds to maximum firing rate measured in each unit, in this and all figures. Raw data (left) and Gaussian fit of normalized responses (right) of one neuron for control (black) and post-ketamine (red) showed that the initially preferred orientation of 23.16° changed to 72.43°. The shift is 49.27°. (D) Results for a different neuron showing the same orientation selectivity after ketamine administration. Raw data (left) and Gaussian fit of normalized responses (right) of one neuron for control (black) and post–ketamine (red) showed that the initially preferred orientation of 53.31°changed to 54.53°. The shift is not significant (1.22° < 5°). (E) Two examples of Gaussian tuning curves showing optimal orientation shifts in cat. The initial preferred orientations were reinstated (illustrated by the blue Gaussian fit). In C, D and E, vertical broken lines indicate optimal orientations, and the horizontal arrowhead stands for the shift of the orientation tuning curve peaks. (For interpretation of the references to color in this figure legend, the reader is referred to the web version of this article).

The following analyses were carried out on mouse data. Fig. 3.2 A to D display representative tuning curves which were generated for each trial (twenty-five) of all presented orientations before and after ketamine application. This figure (Fig. 3.2 left same cell and B-D right same cell) shows examples of shifts of the optimal orientation in all 25 presentations for two typical cells. In A (control condition, total average: 216.4 spikes/bin) and C (after ketamine application, total average: 56.3 spikes/bin) there is a decline of 73.9% of the magnitude of original optimal firing rate, while the firing at the novel optimal orientation (67.5°) almost doubled with averages of 79.3–149.81 spikes/bin (pre-, post-ketamine respectively, 88.6%, Fig. 3.2 C). The second example in Fig. 3.2 (B and D) shows that the initial optimal orientation at 22.5° is virtually abolished with ketamine since the average firing falls from 104.4 spikes/bin to 4.6 spikes/bin, (96.2%). Nevertheless, it is at about 90° orientation that the firing rate becomes highest (9.24 spikes/bin, an increase of 32.4%, relative to pre-ketamine value) in comparison to other presented orientations. (See Gaussian fit inserted above raw values in Fig. 3.2D, broken red line indicates optimal orientation). It may be worth emphasizing that the strongest firing modulations are mostly restricted to preferred orientations. These shifts in optimal orientation are unlikely to be due to spontaneous fluctuations of the preferred orientations since several investigations showed the stability of visual field maps (Wandell et Smirnakis, 2009). Interestingly, the illustrated curves display, in control conditions, a rather unwavering optimal orientation even though the level of discharges may fluctuate.

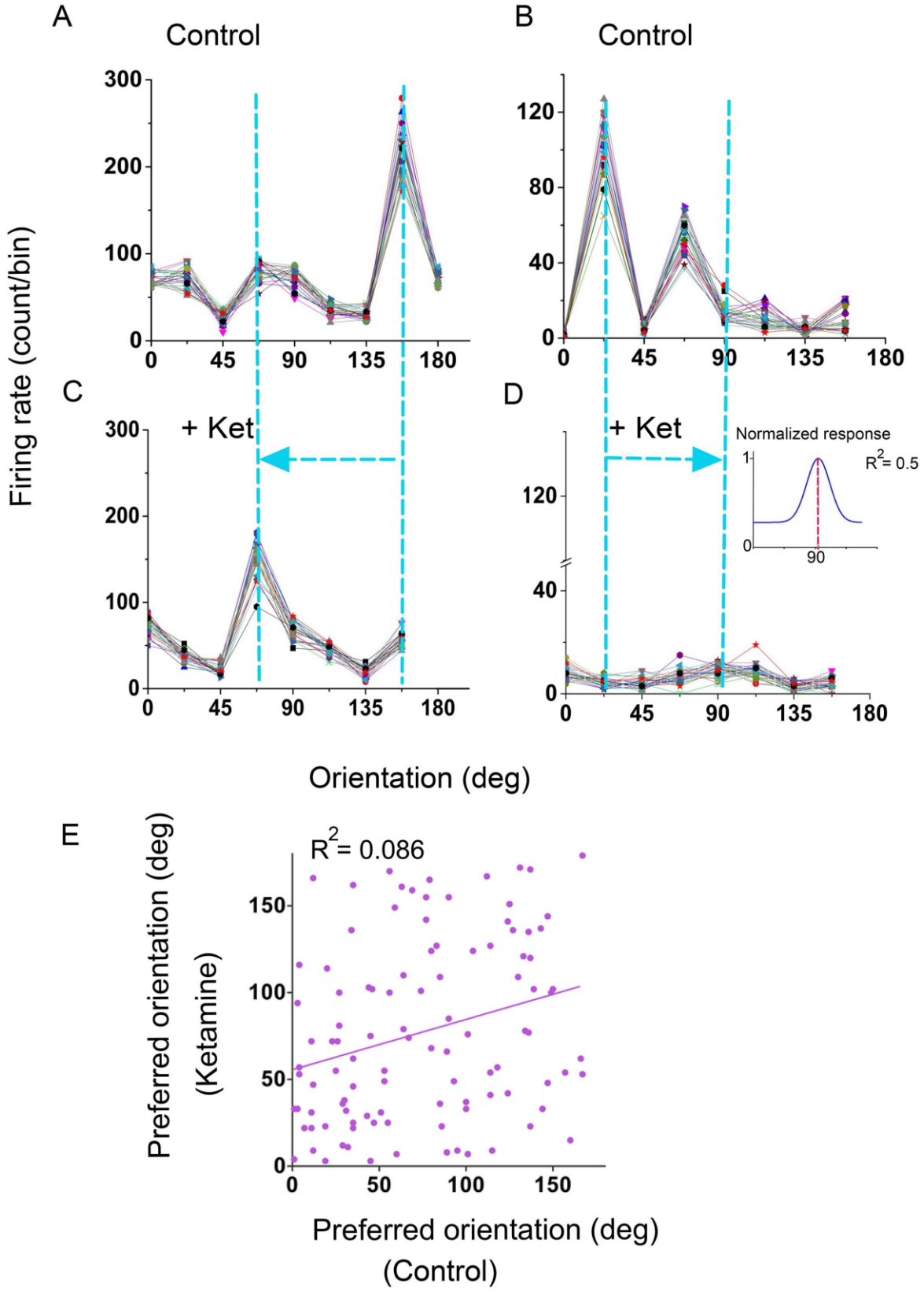
A
Control
B
Control
C
+ Ket
D
+ Ket
Normalized response
R^2= 0.5
Firing rate (count/bin)
Orientation (deg)
E
R^2= 0.086
Preferred orientation (deg)
(Ketamine)
Preferred orientation (deg)
(Control)

Fig. 3.3. The figure shows that in the presence of ketamine the maximum firing rate, evoked by the preferred orientations, drops to the level of non-preferred orientations. The figure illustrates two typical examples of ketamine's impact upon orientation tuning curve in area V1 in mouse. The cell's firing magnitudes displayed in A, B (prior to) and respectively C, D (ketamine) illustrate the orientation tuning curves for every twenty-five presentations of the sine-wave gratings. It is worth emphasizing that in spite of random presentations of orientations the outlines of the tuning curves remain even. As expected, the original optimal orientations (157.5° and 22.5° for cell A and B, respectively) remained unchanged for every application of the stimulus, while the firing rates fluctuated. The bin lasts 4.096s (Fig. 3.3A and 3.3B). Following ketamine application, the first cell shifted its optimal orientation to 67.5° (Fig. 3.3C), and the second cell to 94.37° (Fig. 3.3D); see insert, the red broken line indicates the peak of the tuning curve (Gaussian fit). For the second cell, the tuning curve shows high responses around 90° suggest a broadening of the curve profile (Fig. 3.3D). Furthermore, the responses to the initial optimal orientation diminished considerably in both cells (73.97% for the first cell, and 96.2% for the second cell). Such dual effects in both cells (a decrease of the response at the preferred orientation, and its increase at the acquired new optimal orientation) allude to rather specific effects of ketamine that are circumscribed to specific orientation driven inputs. In this and all figures, vertical broken lines indicate optimal orientations. Horizontal arrowhead stands for the shift of the orientation tuning curve's peaks. Fig. 3.3E: a significant correlation (linear regression function $F = 8.544$, $P = 0.0043$, and Spearman correlation coefficient: $r = 0.2856$, $p = 0.0031$) is observed between the optimal orientation in control and post-ketamine conditions ($R^2 = 0.086$). (For interpretation of the references to color in this figure legend, the reader is referred to the web version of this article).

The low p values of the linear regression function ($F = 8.544$, $P = 0.0043$) and Spearman correlation function (Spearman correlation coefficient $r = 0.2856$, $P = 0.0031$) indicate a significant correlation between the initial preferred orientation and the new one following ketamine administration (Fig. 3.3E). However, the low R square, in regression analysis, shows that the variability of data around the regression line is high. Such large scatter may be due to salt and pepper organization of the mouse visual cortex, that is, cells with different orientations are close to each other. Thus, when one particular cell shifts its original preferred orientation, the initial equilibrium is sufficiently disrupted to induce broad orientation changes in neighboring neurons. Furthermore, very few cells (7.7%) exhibited the original preferred orientation with ketamine application. It is worth mentioning that solvent application did not affect neurons' properties (firing rate and orientation selectivity). Take the example of one single cell with its preferred orientation of 45° and its firing rate for this orientation of 57.84 spikes/bin (4.096 s). Five minutes and one hour following solvent application, the preferred orientation was maintained (45°), and the firing rate was not affected with 54.12 and 58.52 spikes/bin, respectively.

3.2.2. Ketamine does not affect bandwidth but decreases the orientation selectivity index

The tuning bandwidth at half height of each cell was measured from the Gaussian fit. Fig. 3.4A suggests no significant difference between means of bandwidth before and after drug administration (Wilcoxon matched-pairs test: $W = -185.0$, $P > 0.05$).

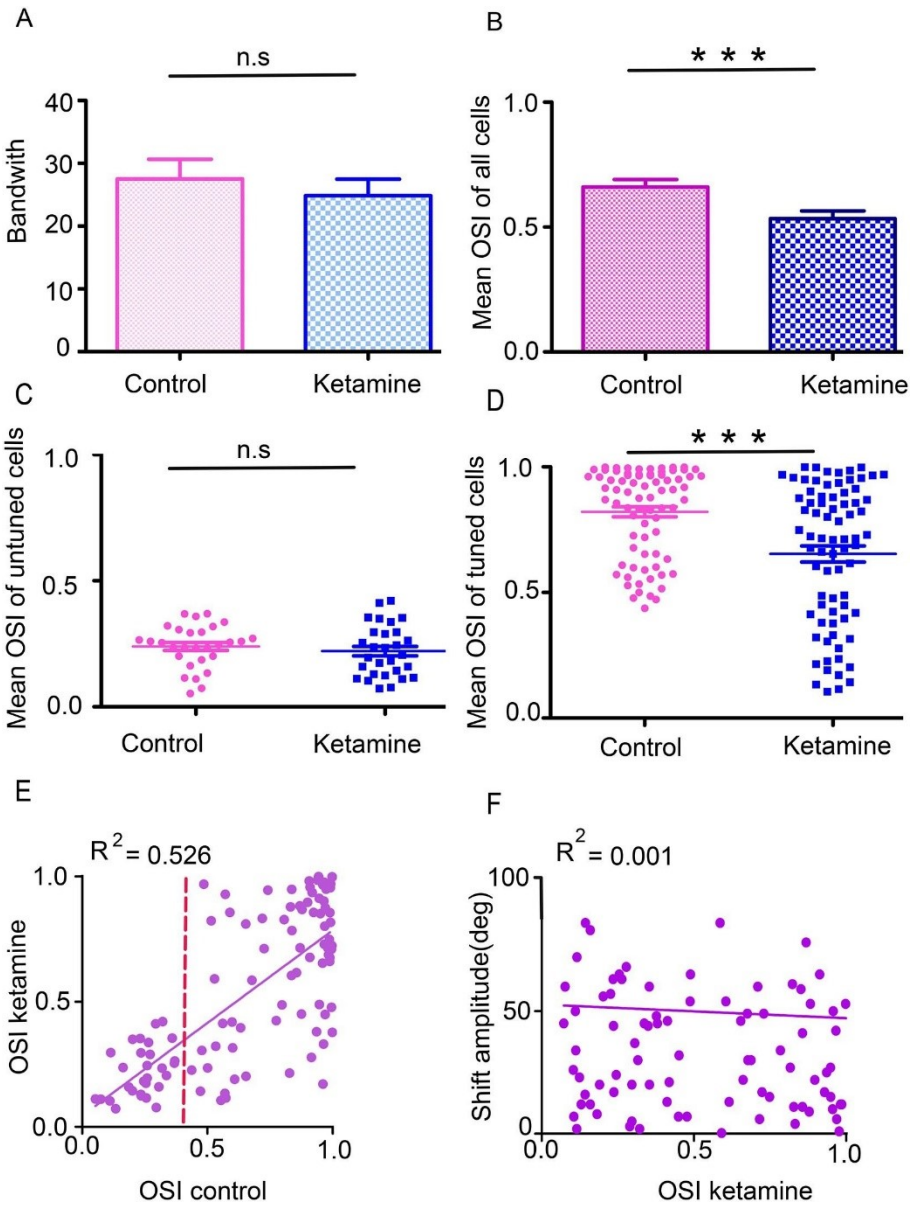

Fig. 3.4. A: Mean of tuning bandwidth at half magnitude (BW) of all the cells used for the present study (n = 103) before (pink) and after (blue) ketamine application. Bandwidths are measured from the Gaussian fit based on the full width at half magnitude (FWHM) to deduce the width of orientation tuning curves of the neurons. No significant difference between the two conditions was

observed. Wilcoxon matched-pairs test was used: $W = -185.0$, $P > 0.05$. Shapiro-Wilk normality test with 95% confidence interval: $p < 0.0001$, for control condition $W = 0.7014$, and for drug condition $W = 0.7244$. 4B: Distribution of neurons according to OSI following ketamine. Mean OSI control decreases after ketamine administration (Wilcoxon paired test: $P < 0.0001$). For A and B, the error bars represent standard errors of mean (SEM), for this and all Fig. 3.4C: A significant correlation between the mean OSI before and after ketamine (linear regression: $F = 114.6$, $P < 0.0001$, Spearman $r = 0.6921$, $P < 0.0001$). $R2 = 0.526$. Vertical broken line indicates the OSI threshold (0.4). 4D: Linear regression function and Spearman correlations show no significant correlation between the two parameters (OSI post-ketamine and shift) after drug administration (linear regression: $F = 0.1986$, $P = 0.6568$), Spearman correlation coefficient: $r = -0.04016$, $P = 0.6842$. $R2 = 0.001$. (For interpretation of the references to color in this figure legend, the reader is referred to the web version of this article).

We calculated the orientation selectivity index (OSI) of each neuron before and after ketamine administration. Out of a total of 103 cells, 2 cells (1.94%) showed no preferred orientation as OSI of tuning curves was inferior to our threshold of 0.4 in control condition but exhibited tuning after ketamine application ($OSI > 0.4$); 25 cells (24.27%) displayed no preferred orientation prior to and following ketamine application. Finally, 16 cells (15.53%) were tuned before drug administration but lost their orientation selectivity with ketamine. The majority of cells (58.25%) retained their tuned property. These results summarize effects of ketamine, they also suggest that the drug may have a broad spectrum of effects on cells' responses and hence properties. It may induce orientation selectivity in cells originally lacking orientation selectivity, and vice-versa. Finally, 25% of neurons remained poorly tuned to orientation in all conditions.

Globally, the mean OSI between control and ketamine conditions was calculated. Wilcoxon paired test shows a significant decrease ($P < 0.0001$) (Fig. 3.4B). To further understand this result, we compared the neurons in two different sub-populations: untuned ($OSI < 0.4$) and tuned neurons ($OSI > 0.4$). Results showed that only tuned neurons were affected by ketamine (untuned population: Paired t-test, $P = 0.3246$; tuned population: Wilcoxon paired test, $P < 0.0001$). It may be argued that the decrease of orientation selectivity is due to neuronal fatigue. However, this appears unlikely since we observed an increase in firing for a novel preferred orientation since peaks of orientation tuning curves shifted. As shown in Fig. 3.4C, linear regression and Spearman correlation show a significant correlation between OSI pre- and post-ketamine (linear regression: $F = 114.6$, $P < 0.0001$, Spearman correlation coefficient $r = 0.6921$, $P < 0.0001$). The interrupted vertical line indicates the OSI threshold. It appears that units within this limit sustain their lack of

orientation preference. Fig. 3.4D illustrates that the shift magnitude was uncorrelated to the OSI with ketamine on a cell-by-cell basis. In summary, ketamine application leads to a selective decline of orientation selectivity index in tuned cells, suggesting that in these cells the new preferred orientation is not as dominant as the original one; however, the neuron seems to retain its functional range of orientation.

3.2.3. Ketamine induces more regularity of neurons' firing rate

Neural variability of spike firing is analyzed by the Fano factor (F), which was calculated for each neuron. Bin counts were carried out in a sliding window over the duration of the trial (4.096 s). It is assumed that a Fano factor value greater than one is an indication of cross-trial firing-rate variability (Buračas et al., 1998). Fano factor modulations are interpreted as reflecting changes in the response variability between trials. Hence, the larger the Fano factor is, the bigger the variability of the neuronal response, and vice versa. To begin, we compared the Fano factor values across our various steps: control, ketamine application, black screen (spontaneous activity), and grating presentations. The comparison of evoked response variability before and after ketamine application shows that the mean F value during ketamine application decreases significantly (Mann Whitney $U = 2575$, $P < 0.0001$). This decline of variability may suggest more regularity in cellular responses (Fig. 3.5A). In this analyses F is calculated for all responses to all orientations. The overall variability is larger since OSI is greater prior to ketamine application (this is the consequence of the fact that firing to optimal orientation is much higher than to non-optimal orientation). During ketamine presence, the OSI is smaller, implying that the difference between response magnitudes to orientations is much weaker, hence the variation is smaller. Interestingly, the mean difference of F values of spontaneous activities calculated before and during ketamine application remains insignificant (Mann Whitney test: $U = 4223$, $P > 0.05$) (Fig. 3.5B). This reveals that ketamine doesn't affect the spontaneous firing variability and its effect is not global, but is targeted to evoked responses, which result from neurotransmission. Moreover, Fig. 3.5D demonstrates that following ketamine application the mean F value of spontaneous and evoked firing remains similar (Mann Whitney test: $U = 3860$, $P > 0.05$), while these values were significantly different in control condition (Fig. 3.5C) (Mann Whitney test: $U = 2775$, $P < 0.0001$). This suggests that ketamine affects variability of neuronal discharges differently in relation to evoked and spontaneous firing. It is worth noting that the F of cortical neurons firing rate in vivo doesn't fluctuate. Indeed, F in V1 neurons as in all cortical neurons is consistently found to be near

or above one (Buracas et al., 1998; Gershon et al., 1998). For example, neurons from the middle temporal area of alert monkeys were reported to have an F of 1.3 (Buracas et al., 1998). Thus, the decrease following ketamine cannot be attributed to regular spontaneous fluctuations.

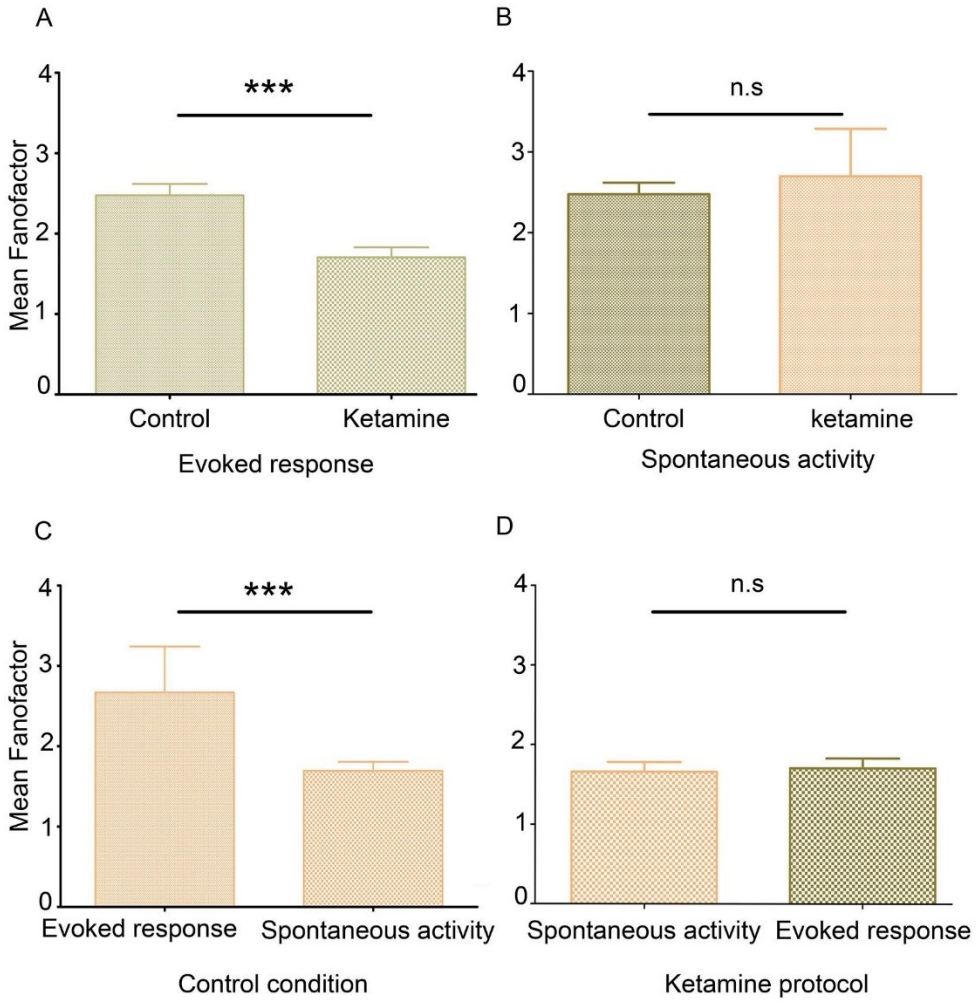

Fig. 3.5. Effect of ketamine application on neurons' variability response characterised by Fano factor (F). 5A and 5B show a significant decrease (Mann Whitney $U = 2575$, $P < 0.0001$) or not (Mann Whitney test: $U = 4223$, $P > 0.05$) of the mean F after ketamine application on evoked response and spontaneous activity, respectively. Fig. 3.5C and 3.5D show a significant difference (Mann Whitney test: $U = 2775$, $P < 0.0001$) or not (Mann Whitney test: $U = 3860$, $P > 0.05$) of the mean of F between spontaneous and evoked activities in control condition and following ketamine application, respectively.

3.3. Discussion

The major findings of the current study are that ketamine leads to shifts in the optimal orientation of neurons, and that it induces less sharp orientation selectivity. In addition, F computations indicate that ketamine reduced variability of evoked responses, increasing firing stability, and, interestingly, not the spontaneous activity.

3.3.1. Ketamine changes preferred orientation

Results show that most cortical orientation-tuned cells displace their peaks of tuning curves in the presence of ketamine. It seems that ketamine, an NMDA non-competitive antagonist, locally modifies the orientation preference map. This type of shift may be explained by results reported in mouse (J. M. McNally et al., 2013). In this study it was shown that chronic ketamine elicits behavioral effects and structural alterations of cortical interneurons similar to those observed in schizophrenia. Such outcomes are mediated by local circuit structural alterations in the prelimbic cortex, suggesting that similar effects might occur in V1. It was also shown that in rats N-methyl-d-aspartate receptor (NMDAR) antagonists induced a decrease in glutamic acid decarboxylase (GAD67), a key enzyme for γ-aminobutyric acid (GABA) synthesis. This reduction in GAD implies a decrease in functional inhibition(Zanos et Gould, 2018). It appears that NMDAR blockade changes the balance between excitation and inhibition in the cortical circuitry (Homayoun et Moghaddam, 2007). Therefore, the decrease of local inhibition may induce the activation of an alternate group of orientation driven synapses resulting in the optimal orientation shifts. Hence, ketamine might produce a change in synaptic weights leading to the emergence of a different synaptic cluster allowing new orientation selectivity. Furthermore, ketamine exerts a very specific effect since it targets a narrow range of orientations, although globally the OSI decreases. Additionally, our data suggest that synaptic weight fluctuations are occurring within a relatively brief time window. Very recently it was demonstrated that ketamine restores eliminated spines (Moda-Sava et al., 2019). Our data further complement these results as they suggest an increase of synaptic efficiency which results in the emergence of a novel selectivity. Shifts may be attributed to decrease of the cell's responsiveness to its dominant orientation by the blockade of NMDAR. Several processes may be involved in these changes such as spike thresholds, intracortical excitation, and intracortical inhibition (Atallah et al., 2012; Douglas et Martin, 2007;

Priebe et Ferster, 2008). It should be noted that the shifts of orientation tuning curve peaks, induced by ketamine application, were observed on V1 mouse and cat neurons, suggesting that it is a process that may be occurring in other mammals as well.

It has previously been demonstrated that shifts of optimal orientations and spatial frequencies are of cortical origin (Bachatene, Bharmauria, Rouat, et al., 2012; Bouchard et al., 2008). We call these orientation shifts plasticity since cells acquire a novel preferred property. Of course, the modification of neuronal selectivity may be related to changes to cellular properties caused by ketamine, yet the acquisition of a novel orientation selectivity may be defined as a plastic change since the neurons gained a novel and unique preferred characteristic. Furthermore, this drug might induce visual plasticity by a different pathway than glutamatergic. This visual plasticity following ketamine application is supported by the results of several recent studies (Aleksandrova et al., 2017; Zanos et al., 2016) suggesting that synaptogenic signaling of mTOR (mechanistic target of rapamycin), BDNF (brain-derived neurotrophic factor), and protein synthesis through EEF2 dephosphorylating (eukaryotic elongation factor 2), increases following ketamine application (Autry et al., 2011; Lepack et al., 2015; Park et al., 2015). Given their respective molecular operations, the activation of these different classes of molecules after ketamine application have permitted the restoration of synaptic strength, connectivity, and, hence, plasticity in the hippocampus and prefrontal cortex (Zanos et al., 2016).

Our results suggest that 26.21% of examined cells were untuned; among this group of cells, 7.4% became tuned following ketamine application. This large proportion of cells that are weakly tuned is compatible with previous studies (Jeyabalaratnam et al., 2013b) and might be explained by the fact that cortical cells in mouse are driven by afferent axons displaying a large spectrum of orientations (Jia et al., 2010). However, following ketamine application, the same cells showed quite strong orientation tuning, even though the same gratings were presented. Such emergence of orientation selectivity suggests that ketamine allows one specific orientation to strengthen its drive over the other inputs. This effect may be due to a local disinhibition which increases pyramidal activities and in turn results in an acquisition of novel orientation selectivity. Previous investigations suggested that NMDAR blockade leads to increased excitability of pyramidal neurons (Homayoun et Moghaddam, 2007). It is important to emphasize that our results are not global for all untuned cells. One possibility to reconcile this result is that the number and the

subunit composition of NR1 and either NR2A or NR2B, C or D subunits of the NMDA receptor varies in cortical cells, and it is the blockade by ketamine that leads to differential effects. Ketamine is not selective for the NR2A, C or D subunits of the NMDA receptor (Avenet et al., 1997). However, other investigation shows that ketamine is mediated by the NMDARs containing the NR2A subunit (Narita et al., 2001). In addition, in contrast to the blockade of NR1/NR2A subunit of the NMDAR by ketamine that induces critical changes in gamma activity; the blocked of NR2B-2D subunit-containing receptors have negligible effects(Kocsis, 2012). Furthermore, investigations show that the threshold for synaptic modifications is regulated by the NR2A:NR2B ratio (Chen et Bear, 2007; Sawtell et al., 2003; Tongiorgi et al., 2003). It is unlikely that response modulations (acquisition of orientation selectivity for some untuned cells and the shift of the preferred orientation for some other tuned cells) reported in the present study are due to a sudden surge of electrical activity and not to ketamine effects, because our data showed that, in parallel to the decrease of responses to the initial preference, cells exhibit an increased response to a new orientation preference, which is incompatible with a global fluctuation and uniform modulation of firing rates. In addition, the post-ketamine preferred orientations are roughly correlated to the initial preferred orientations which is irreconcilable with a random modification of evoked responses.

3.3.2. Ketamine decreases both OSI and the variability of evoked responses

As stated earlier, individual neurons in mouse V1 receive inputs that are tuned to widespread orientations, and the overall orientation preference is determined by the integration of the large spectrum, tuned synaptic inputs (Jia et al., 2010). To assess the degree of orientation selectivity, and the variability of neurons' activities, we used the orientation selectivity index (OSI) (Niell et Stryker, 2008) and the Fano factor (F), a standard measure of firing variability, for both control and following ketamine conditions. Interestingly, across our sample population of recorded neurons, average orientation selectivity (OSI) and average response variability (F) were consistently lower following ketamine than in control condition. It appears that the functional significance of the decrease of both OSI and F is that ketamine locked the local circuit involved in the orientation selectivity. It seems that synaptic connections govern the establishment of the orientation selectivity in the cortex. This assumption is supported by a study demonstrating that the maturation of orientation-selective responses in ferret primary visual cortex requires cortical

neuronal activity (Chapman et Stryker, 1993). Since ketamine, as cited above, mostly deteriorates the original synaptic connections established during the critical period (J. McNally et al., 2013), it leads to lower OSI. It was also shown that orientation selectivity depends on the balance between excitation and intra-cortical inhibition (Atallah et al., 2012; Katzner et al., 2011; Priebe et Ferster, 2008). Furthermore, recent studies have shown that ketamine induces dysfunction of a subset of cortical fast-spiking inhibitory interneurons with loss of expression of parvalbumin phenotype in GABAergic interneurons (PV) (Behrens et al., 2007; Featherstone et al., 2012). These changes cause disruption in local neuronal ensembles (Hamm et al., 2017), which suggests that ketamine, by modulating the number or the synaptic efficacy of dendritic spines, decreases orientation selectivity. Our results are consistent with a recent investigation at the single cell level showing that chronic ketamine application decreased OSI values due to disinhibition, leading to larger calcium transients and reduced orientation selectivity (Hamm et al., 2017). The same study revealed that pharmacogenetic suppression of PV interneurons or acute ketamine injection inducing blockade of NMDARs was sufficient to disinhibit neuronal activity at similar levels as chronic ketamine application. It is worth mentioning that there is a relationship between the original map and the new selectivity, and this might lead to perceptual changes. Along this line, in humans it has been shown that orientation or contrast adaptation degrades test gratings discrimination (Regan et Beverley, 1985), and these effects increase along the hierarchy of visual areas (Boynton et Finney, 2003). Indeed, adaptations by modifying orientation selectivity lead to a reorganization of orientation cortical maps in V1 in adult cat (Cattan et al., 2014). Furthermore, the correlation between OSI before and after ketamine could explain the modifications of visual perception, since it has been shown in humans that ketamine (injected intravenously) modifies neural detection of object identification (van Loon et al., 2013). Our results indicate that F values decreased following ketamine protocol, which reflects an increase of firing regularity in response to different inputs. It has been shown that in adult anesthetized rats, neocortical neurons fire highly irregularly to constant sensory stimulation, but in slice preparations, they fire regularly in response to constant current injection (Stevens et Zador, 1998). The authors set out to study the source of this large firing variability and they argue that it arises from the synchronous arrival of inputs from many neurons. Since variability diminishes with ketamine, this might be attributed to decline of synchrony. This assumption is supported by above cited data (Hamm et al., 2017) revealing that ketamine actions disrupt synchrony, and strengthen/weaken functional correlations at the network

level. We provide some evidence that ketamine changes neurotransmission, disrupting existing functional ensemble patterns in the cortex since the drug affects almost selectively evoked responses rather than spontaneous discharges (Fig. 3.5 A, B and Fig. 3.3).

Our results, together with recently accumulating evidence from above studies, suggest a critical (if not primary) role of glutamatergic synaptic deficits in the decrease of orientation selectivity, the depression of the output variability and perhaps synaptic stability and plasticity. Since ketamine modifies the preferred orientation of visual neurons established during the critical period of development, we conclude that it induces plasticity in V1 neurons that might be operated by a different pathway than NMDAR.

3.4. Experimental procedure

3.4.1. Ethical approval

The animal surgery and electrophysiological recording procedures were performed on the primary visual cortex of CD-1 strain adult mouse and adult domestic cat (*Felis catus*) and followed the guidelines of the Canadian Council on Animal Care and were approved by the Institutional Animal Care and Use Committee of University of Montreal. Animals were provided by the Division of Animal Resources of University of Montreal.

3.4.2. Animal preparation

CD-1 strain adult mouse (19 mice 28–31 g and aged from 9 to 11 weeks) were used in this study and prepared in conventional fashion. In order to record from the primary visual cortex, a general anesthesia was achieved with 10% urethane (1.5 g/kg) injected intraperitoneally. Lidocaine hydrochloride 2% (Xylocaine) was injected subcutaneously as a local anesthetic at surgical and pressure sites. To evaluate the proper depth of anesthesia, pinch reflexes were applied throughout the duration of the experiment. Animals were then placed in a custom-made stereotaxic apparatus allowing visual stimulation of the entire contralateral visual field; the skull was fixed in a head holder. A heated pad was used to maintain an optimal body temperature. Craniotomy was carried out (dissection of the skull and dura mater (2.5 × 2.5 mm) over the visual cortex). A thin layer of silicone oil was applied on the mouse's stimulated eye to prevent drying the cornea, allowing a clear optical transmission. The unstimulated eye was closed. Within the period of recordings eye

movements were negligible. At the end of each experiment, a lethal dose of urethane was injected intraperitoneally in order to euthanize the animals.

The cat preparation was conventional and described in detail in our previous publications (Bachatene et al., 2013). Briefly, adult cats were initially anesthetized with acepromazine maleate (1 mg/kg, i.m., Atravet; Wyeth-Ayerst, Guelph, ON, Canada), atropine sulfate (0.04 mg/kg i.m., ATRO-SA; Rafter, Calgary, AB, Canada) and ketamine hydrochloride (25 mg/kg, i.m., Rogarsetic; Pfizer, Kirkland, QC, Canada). The general anesthesia was achieved with isoflurane (0.5% AErrane; Baxter, Toronto, ON, Canada) and a mixture of N2O/O2 (70:30). The pupils were dilated with atropine sulfate (1%, Isopto-Atropine; Alcon, Mississauga, ON, Canada) and plano contact lenses with artificial pupils (5 mm diameter) were placed on the cat's eyes. Recording electrodes were lowered in V1. It must be emphasized that cat recordings were carried out solely to replicate mouse experiments with the intention to see if ketamine induces the same effects in both species, namely shifts of the peak of orientation tuning curves. All analyses were carried out on data obtained from mouse.

3.4.3. Experimental steps

Fig. 3.1 illustrates key experimental steps. In A (left) the black square on mouse cortical surface schematizes the positioning of the custom-cut filter paper (1 × 1 mm) soaked in ketamine (see below), while the red dot underlines electrode penetration site. On the right, we illustrate the degree of the drug dispersion. Two electrodes were positioned laterally (inter-electrode distance 0.7 mm). The strip of filter paper impregnated with ketamine was placed beside electrode E2 (black square). Section B (Fig. 3.1) displays experimental phases: control recordings of the orientation tuning curves (including spontaneous activity: dark screen). This phase is followed by drug application, during which orientation selectivity tests are repeated. In C (Fig. 3.1) multi-unit activity in the primary visual cortex was recorded with two glass microelectrodes (inter-electrode spacing <1 mm) filled with saline (0.9% NaCl used as solvent) inserted in V1. Evoked and spontaneous extracellular neuronal activities were recorded from superficial layers at an average cortical depth of less than 1 mm (Fig. 3.1A). The signal from the microelectrode was band-pass filtered (300 Hz–3 kHz), amplified, displayed on an oscilloscope, and audio-monitored, then digitized and recorded with data acquisition software (Spike 2, Cambridge Electronic Design, CED Limited, Cambridge, England). Action potentials were sorted using the off-line spike sorting method which is based on

cluster classification in reduced space. Visual control of the cluster disposition and the waveform shape were required to verify qualitatively the stability of each cell's activity across conditions (Fig. 3.1C middle). Auto-correlograms showing a total depression at its center (deep at zero) was systematically carried out to ensure proper single-cell capture (Fig. 3.1C right). Since the excitatory receptive field in mouse is rarely smaller than 10° (Mangini and Pearlman, 1980), the recording of the multi-unit electrical signal doesn't require making any attempt to stimulate the receptive fields. The stimulating grating covered 157.5° of the mouse monocular field. In part D we show that diffusion of ketamine application remained limited to a radius less than 1 mm. Two electrodes (E1 and E2) were lowered with inter-electrode distance of 0.7 mm. Gaussian orientation tuning curves recorded simultaneously indicated that under the ketamine application (electrode at E2) the peak of the tuning curve shifted by 48.08°; in contrast, 0.7 mm away (E1) yielded two almost identical tuning curves, as the crest of both curves were close to each other, suggesting that the drug did not reach this recording site. In cat, the gratings were positioned within the receptive fields of the cells.

3.4.4. Visual stimulation protocol and drug administration

For the entire study, stimulation was monocular, the eye screen-distance was 30 cm, the visual stimuli were generated with a VRG Volante 34,020 graphic board (Vision Research Graphics, New Hampshire, USA), and displayed on a 21-inch monitor (60 Hz refresh rate, Mitsubishi FHS6115SLK Color Display Monitor, Tokyo, Japan) with 1024 × 512 pixels placed 30 cm from the mouse's eye. Parameters of stimulus (contrast at 80%, mean luminance at 40 cd/m2, spatial and temporal frequency set within 0.1–0.5 cycles/deg and 1.0–2.0 Hz respectively, velocity and temporal frequency at 4 °/s and 0.07 cycles/deg respectively) were set to evoke optimal responses and were maintained constantly throughout the duration of the experiment. The center of the monitor was positioned at about 30.7° azimuth, 0° elevation. The blank screen was uniformly gray (35 cd/m2) and applied for recording spontaneous activity in blocks of 25 trials lasting 4.096 s each with a random inter-trial interval (1.0–3.0 s). Spontaneous activity was recorded using a blank black screen (Fig. 3.1B). In cat experiments, sine-wave patches were placed in the cellular receptive field characterized manually (contrast 80%, mean luminance 40 cd/m2, 0.1–0.5°; 1.0–2.0 Hz, values chosen to evoke best responses).

Eight orientations equally spaced with a 22.5° interval between orientations were selected and applied for this study, covering a span of 157.5°. Test orientations were used in a random order. Each oriented stimulus was presented in blocks of 25 trials lasting 4.096 s each, with a random inter-trial interval (1.0–3.0 s) during which no stimulus was presented. Thus, a recording session lasted for 40–50 min. Once control orientation tuning curves were characterized, ketamine was applied in a fashion as described in (Bachatene et al., 2013), using a custom-cut filter paper (1 × 1 mm) soaked in 10 mM ketamine and applied topically on the cortical surface, next to the recording site. Multi-unit activity before and five minutes after ketamine application were recorded (Fig. 3.1C left). Thereafter, we aimed to test the degree of substance dispersion. Since both electrode sites are presumably being affected similarly by the solvent (0.9% NaCl) as well as ketamine, and to be sure that the effect (if there is) on the recordings is indeed due to ketamine; we placed a strip of filter paper impregnated with only solvent over the cortex. Neuronal responses were recorded before, five and 60 min after the solvent application. For cat, the drug was applied as described above in mouse. Spontaneous activity was recorded using a blank black screen. The electrophysiological recordings of evoked responses, the visual stimulation in control condition and following ketamine application were performed based on the methods of our previous publication (Bachatene et al., 2013). Following a recovery period, test orientations were applied in random order. Thus, recovery tuning curve measurements were performed.

3.4.5. Data analysis

For cat and mouse, once single cells were sorted out off-line from the multi-unit activity recorded during data acquisition, in all steps of the protocol, orientation tuning curves of spontaneous and evoked response in control and following ketamine administration were constructed from the raw data derived from peri-stimulus time histograms (PSTH) which provided cellular firing rates. Because the 22.5° interval between the stimulus orientations is large, tuning curves derived from raw data may be imperfect. In order to determine the preferred orientation of neurons with precision and then to measure shifts in orientation preference, orientation tuning curves were fitted by using the Gaussian function. Since orientation tuning is best described with Gaussian-like functions, we fitted our raw data with the von Mises function (Kohn et Movshon, 2004; Mangini et Pearlman, 1980; Swindale, 1998). The von Mises function is defined as:

$$M(\Theta) = A.e^{b[\cos(\Theta - c)]} + d$$

where A is the value of the function at the preferred orientation, c, and b is a width parameter. An additional parameter, d, represents the spontaneous firing rate of the cell (Kohn et Movshon, 2004; Mangini et Pearlman, 1980). In the aim of ensuring that cells in our sample were properly tuned for orientation we analyzed cells whose tuning fitted well with the von Mises function over the (157.5°) range of stimulus orientations. A fit was considered satisfactory if it accounted for at least 80% of the variance in the data. Other cells were considered as untuned.

For all of the next section, data analysis concerns only mouse.

We measured also an orientation selectivity index (OSI) by dividing the minimum firing rate (baseline of the tuning curves) by the firing rate for the preferred orientation, and subtracting the result from 1 (Ramoa et al., 2001a). The closer the OSI is to 1, the stronger the orientation selectivity. Thus, a small baseline/preferred orientation ratio implies that the firing rate at the preferred orientation is much greater than the baseline firing rate, and vice versa. OSI values were measured from fitted data; therefore, the figures presented in the results section are from fitted data. To compare the mean OSI between control, and post-drug administration, a Wilcoxon paired test was performed with a significance level of 95% (Shapiro-Wilk normality test with $P < 0.0001$, $W = 0.8741$ OSI pre-ketamine, $W = 0.9017$ OSI post-ketamine). In addition, regression and Pearson correlation function with 95% confidence interval were used to test potential correlation between OSI pre- and post-ketamine.

The distance between peak positions of the fitted tuning curves pre- and in the presence of the drug allowed measuring ketamine-induced shifts. The shifts of peaks of tuning curves between pre-and post-ketamine conditions were calculated from the Gaussian fits using following formula:

$$\textbf{Shift} = |\boldsymbol{XC}\ \textbf{post} - \boldsymbol{XC}\ \textbf{pre}|$$

Where XC is the central value derived from the Gaussian fit. Only shifts larger than 5° in preferred orientation were statistically significant (paired sample two tailed t-test, $P < 0.01$) (Ghisovan et al., 2008).

Another parameter: the tuning bandwidth at half magnitude was calculated based on the full width at half magnitude (FWHM) of the Gaussian fit for each cell (Ringach et al., 2002).

$$\text{FWHM (Bandwidth)} = 2\sqrt{2\text{In}2}\,\text{c} = 2.35482\text{c}$$

where In is the logarithm and c is the Gaussian root mean square width. Wilcoxon paired tests were carried out to verify the significance of the differences between control and drug condition. Linear regression function with 95% confidence interval was used to verify a potential correlation between the OSI and ketamine–induced shift. Moreover, other regression and Spearman correlation functions with 95% confidence interval were used to test potential correlation between the preferred orientation pre- and post-ketamine.

To assess and describe the variability of a neuron's response, a Fano factor (F) was calculated for each neuron by dividing the variance by the mean of firing rate of this neuron as following:

$$\text{F} = \frac{\sigma_{\text{W}}^2}{\mu_{\text{W}}}$$

where σ^2_W the variance and μ_W is the mean of a random process in some time window W. The smaller the Fano factor value, the less neuronal response will vary. The Whitney test (95% confidence limit) was used to compare on the one hand, the F of spontaneous firing activity before and after ketamine application, and on the other hand, the F of evoked firing response before and after ketamine application. With the same statistical test, we compared the spontaneous activity to the evoked one for each neuron in the two conditions (pre- and post- ketamine).

All statistical tests described in the results were chosen after using the Shapiro-Wilk normality test with 95% confidence limit and were computed using the numerical software GraphPad Prism version 5.03 (GraphPad Software Inc., CA, USA).

Acknowledgments

We acknowledge the Conseil de Recherche en Sciences Naturelles et en Genie du Canada (CRSNG) to support the completion of this study and Steve Itaya for his comments of the early version of the manuscript

4. Ketamine promotes adaption-induced orientation plasticity and vigorous network changes

Ouelhazi A, Lussiez R, Molotchnikoff S

Publié dans : Brain Research, vol 1797 December 2022, 148111

Numéro CDEA : **20-068**

Rôles des auteurs :

Conceptualization, A.O.; Methodology, A.O. and R.L.; Software, A.O.; Validation, O.A., and S.M.; Formal Analysis, A.O.; Investigation, A.O.; Resources, A.O., and M.S.; Data Curation, A.O.; Writing Original Draft, A.O.; Writing – Review & Editing, A.O., and S.M.; Visualization, A.O.; Supervision, S.M. and O.A.; Project, S.M.; Funding Acquisition, S.M. and NSERC Canada.

https://doi.org/10.1016/j.brainres.2022.148111

Graphical Abstract Text:

Electrophysiological recordings in cat and mouse V1 reveal that ketamine influence depends on the post-adaptation shift amplitude. It alters the orientation selectivity acquired following adaptation and induces plasticity in the primary visual cortex in both species, even though they exhibit different organization of V1. In addition, ketamine adjusts the configuration of involved connectomes.

Image: Ketamine affects post-adaptation shifts according to the amplitude and reorganizes pre-existing neuronal networks

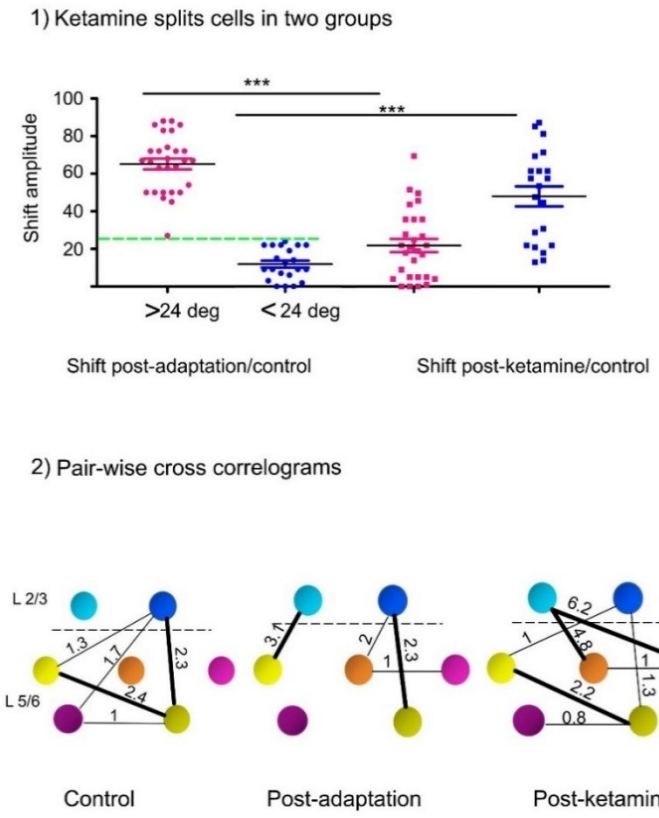

Abstract

Adult primary visual cortex features well demonstrated orientation selectivities. However, the imposition of a non-preferred stimulus for many minutes (adaptation) or the application of an antidepressant drug, such as ketamine, shifts the peak of the tuning curve, assigning a novel selectivity to a neuron. The effect of ketamine on V1 neural circuitry is not yet ascertained. The present investigation explores (in control, post-adaptation, and following local ketamine application) the modification of orientation selectivities and its outcome on functional relationships between neurons in mouse and cat. Two main results are revealed. Electrophysiological neuronal responses of monocular stimulation show that in cells exhibiting large orientation shifts after adaptation, ketamine facilitates the cell's recovery. Whereas in units displaying small shifts following adaptation, the drug increases the magnitude of orientation shifts. In addition, pair-wise cross correlogram analyses show modifications of functional relationships between neurons revealing updated micro-circuits as a

consequence of ketamine application. We report in cat but not in mouse, that ketamine significantly increases the connectivity rate, their strengths, and an enhancement of neuronal synchrony.

Key words:
Cross correlation, Ketamine, Orientation selectivity, Plasticity, Synchrony, Visual adaptation

4.1. Introduction

Cortical plasticity is a foundational brain function associated with development, memory, learning, and recovery from injuries. Investigations of plasticity have shown that neurons may change their stimulus selectivity following appropriate experimental interventions, such as adaptation (imposition of a non-preferred stimulus for several minutes) (Dragoi et al., 2000; Dragoi, Turcu, et al., 2001). At the single cell level, adaptation outcome can be measured as shifts of peaks of orientation tuning curves after testing the neuron with an adapter from several seconds to a few minutes. The consequence of modifying orientation selectivity (OS) is a reshuffling of cortical orientation maps (Cattan et al., 2014; Dragoi, Turcu, et al., 2001; Kohn, 2007). Interestingly and comparably, OS is modified by the local application of drugs such as fluoxetine (a selective serotonin reuptake inhibitor) (Bachatene et al., 2013; Benfield et al., 1986; Fuller et al., 1991), and ketamine (a non-competitive glutamatergic NMDAR (N-methyl-D-aspartate receptor) antagonist) (Church, 1990; Ouelhazi et al., 2019). NMDARs are required in the rapid processing of continuous visual inputs and for the faithful neuronal firing to sensory stimulation. In addition, by mediating Ca2+ ion influx (Sobczyk et al., 2005) and their coupling to intracellular signaling partners (Barria et Malinow, 2005), NMDARs are implicated in many forms of synaptic plasticity (Malenka et Bear, 2004). Changes of the receptor attributes or its blockage are likely to influence synaptic transmission and thereby alter the encoding of stimuli.

As neurons change their selectivities, it is conceivable that their distinctive functional relationships are modified. Cross-correlograms (CCGs) between spike trains of identified neuronal pairs is a tool revealing these functional relationships in a cell assembly (Denman et Contreras, 2014; Fujisawa et al., 2008; Malenka et Bear, 2004; Perkel et al., 1967). It is hypothesized that synaptic strength corrections may possibly support cortical map reorganization and reveal changes of dynamic functional connectivity (Alloway et Roy, 2002; Wise et al., 2010). Yet, the relations between orientation shifts, and inter-neuronal functional interactions have not been investigated.

The aims of the current paper are twofold. 1) We investigated the effects of local ketamine application on the adaptation-induced OS shifts in mouse and cat, which display salt-and-pepper and columnar organizations, respectively; that is, we explored the effect of ketamine on visual adaptation. 2) The second goal was to study the dynamics of the functional networks in V1 when ketamine is applied, and to look for drug induced network changes. Following adaptation, we split cells into two groups according to the amplitude of the post-adaptation shift, and the effect of ketamine is different between the two groups: in cells displaying large post-adaptation shifts, the drug reverts the orientation tuning curve toward its original value, whereas in neurons weakly affected by adaptation, ketamine strengthens the shifts. The specific changes of OS are suggestive of a reorganization of cortical orientation networks which are supported by an enhancement of spiking synchrony. Indeed, these novel results show that under ketamine influence neurons' spiking activity is more correlated and synchronized in cat, but not in mouse. The acquisition of a new selectivity, following adaptation or local ketamine application, might be attributed to pair-wise relationship dynamics. A supplementary effect of ketamine is enhanced neuronal synchronization which may influence the orientation discrimination in cat.

4.2. Results

We performed extracellular recordings in V1 of adult anaesthetized mouse and cat. Neuronal activity was measured in response to orientated gratings in control, after adaptation, and after ketamine application. The schematic and steps of the experiment are displayed in Fig. 4.1.

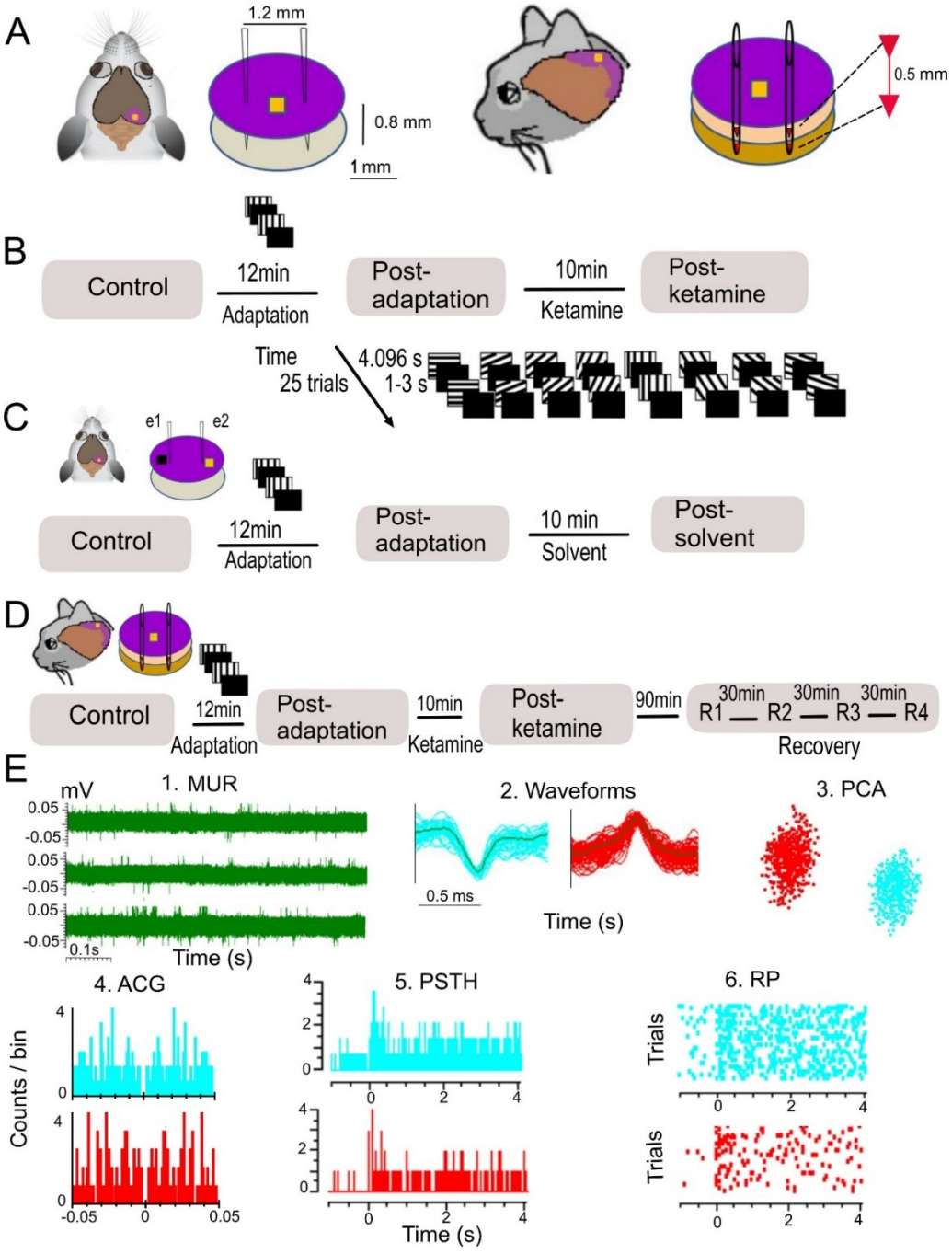

Fig. 4.1 A schematic of the experiment protocol and neuronal spike sorting method. (A) Presentation of the positioning of electrodes, the inter-electrode distance (1.2 mm) and recording depth in mouse (left) and cat (right). In cat, two depths (inter-electrode distance 0.5 mm) for layers 2/3 and 5/6 (area 17) in which electrode tips contact V1 are shown. Ketamine deposit site is shown by the yellow square. (B) Cartoon of sine-wave drifting gratings presented in a random fashion on the screen in 25 trials with arbitrary intervals in control, after 12 min of exposure to 90° (adaptation), and after 10 min of acute ketamine application. (C) Ketamine diffusion was assessed

in mouse by recordings from two electrodes (e1 and e2) 1.2 mm apart in control condition, post-adaptation, and after 10 minutes of solvent application closer to e1 (black square) or ketamine application closer to e2 (yellow square). (D) To test if the observed effect of ketamine is reversible or not, four recovery periods were performed in cat (the first recording was done 90 minutes following the post-ketamine phase and the three other recordings were performed every 30 minutes). (E) Spike sorting analysis. (E1): Example of the multi-unit recordings (MUR) for control (above), post-adaptation (middle), and drug diffusion (below) conditions. Two cells (cyan and red units) sorted from a MUR. Neurons have distinct waveforms (E2) and well-dissociated clusters (E3). (E4) corresponding autocorrelograms (ACG), (E5) peri-stimulus time histograms (PSTH), and (E6) raster plots (RP), for both isolated neurons are displayed.

The focus of the current investigation was to examine if acute ketamine application influences the neuron's orientation preference induced by visual adaptation and, if it is the case, how it affects the functional neuronal connectivity. In total, 95 tuned cells were sorted in mouse (over a total of 175 cells), 33 tuned cells in cat: 14 units within layers II/III and 19 units within layers V/VI (over a total of 40 cells) that could be tracked in all phases of our recording sessions. In this study, across all recorded units in mouse and cat, the fit curves had R2 values ranging between 0.6 and 1.

4.2.1. V1 cells in mouse and cat exhibit mostly attractive shifts following adaptation

In the control condition and following twelve minutes of presenting an uninterrupted sine-wave grating at 90° (adaptation) off the initial preferred orientation (PO), new orientation tuning curves were generated and fitted using a von Mises function (see Materials and methods). To assess the statistical significance of tuning shifts, curve fits were generated separately for each of the 25 trials, and the mean difference was tested by a paired t-test (Dragoi et al., 2000). Results show that only shifts in orientation preference greater than 5° were significant (paired sample two-tailed t-test, $p < 0.01$) in mouse (Jeyabalaratnam et al., 2013a) and in cat (Ghisovan et al., 2009; Lussiez et al., 2021). Moreover, neurons adapting to a non-preferred orientation in mouse and cat leads to shifts of peaks of orientation tuning curves towards the adapting orientation (attractive shift) or away from it (repulsive shift). Only a few cells retained their original PO and were characterized as refractory cells.

In mouse, out of 95 tuned cells, 72.22% of units showed attractive shifts, whereas tuning curves of 21.29% of cells reacted with repulsive shifts. Only 6.48% units were refractory cells. In cat, out of a total of 33 tuned cells, 69.69% of units displayed attractive shifts following the orientation adaptation, whereas tuning curves of 27.27% of cells shifted away from the adapter. Only 3.03%

showed no significant shifts. Typical examples are illustrated in Fig. 4.2A for mouse. In upper curves (raw data in inserts in each case) van Mises fits of normalized responses of three neurons recorded simultaneously for control (black) and post-adaptation (red), showed that the initial PO can shift toward 90° (M1.1), away from 90° (M1.2) or remain unchanged (M1.3). Thus, 97.99% of mouse cells and all cat cells (100%) displayed a shift from the original PO at least for one condition (post-adaptation or post-ketamine).

4.2.2. Dual effects of Ketamine

For a small group of cells, 9.48% in mouse and 9% in cat, ketamine does not affect the neurons' orientation selectivity following adaptation. However, for most cells, 90.52% and 91% in mouse and cat, respectively, ketamine shifts the new PO acquired after adaptation (Fig. 4.2B). The multiplicity of cellular reactions between adaptation and ketamine protocols suggests the complexity of the mechanism allowing OS formation. In 73.25% of cells in mouse, and 83.88% in cat, adaptation induced shifts with a magnitude larger than 24° (dark orange pie chart in Fig. 4.2B). For the rest of cells, the adaptation-shift magnitude is smaller than 24°. Since we divided our cell population after visual adaptation into two groups according to their post-adaptation shift amplitude, we examined the ketamine effects on the OS of the two cell groups. Results show two major effects of ketamine on the adaptation-induced changes of OS. Moreover, Spearman correlation function revealed a significant correlation between post-adaptation - control shifts and post-ketamine - control shifts in mouse ($r = -0.4655$, $p = 0.0042$) and in cat ($r = -0.5929$, $p = 0.0011$) (Fig. 4.2C).

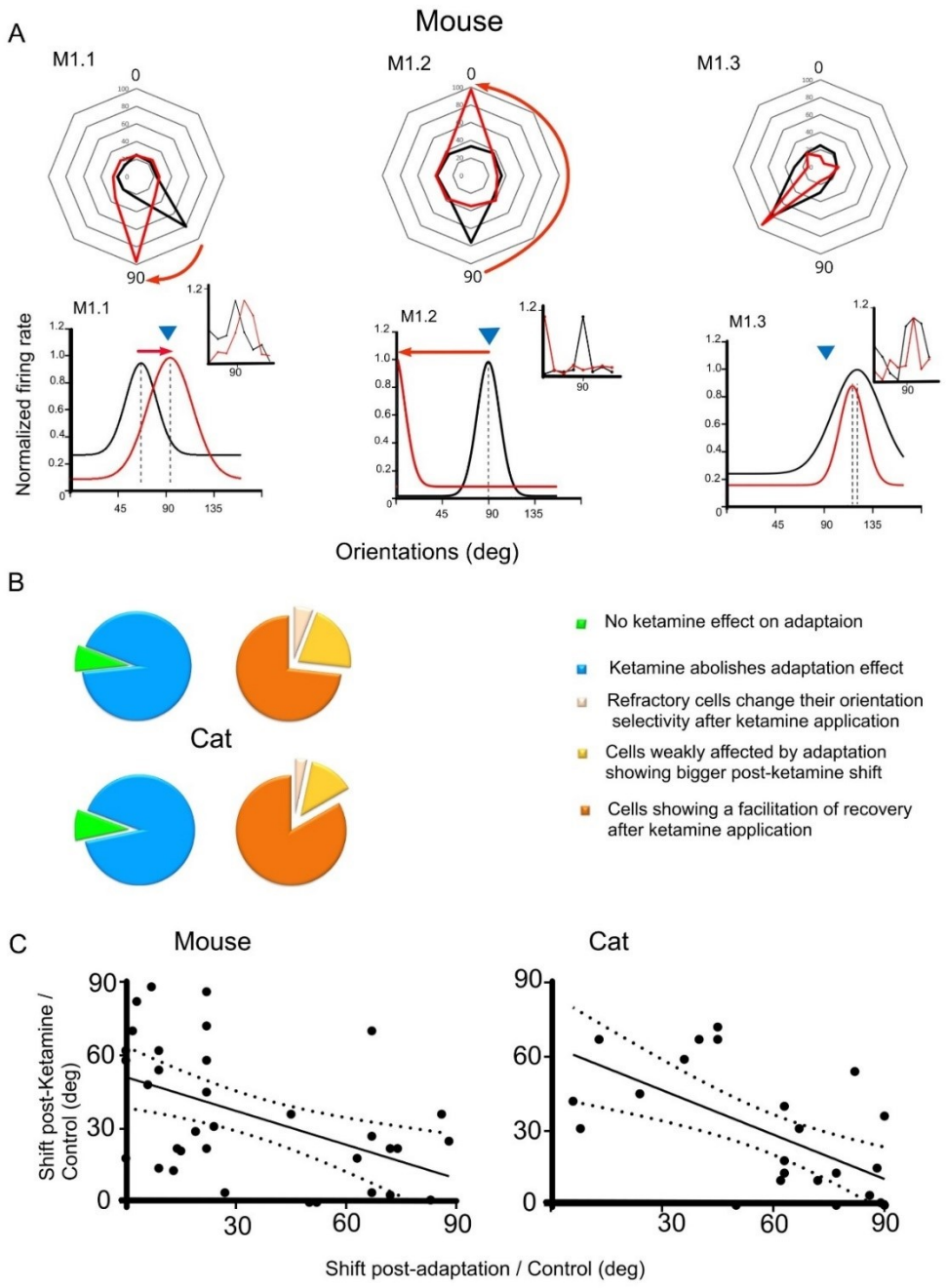

Fig. 4.2 Adaptation and ketamine effects on cells' orientation selectivity and correlation between post-adaptation and post-ketamine shifts. (A) Circular plots and Van Mises fit of normalized responses and raw values (inserted above Van Mises fits) of three mouse neurons in control, and after adaptation of 12 minutes to 90°. Blue triangle represents adapting orientation. The peak tuning curve (Control R2 = 0.75) of the unit M1.1 shifted by 25.8° (68.49° to 94.37°) in the attractive direction (Adaptation R2 = 0.98). while the peak tuning curve (Control R2 = 0.96) of the unit M1.2 shifted by 89.64° (from 89.64° to 0°) in the repulsive direction (Adaptation R2 = 0.97). Finally, unit M1.3 exhibited the same PO after adaptation (Control R2 = 0.73, Adaptation R2 = 0.85), as

shifts were smaller than 5° (from 116.15° to 111.73°). (B) Percentage of cells in mouse and cat according to ketamine effect on adaptation PO. Blue and green pie chart: following ketamine administration, 9.48% cells in mouse and 9% in cat display no significant shift. Out of this small group (green section), for most cells (blue section) 90.52% in mouse, and 91% in cat, the effects of adaptation were not maintained after ketamine application. Orange, yellow, and beige pie chart: out of 86 investigated cells in mouse and 30 units in cat, 63 mouse units, and 25 cat units show an adaptation-induced shift larger than 24°. For all cells in this group, ketamine facilitates the cell's recovery (73.25% and 83.33% cells in mouse and cat, respectively). Beige pie chart: refractory cells, 5.81% in mouse and 3.33% in cat. Yellow pie chart: cells weakly affected by adaptation, 20.93% in mouse and 13.33% in cat. For refractory cells, ketamine induced shifts of the tuning curve peaks, and for cells weakly affected by adaptation, ketamine potentiates the shift. (C) Correlation between the adaptation and ketamine effects on the PO. Spearman correlation function revealed a significant correlation between post-adaptation - control shifts and post-ketamine - control shifts in mouse ($r = -0.4655$, $p = 0.0042$) and in cat ($r = -0.5929$, $p = 0.0011$). The area bounded by the two dotted lines represents the best fit values.

4.2.2.1. Ketamine facilitates cells' recapture of initial preferred orientation

For all cells exhibiting large shifts (> 24°) following visual adaptation, ketamine displaced the adaptation orientation tuning peak back toward the control PO. Fig. 4.3A illustrates, in mouse, a typical example of two neurons (M3.1 and M3.2) showing a post-adaptation shift superior to 24° (respectively 31.24° and 71.96°), and the displacement direction of orientation tuning curve peak induced by ketamine, back to control values. In cat, the units C3.1 and C3.2 show a post-adaptation shift larger than 24°, and a change back to the control position post- ketamine application. In addition, recovery from ketamine effects was carried out four times (green curves) for all the sorted cells, the first recovery session 90 minutes after drug application phase (R1 in Fig. 4.3A) and at 30-minute intervals for second, third and fourth recovery periods (R2, R3, R4 in Fig. 3B). The full recovery was observed after 180 min (after the last recovery period R4). In mouse and cat, the ketamine effects are unrelated to OSI (Orientation Selectivity Index) values (high or low). The two cells displayed in Fig. 4.3A for mouse (M3.1 and M3.2) and for cat (C3.1 and C3.2) have different OSI in control condition. However, the effect of ketamine application is the same in the two examples: low OSI = 0.32 (unit M3.1), and 0.34 (unit C3.1); and high OSI = 0.95 (unit M3.2) and 0.63 (unit C3.2) (Fig. 4.3A).

4.2.2.2. Ketamine potentiates shifts in cells weakly affected by adaptation.

We call cells "refractory" that did not show any significant shift of their PO after an adaptation period, and cells "weakly" affected by adaptation as neurons displaying a shift between 5° and 24°. For all refractory neurons, ketamine resulted in mean shifts of 59°±11.26 in mouse and 62°± 8.52 in cat. Typical examples of refractory neurons in mouse (M3.4) and in cat (C3.4) are illustrated in Fig. 4.3B. For those cells, after ketamine application, small shifts induced by adaptation increased by 18° and 67° in mouse and cat cells, respectively. For all neurons weakly affected by adaptation, the amplitude of the mean shift increased after ketamine administration (amplified shift effect) from 16°±1.63 (post-adaptation) to 41°±5.29 (post-ketamine) in mouse, and from 13°±4.028 (post-adaptation) to 46°±7.54 in cat (post-ketamine). Fig. 4.3B shows the effectiveness of ketamine in further driving the peak of the tuning curve away from the original PO. Thus, in mouse, adaptation induced a shift of 22.4° and following ketamine application, the peak of the tuning curve migrates to 157.5° (M3.5). In cat, the peak of the tuning curve shift was amplified from 8° to 31° (C3.5). The recoveries shown in Fig. 4.3C indicate that the observed ketamine effects are reversible. Our data seem to suggest that ketamine influences only certain properties, since firing rates, initial PO, and cortical depth do not allow sorting ketamine impact along these parameters. It is worth noting that NO2, used in the anesthesia for the cat, is known to act as a non-competitive NMDAR antagonist (Gawaskar et al., 2015). However, it is unlikely that this might impact the results since constant NO2 anesthesia started at the beginning of the experiment, and it can-not induce such repeatable, precise shifts of the tuning curve in a short time window right after ketamine local application. In addition, anesthesia lasts for the duration of the experiment.

4.2.2.3. In absence of ketamine, the effects of adaptation persist

As a supplementary control to rule out a random fluctuation of cells' activity, we proceeded to record simultaneously from two electrodes placed over the mouse and cat cortex. One strip of filter paper impregnated only with solvent was placed next to the electrode (e1), and a ketamine soaked-filter paper was positioned next to the second electrode (e2) (see Fig. 4.1C). Recordings from e1 and e2 occurred simultaneously following 10 minutes of solvent or ketamine application. Results show that following solvent administration, cells maintained their PO (shift < 5°); in contrast, following ketamine application, cells exhibited shifts (Fig. 4.3D). A typical example of two cells (M3.7 in mouse and C3.7 in cat) recorded at increasing distances from the ketamine site revealed that the effect of the drug was only observed in the unit closer to electrode e2. Thus, for the same

period (10 minutes), in absence of ketamine (e1) no effect was seen and the neurons' acquired PO following adaptation in mouse (M3.6) and in cat (C3.6) were maintained. One might think that the reported ketamine effects could be attributed to a random fluctuation and not to the drug. For instance, adaptation could induce large shifts (i.e., due to noise), then in the subsequent measurements, regression to the mean could contribute to smaller shifts. This assumption lacks evidence since orientation tuning has been described as one of the most stable features of V1 cortical cells. Noise could contribute to the FR fluctuation between trials; hence, it could change the tuning width or the amplitude of the tuning curve, but overall once PO is reached, it remains invariant. It was shown that simulations with two different noise levels (10% and 25%) don't produce spurious peaks in the orientation of V1 output (Teich et Qian, 2003), which means that the neurons' tuning curves are stable even with noise much greater than those introduced by Carandini and Ringach (1997). In addition, noise is an inevitable component in any neural system; it is present in all conditions (control, adaptation, and ketamine), so it would be very surprising with its constant presence, that noise induces specific changes in PO, that is, following adaptation, shifts increased, then decreased following ketamine application and this effect is systematically observed for all the cell groups. To further confirm that the shifts are indeed due to ketamine and not to a variation in the dynamics of the PO after adaptation, extra recordings after 30 minutes were carried out from e1 in mouse and cat. A typical example of two units in mouse (M3.6) and in cat (C3.6) showed that once a new preferred orientation (PO) was reached, it remained stable up to 30 minutes (R' in Fig. 4.3D). This experiment tests also the degree of spread of the drug and shows that the effects of ketamine are locally restricted (less than 1.2 mm).

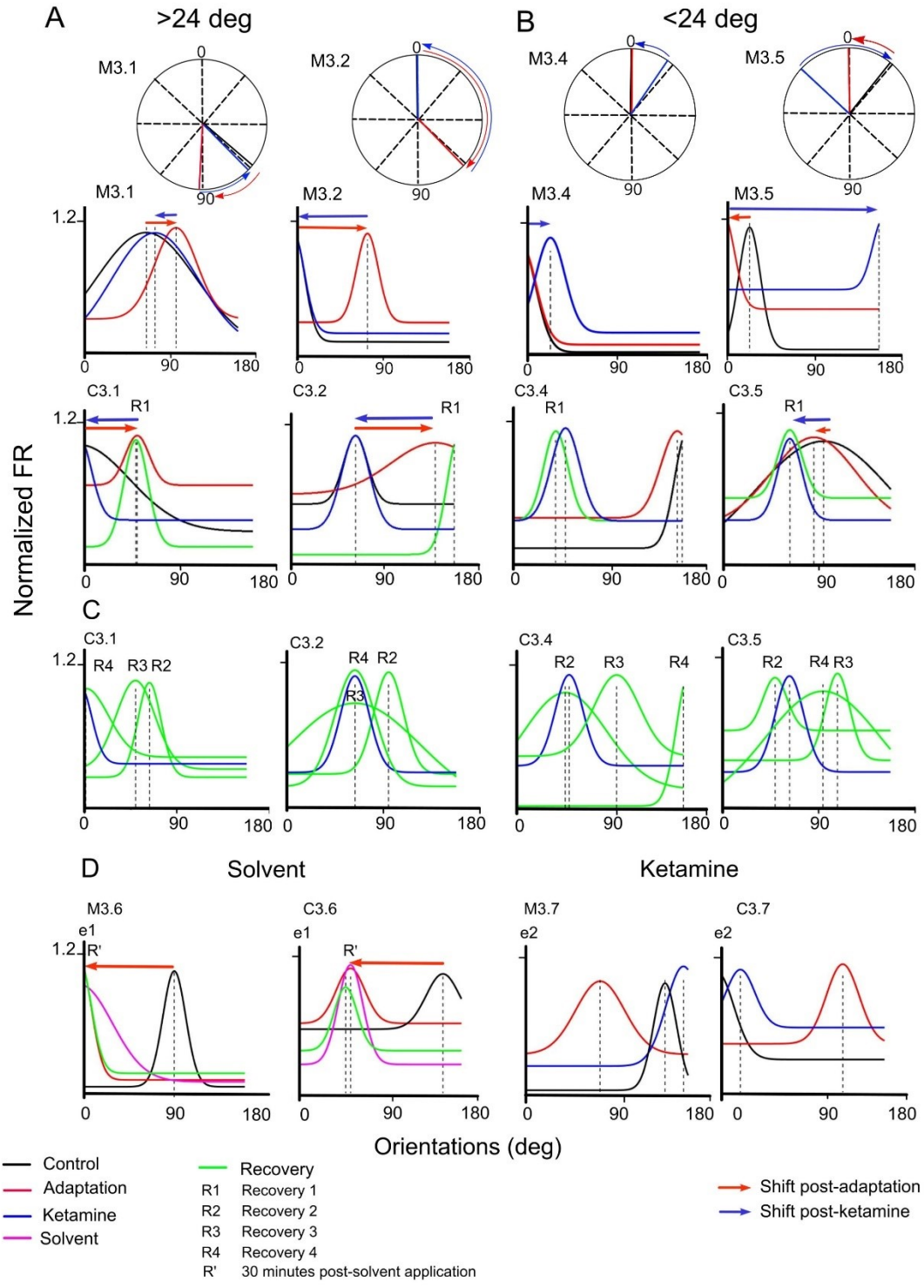

Fig. 4.3 The impact of the presence or not of ketamine on maintaining the adaptation- induced shift in mouse and cat. (A) For adaptation shifts bigger than 24°, ketamine facilitates the cell's recovery regardless of their control OSI value. Van Mises fit of normalized responses of two mouse neurons (M3.1 and M3.2) and two cat neurons (C3.1 and C3.2) for control, post- adaptation, and 10 minutes

post-ketamine application. The control PO of the unit M3.1 (OSI = 0.32, Control R2 = 0.79) is 63.13°, shifts to 94.37° following adaptation (Adaptation R2 = 0.62), and to 71.96° post-ketamine application (Ketamine R2 = 0.81). The PO (0°) of the unit M3.2 (OSI = 0.95, Control R2 = 0.80) shifts to 71.96° following adaptation (Adaptation R2 = 0.73) and ketamine application (Ketamine R2 = 0.78) brings back the neuron's PO to its control value. The amplitude of the shift post-adaptation decreased in neuron C3.1 (OSI = 0.34, Control R2 = 0.74, Adaptation R2 = 0.79) from 49.55° to 0° in the presence of the drug (Ketamine R2 = 0.82) and attained that of the original PO (0°). In neuron C3.2 (OSI = 0.63, Control R2 = 0.78), ketamine derived the peak of the post-adaptation tuning curve (139.50°) to the control PO (63.12°) (Adaptation R2 = 0.88, Ketamine R2 = 0.85). (B) Ketamine potentiates shifts in cells weakly or not affected by adaptation. Following adaptation, the neuron M3.4 (Control R2 = 0.97, Adaptation R2 = 0.82) retained the same orientation selectivity (0°), but the PO shifted to 18° post-ketamine application (Ketamine R2 = 0.81). The neuron M3.5 shows a preference to 22.40° in control condition (Control R2 = 0.90), to 0° following adaptation (Adaptation R2 = 0.82) and to 157.5° post-ketamine application (Ketamine R2 = 0.82). Thus, the shift increased from 22.4° to 44.9°. In A and B, Circular graphical representation of the PO in mouse was added to show the shifts of the PO through conditions. C3.4 is a typical example of a refractory cell in cat. Original PO was 157.5° (Control R2 = 0.83), post-adaptation PO was 153.08° (Adaptation R2 = 0.89) and the post-ketamine PO was 49.55° (Ketamine R2 = 0.83). Similar potentiation of post-adaptation shift for C3.5 following ketamine administration. Original PO was 94.37° (Control R2 = 0.79) shifted to 85.54°, that is, the post-adaptation PO (Adaptation R2 = 0.83). In the presence of the drug, the amplitude of shift increased from 8.83° to 82.41° (the post-ketamine PO was 63.13°) (Ketamine R2 = 0.86). In cat, four recovery sessions followed the ketamine application were performed (green curves). The first recording (R1) was done 90 minutes following the post- ketamine phase and shows that none of the cells has recovered. (C) The other recovery recordings (R2, R2, and R4) were done every 30 minutes and shows the full recovery in R4. (D) In absence of ketamine, the adaptation induced changes are maintained. Typical examples of Van Mises fit of normalized responses of two pairs of neurons (M3.6 - M3.7 in mouse, and C3.6 – C3.7 in cat) recorded simultaneously from the two electrodes e1 and e2 with 1.2 mm distance separating them. The filter paper soaked with the solvent is beside e1 and the filter paper soaked with the drug is beside electrode e2. M3.6 (Control R2 = 0.78, Adaptation R2 = 0.83, Solvent R2 = 0.61) and C3.6 (Control R2 = 0.67, Adaptation R2 = 0.76, Solvent R2 = 0.98) retained their adaptation PO after solvent application. Extra recordings 30 minutes post-solvent application (R') were carried out from e1 in mouse (Recovery (R') R2 = 0.71) and cat (Recovery (R') R2 = 0.87) and showed that the post-adaptation PO were maintained up to 30 minutes. Cells recorded from e2 (M3.7 (Control R2 = 0.99, Adaptation R2 = 0.87, Ketamine R2 = 0.84) and C3.7 (Control R2 = 0.93, Adaptation R2 = 0.73, Ketamine R2 = 0.79)) exhibited a new PO following drug application.

To conclude, in cells exhibiting a shift greater than 24°, ketamine facilitates recovery toward the original orientation (Fig. 4.4A), significantly narrowing the post adaptation gap from 65.14° ±2.88 to 22° ±3.52 (Fig. 4.4C) (Wilcoxon paired test, p = 0.000000015). For the whole population of cells showing a weak or no shift after adaptation, ketamine significantly potentiates the post adaptation shift from 11.85° ±1.83 to 48.43° ±5.36 (Fig. 4.4B and C) (Wilcoxon paired test, p = 0.0000038147). Contrary to the effects observed on the post-adaptation PO after ketamine application (Fig. 4.4D), no changes were noted in the absence of the drug (Fig. 4.4E). In addition, the effect in ketamine was significantly different than the effect in the solvent condition (t-test, p = 0.0001, t = 4.930, df = 18).

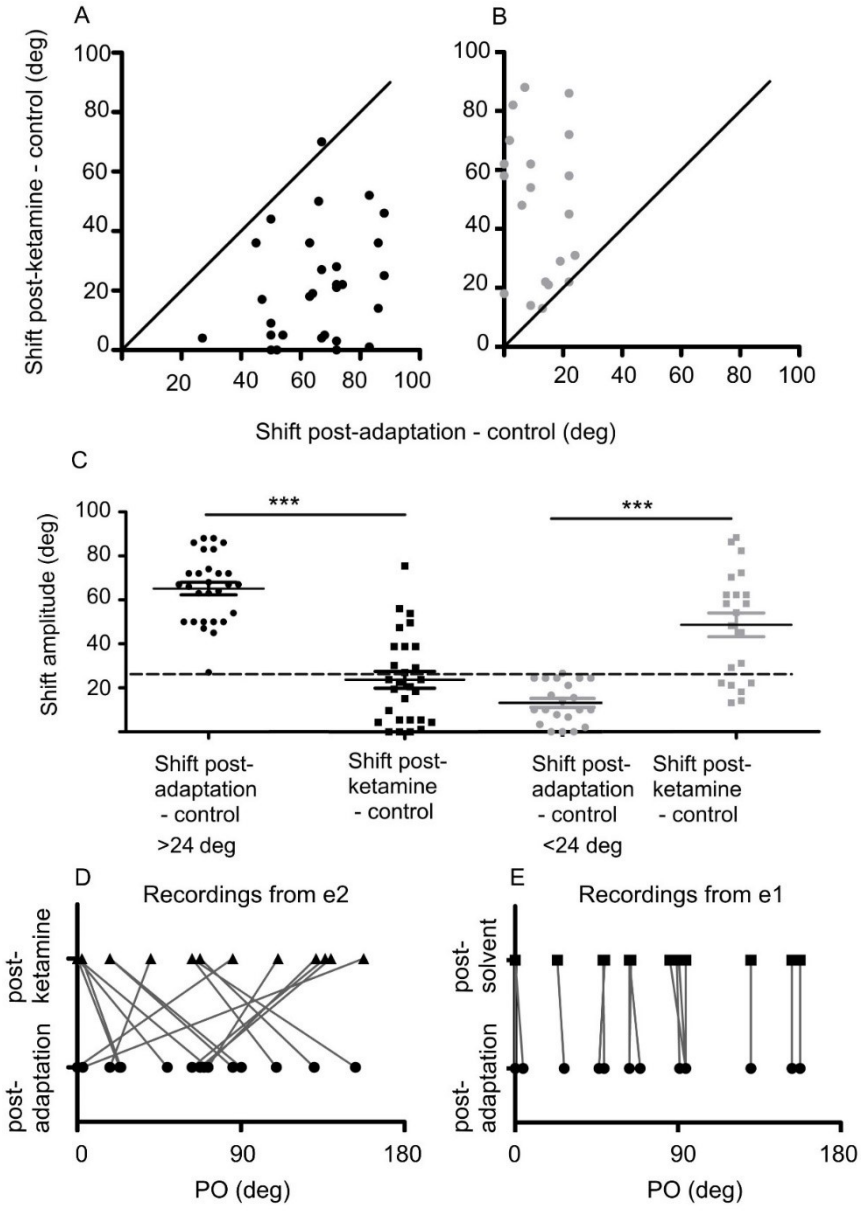

Fig. 4.4 Impact of ketamine on the orientation selectivity acquired following adaptation according to the magnitude of adaptation-induced shift in mouse. (A) Scatter plots of shifts post-adaptation – control (larger than 24°) vs post-ketamine – control. Each black point is a single unit. (B) Scatter plots of shifts post-adaptation – control (smaller than 24°) vs post-ketamine – control. Each grey point is a single unit. (C) Average and standard error of mean of the shift amplitude induced by adaptation vs the shift amplitude between ketamine and control condition for cells highly (black with shifts > 24°) or weakly (grey with shifts < 24°) affected by adaptation. The post adaptation shift for black cell population decreases significantly from 65.14°±2.88 to 22°±3.52 after ketamine application (Wilcoxon paired test: P = 0.000000015). However, for grey cells, it increases significantly from 11.85°±1.83 to 48.43°±5.36 (Wilcoxon paired test: P = 0.0000038147). Dotted black line marks the shift threshold of 24° while the solid black line marks the equality line. (D) The post-adaptation PO of cells recorded from e2 shifts following 10 min of ketamine application. (E) After 10 min of solvent application, no effect was observed on the post-adaptation PO of cells recorded from e1.

4.2.3. Network-dynamics of the assembly

To investigate the dynamics of functional links between simultaneously recorded neurons from a microelectrode (termed in our paper a "cell-assembly") in relationship to applied orientations and in different conditions, Cross-correlograms (CCGs) were computed between spike trains of neuron pairs in mouse and cat for each recording (95 units and 33 units in total in mouse and cat, respectively). In the next sections we distinguish neuronal synchrony from functional relationships. Neuronal synchrony is a special case of a functional relationship where two cells receive common input from a third neuron and it applies when the central peak of the CCG is within the time window -1 to +1 ms bin adjoining the central zero point, while functional relationships refer to cases when the highest significant peak of CCG is within +/- 5 ms of the central point in the CCG.

4.2.3.1. Adaptation activates dedicated networks and ketamine reorganizes them

A functional feature of cats' V1 is the organization of neurons into orientation columns (Hubel et Wiesel, 1969; Mountcastle, 1957). Therefore, neurons sharing functional properties (belonging to a column) respond in unison which implies the existence of specific connections between them (Shadlen et Newsome, 1998; Stepanyants et al., 2008) . In addition, there are projections between columns (Binzegger et al., 2004; Kisvarday, 2000; Michalski et al., 1983; Stepanyants et al., 2008). However, how pair wise connections change in response to ketamine application has not yet been explored. Fig. 4.5 shows a typical example of functional connections between neurons recorded

simultaneously in cat when a 0° oriented sine-wave drifting grating was presented within the receptive field. Thus, we examined the putative pair-connections between a reference (blue neuron) and five targets (other colored neurons) throughout the several conditions of the experiment. In control condition, no functional connections were revealed between the reference blue neuron and target cells as the CCG indicated no significant peaks within a 5 ms time-window around the zero mark. Following adaptation, the blue neuron (reference) impacts the target unit (purple). The black connecting line between the two cells depicts the functional connections as revealed by CCGs (significant peak p = 2%). The cumulative histogram (above CCG) of the FR (firing rate) of the target cell further illustrates that once the source unit produced a spike, the firing rates of the target neurons increased. This increase may be attributed to changes in intrinsic properties or intensified excitation from the source unit. It must be underlined that crosscorrelations are not related to firing rates but to temporal relationship between action potentials of both trains (Bharmauria et al., 2016; Rolls et Treves, 2011). Following ketamine administration, CCGs show that the same reference and five target neurons simultaneously increase their firing rates (red line linking cells). The cumulative histogram shows that reference and target units were excited synchronously with different probabilities (p = 5.9% for the orange, 8.1% for the green, 4.3% for the yellow, 5.3% for the cyan, and 5.9% for the light green unit). This suggests synaptic weights are changing between neurons (Alloway et Roy, 2002). Therefore, after ketamine application within this example of a neuronal network, the functional connections were redeployed between 37 neuron pairs and the connectivity pre- and post-ketamine were found to be significantly different (Pearson coefficient = 0.11, p = 0.6552). Following a period of recovery, no connections were observed, and the functional network recovered its initial dynamics observed in control condition. The large increase in excitation under ketamine is in line with recent results showing multiplicative gain of responses in auditory cortex (Deane et al., 2020).

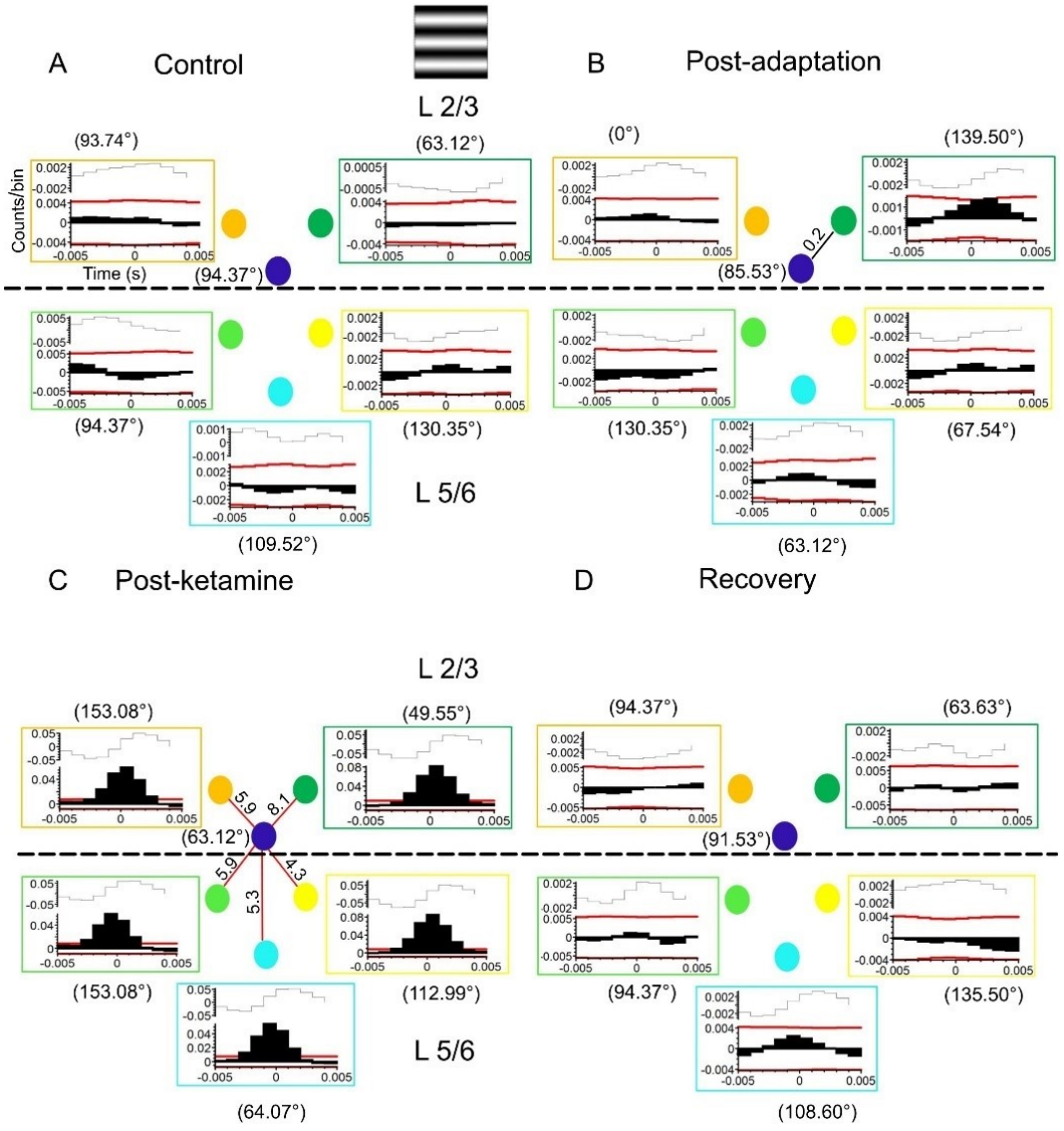

Fig. 4.5 Dynamics of the functional network between neurons recorded simultaneously from multisite microelectrodes in cat, throughout conditions at the orientation 0°. For this entire figure, three neurons (blue, orange, and green units) were isolated from layer 2/3 and three neurons were isolated from layer 5/6 (yellow, cyan, and light green units). The cells belonging to each layer were separated by the black dashed line and were labelled by different colors (the colour scheme is respected throughout the figure). Blue circle indicates the reference neuron in the pair and the others are targets. The functional network between pairs (reference and each target) was revealed by the crosscorrelogram (CCG) which is shown adjacent to each cell. All CCGs were shift-corrected. X axis in the CCG represents the time window (-5 ms to 5 ms), and Y axis the probability (p) of the cell discharge. The red curved line indicates the significance level. The significant peak (shown by a number) suggests a functional link between a pair of cells (shown by the black line in B). Numbers in brackets shows the cells PO. The curve above the CCG depicts the cumulative

sum histogram of the discharge of the target cell. Red line in C marks the simultaneous inputs. (A) Functional network in control condition revealed no putative connection between the reference (blue cell) and the target neurons. (B) Functional network following adaptation revealed a putative connection between the blue – green pair (p = 0.2%). (C) Functional network following ketamine application revealed synchronous inputs between blue - orange pair (p = 5.9%), blue – green pair (p = 8.1%), blue – yellow pair (p = 4.3%), blue - cyan pair (5.3%) and blue – light green pair (p = 5.9%). Example of a neuronal network before and after ketamine revealed that functional connections between synchronously recorded cells are significantly different (Pearson coefficient = 0.11, p = 0.6552, 37 neuron-pairs). (D) Functional network following the last period of recovery revealed no putative connection between recorded cells.

In relationship to the work mentioned above, neuronal firing activities of cells were crosscorrelated for all the simultaneously recorded neuron-pairs between the recorded sites. Fig. 4.6A shows the connectivity matrices of all the responsive neuron-pairs in cat. Fig. 4.6C displays a typical example of the connectivity matrices in mouse between six units. Matrices were generated in response to gratings and for each condition. Hence, the values of probabilities (the peak-strengths) for all cell-pairs indicated by the color scale on the right of the matrices can be compared at control, post-adaptation, and post-ketamine conditions. As has been shown previously in cat (Bachatene, Bharmauria, Cattan, Chanauria, et al., 2015), our results reveal that adaptation induces new functional connections in the microcircuits and disconnections in others both in cat and mouse (Fig. 4.6B and D). The connectivity matrices pre- and post-adaptation were found to be significantly different in cat (Pearson coefficient = 0.2411, p = 0.5651, 345 neuron-pairs) and in mouse (Spearman coefficient = 0.0803, p = 0.1366, 346 neuron-pairs). A comparison of the structure of the matrices divulges the emergence of new connections. The relationships between cells, as revealed by CCG analyses, are modulated by adaptation (In Fig. 4.6D for example, at 157.5° consider the pair pink - purple, the peak CCG increased from 1.0% in control to 1.5% post-adaptation). Yet it is important to underline that some functional relationships remain unchanged with the same strength (for example, pink - orange units, p = 1.7%, Fig. 4.6D). Thus, visual adaptation remaps the connectivity in mouse visual cortex microcircuits. Furthermore, to investigate the effect of ketamine on the assembly dynamics and the functional connectomes established following adaptation, we systematically studied connections between co-active neurons at every presented orientation. Results show that following ketamine application, the connections were characterized by a change in their probabilities (p) and thus in synaptic weights linking cells (Alloway & Roy, 2002). The connectivity matrices between all pairs before and after

ketamine administration were found to be significantly different in cat (Pearson coefficient = 0.2682, p = 0.5207, 345 neuron-pairs), and in mouse (Spearman coefficient = 0.005, p = 0.3093, 346 neuron-pairs). It is interesting to mention that, in cat, most of the putative connectivity changes are in the lower left quadrant of the connectivity matrix. To explain this distribution, we looked at many factors, such as cells sorted from infra- or supragranular layers, the preferred orientation in all conditions, the amplitude of post-adaptation, and the post-ketamine shift. However, not one of these factors was conclusive, the only difference between the two groups (cells showing higher connections and cells showing lower connections) is the OSI value. In fact, for the first population, there is a significant increase of OSI between adaptation and ketamine conditions (paired t-test, p = 0.000001, t = 7.801, df = 15) but for the second population there is a significant decrease of OSI value between the two conditions (paired t-test, p = 0.0120, t = 2.834, df = 16). The increase of OSI might favor the connection between cells. A typical example of a CCG peak-modulation after drug application for a neuron pair in cat at 45° (olive - dark blue unit, p post- adaptation = 2.3%, p post-ketamine = 1.3%) is shown in Fig. 4.6B. Some connections were maintained with the same probability (orange unit – magenta unit, p post-adaptation = p post-ketamine = 1%), in some new links were activated (for instance light blue - magenta unit, p post-ketamine = 6.2%), and in others, deactivated (for example orange - dark blue unit). Similar results were observed in mouse as illustrated in Fig. 4.6D; new connections were revealed at the same presented orientation (for example at 157.5° yellow - blue units p = 1.1%), while others disappeared (for example yellow - orange unit). Some links are maintained in all conditions with almost the same strength (p = 1.7% for the pink - orange pair). In short, whatever the PO (original or adaptation induced), ketamine revises it, as if ketamine reworks the neuronal network.

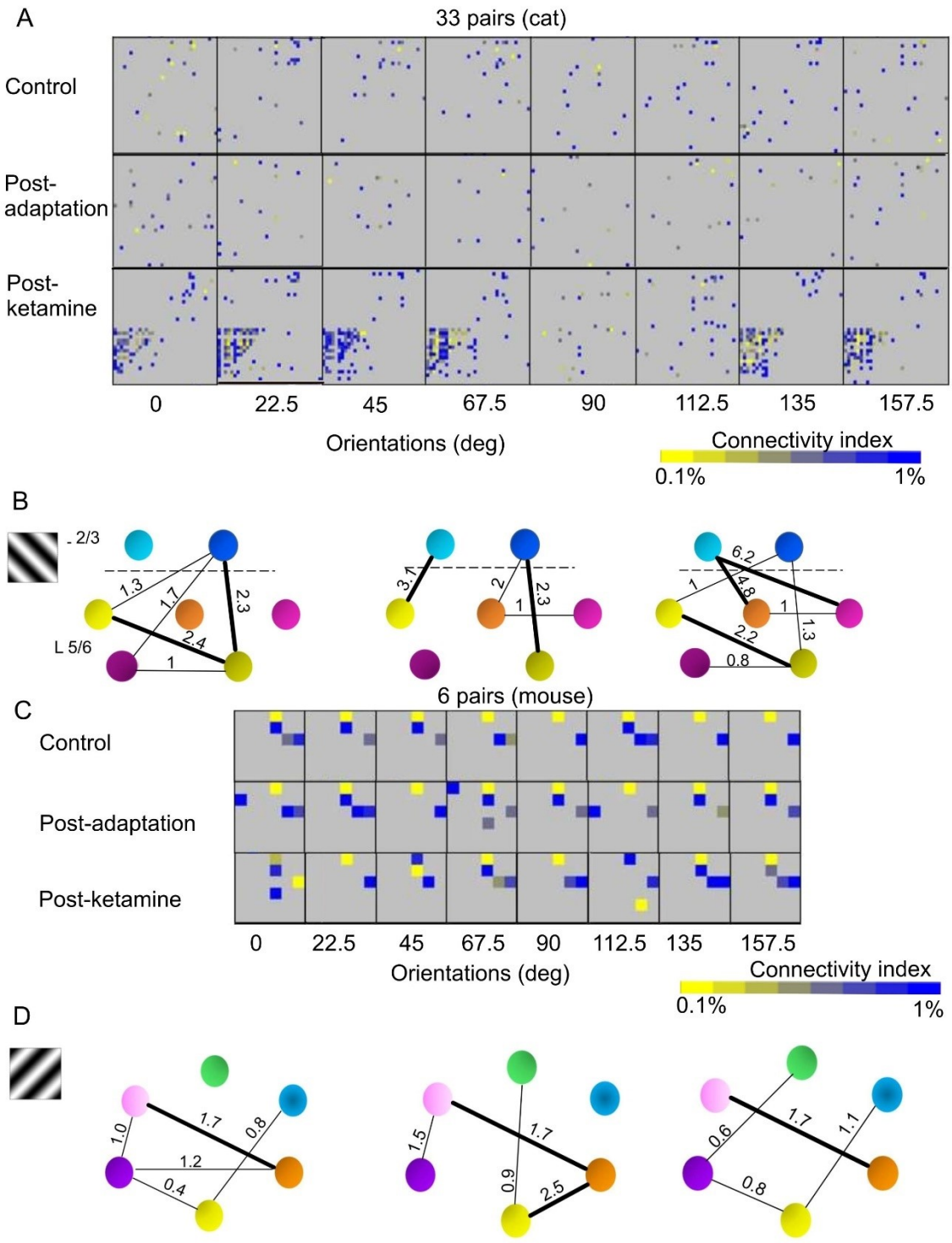

Fig. 4.6 Connectivity dynamics of neuronal microcircuits. (A and C) Strength matrices of a cell assembly (33 × 33 cells) in cat (A), and (6 × 6 cells from two sites) in mouse, at all the tested gratings and in all conditions (control, post-adaptation, and post-ketamine). Same cells were sorted for all conditions and their corresponding activities were cross-correlated. The square in the matrix

represents a significant connection between a neuron on the x-axis and a neuron in the y-axis. The normalized peaks-strengths of connections (peak-probabilities in CCG) are represented by a colored scale (to the right). Pre- and post-adaptation matrices between all pairs were significantly different in cat (Pearson coefficient = 0.2411, p = 0.5651, 345 neuron-pairs), and in mouse (Spearman coefficient = 0.0803, p = 0.1366, 346 neuron-pairs). As well, pre- and post-ketamine matrices were significantly different in cat (Pearson coefficient = 0.2682, p = 0.5207, 345 neuron-pairs), and in mouse (Spearman coefficient = 0.005, p = 0.3093, 346 neuron-pairs). (B and D) Neuronal microcircuits and connectivity strength dynamics in cat and mouse, respectively. Black dashed line in B represents the separation between cells (two units) within supra-granular layers (L 2/3) and cells (5 units) within infra-granular layers (L 5/6). The thick lines correspond to strong connections (by convention, probabilities of connections > 2% in cat and > 1.5% in mouse), and the thin lines correspond to weak connections (by convention, probabilities of connections < 2% in cat and < 1.5% in mouse).

4.2.3.2. Comparative effects of ketamine on functional relationships in mouse and cat

We then quantified the extent of the neuronal assembly reshuffling by adaptation and ketamine by computing the sum of the connection strengths and the number of connections, in both mouse and cat. To this end, in the same cell assembly, we averaged the peak-strengths of all connections at all orientations and the number of connections, in order to compare the global strength of functional connectivity between the same assembly in control, adaptation, and ketamine conditions (Fig. 4.7A-D). In mouse, the mean values for the peak strengths of matrices (Fig. 4.7A) were not significantly different between conditions (Repeated measures ANOVA, p = 0.393, F = 0.996, df = 23). In addition, no significant difference was revealed between the mean values of the sum counts of connections (Repeated measures ANOVA, p = 0.393, F = 0.996, df = 23) (Fig. 4.7B). This analysis suggests the following: Despite the modification of the connectivity of the neuronal network and consequently its dynamics induced by adaptation and ketamine, on average, the global connectivity strength and connection counts in the assembly are maintained regardless of which cells are linked. Interestingly, the results (Sidak's multiple comparisons test was used as post hoc) are different in cat since the mean peak probabilities are significantly higher under ketamine than in control (p = 0.0005) and post-adaptation conditions (p = 0.0001) as well as the mean sum counts of connections significantly increases after ketamine compared to control condition (p = 0.00002) and following adaptation (p = 0.00001) (Fig. 4.7C and D). Our results reveal that these rises of the CCG magnitude and number of connections in cat following ketamine administration are due to an increase of synchrony strength and synchrony counts respectively. Fig. 4.7E and F show a

significant increase of the mean peak probabilities and the mean sum counts of synchrony in the ketamine condition versus control ($p = 0.00003$ and $p = 0.00006$, respectively) and post-adaptation conditions ($p = 0.00009$ and $p = 0.00008$, respectively). It is worth noting that for all the revealed synchronous–time relationships, the firing rate of the post-synaptic target neurons increased as shown by the cumulative histogram (above CCG in Fig. 4.5), which implies a common excitatory input leading to an increase of excitation of network.

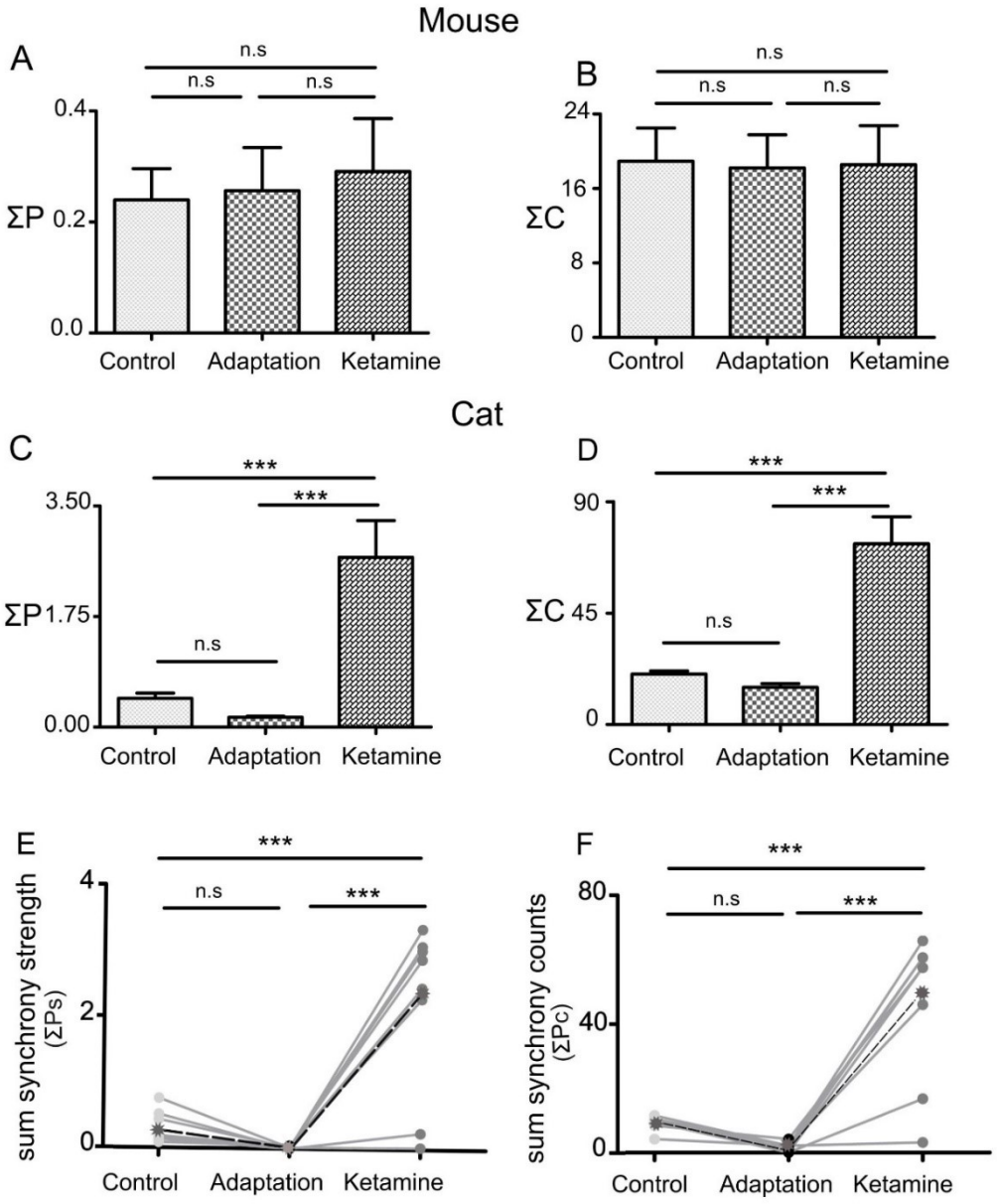

Fig. 4.7 Comparative histograms of averages of summed CCG magnitudes and the mean sum counts of all disclosed connections between neurons at all presented orientations in control, following adaptation, and following ketamine application, in mouse and cat. Error bars in the histogram indicate the standard error of mean. (A) and (B) In mouse, between conditions, no significant difference of the mean CCG magnitude (ΣP) of all summed pairs (ΣP control = 0.24 ± 0.056, ΣP post-adaptation = 0.25 ± 0.077, ΣP post-ketamine = 0.29 ± 0.095 (Repeated measures ANOVA, F = 0.99, df = 7, p = 0.3939)), and the mean sum counts of connections (ΣC) (ΣC control = 19 ± 3.560, ΣC post-adaptation = 18 ± 3.560, ΣC post-ketamine = 19 ± 4.181 (Repeated

measures ANOVA, $F = 0.07$, $df = 13$, $p = 0.9260$)). (C) and (D) In cat, no significant difference in pre- and post-adaptation of the mean sum peak probabilities (ΣP control = 0.45 ± 0.080, ΣP post-adaptation = 0.15 ± 0.017 (Repeated measures ANOVA, $F = 15.42$, $df = 7$; post hoc Sidak's multiple comparisons test, $t = 0.60$, $p = 0.5540$)), and the mean sum counts of connections (ΣC control = 20 ± 1.0253, ΣC post-adaptation = 15 ± 1.524 (Repeated measures ANOVA, $F = 27.42$, $df = 14$, post hoc Sidak's multiple comparisons test, $t = 0.62$, $p = 0.5445$)). The mean sum CCG magnitude is significantly higher in the ketamine condition (ΣP post-ketamine = 2.68 ± 0.58) than in control condition (post hoc Sidak's multiple comparisons test for Ketamine > Control, $t = 4.47$, $p = 0.0005$) and post-adaptation condition (Sidak's multiple comparisons test for Ketamine > Adaptation, $t = 5.08$, $p = 0.0001$). Similarly, the mean sum counts of connections is significantly higher in the ketamine condition ($\Sigma C = 73 \pm 10.88$) than in control condition (post hoc Sidak's multiple comparisons test for Ketamine > Control, $t = 6.08$, $p = 0.00002$) and post-adaptation condition (Sidak's multiple comparisons test for Ketamine > Adaptation, $t = 6.70$, $p = 0.00001$). (E) and (F) Sum synchrony strength (ΣPs) is not significantly different between control and post-adaptation conditions (ΣPs control = 0.30 ± 0.085, ΣPs post-adaptation = 0.18 ± 0.005 (Repeated measures ANOVA, $F = 17.18$, $df = 14$; Sidak's multiple comparisons test, $t = 0.70$, $p = 0.4929$)). Then as well, the sum synchrony counts (ΣPc) is not significantly different between control and post-adaptation conditions (ΣPc control = 9 ± 0.779, ΣPc post-adaptation = 2 ± 0.460 (Repeated measures ANOVA, $F = 26.44$, $df = 14$; Sidak's multiple comparisons test, $t = 1.18$, $p = 0.2559$)). However, ΣPs is significantly higher between control and post-ketamine condition (ΣPs post-ketamine = 2.17 ± 0.460, Sidak's multiple comparisons test for Ketamine > Control, $t = 4.68$, $p = 0.00003$), as well as between post-adaptation and post-ketamine (Sidak's multiple comparisons test for Ketamine > Adaptation, $t = 5.39$, $p = 0.00009$). ΣPc is significantly higher between control and post-ketamine condition ($\Sigma Pc = 44 \pm 7.860$, Sidak's multiple comparisons test for Ketamine > Control, $t = 5.62$, $p = 0.00006$), as well as between post-adaptation and post-ketamine (Sidak's multiple comparisons test for Ketamine > Adaptation, $t = 6.80$, $p = 0.00008$). Black stars represent the mean synchrony strength.

4.3. Discussion

Two major goals were investigated: 1) how ketamine impacts V1 adaptation induced plasticity as characterized by OS changes, and 2) changes in functional relationships between neurons in microcircuits by crosscorrelation analyses. Indeed, ketamine altered OS acquired after adaptation, and simultaneously influenced the dynamic modulation of functional relationships between V1 adapted cells; thus, it modified the network configuration of V1 in mice and cat.

4.3.1. Ketamine impacts the adaptation-induced orientation selectivity

Following adaptation, PO changes in both species. The post-adaptation curves showed mostly an attractive transfer to orientations near the adaptor, and a smaller number of cells exhibited repulsive shifts. The present results are in good agreement with data obtained in related studies in

mouse (Jeyabalaratnam et al., 2013b) and cat (Ghisovan et al., 2009). The main behavioral consequence of orientation adaptation is an improvement of performance for orientation discrimination tasks and a broadening of the perceptual range (Krekelberg et al., 2006) . As suggested, these peak shifts may be involved in a better stimulus discrimination at the adapting orientation (Teich et Qian, 2003), or for increasing detectability (Clifford et al., 2001). In addition, in mouse and cat, following adaptation, cells were divided into two groups according to the shift magnitude (the difference between the initial PO and the post-adaptation PO ($\Delta\theta$)). Thus, we distinguish cells with small $\Delta\theta$ values (0° - 24°) and cells with large shifts (over 24°). It is likely that the larger shift magnitude is a consequence of the greater spectrum of orientation distribution on a particular dendritic branch, whereas cells collecting a narrower range of orientation showed smaller shifts. Thus, the adapter strengthens its drive over the other inputs and leads to an attractive shift or weakens its drive, which favors a bias of one orientation on the opposite side of the tuning curve and therefore a repulsive shift.

We also looked at how ketamine affects the two categories of cells (exhibiting small $\Delta\theta$ or large $\Delta\theta$). Interestingly, the response of the two cell categories to ketamine application was very different. While ketamine reduced the post-adaptation shifts superior to 24° (large $\Delta\theta$) facilitating the cells' orientation recovery, that is, back to the initial PO, conversely, it potentiated the post-adaptation induced shift inferior to 24° (small $\Delta\theta$) by further increasing shift magnitude. For cells exhibiting large $\Delta\theta$, we suggest that ketamine application leads to weakening the synaptic strengths for the adapted orientation (post-adaptation PO) and increases the synaptic weight for orientations close to the original one. This implies that the shift moves toward the original orientation. On the other hand, for cells weakly ($\Delta\theta < 24°$) or not affected by adaptation, ketamine pulled the peak further way from the post-adaptation PO. It is well documented across species and across recording sites that the processing of sensory inputs is under the control of the excitation-inhibition (E-I) balance, and changes in neuronal response can result from altering such balances by ketamine (Li et al., 2010; Populin, 2005; Zanos et al., 2016). Thus, we hypothesize that ketamine leads to the specific pattern of orientation tuning curve shifts due to an imbalance of excitation and inhibition in the network and that the observed dual effect could be explained by the different patterns of neuronal interactions. Indeed, neuronal interactions between excitatory and inhibitory cells determine the output of each neuron for each presented orientation. In the cerebral cortex, cortical inhibition orchestrates sensory-driven activity (Isaacson et Scanziani, 2011). Considering that

parvalbumin-expressing (PV) inhibitory cells are the initial locus underlying ketamine's effects (Grieco et al., 2020; Zhou et al., 2015), the result of the interactions between neurons and ketamine depends on the cell types and their output according to the network composition to which they belong. While the decrease of the connection of PV with excitatory neurons leads to increased excitation (Browne et Lucki, 2013; Homayoun et Moghaddam, 2007)in some networks, the depression of interconnections between inhibitory cells may lead to a decrease of excitation in other microcircuits. Indeed, in addition to the connection of inhibitory with excitatory neurons, several studies have described connections between PV cells and other inhibitory units (Avermann et al., 2012; Bachatene, Bharmauria et Molotchnikoff, 2012; Dalezios et al., 2002; Pfeffer et al., 2013). Then the disinhibition induces facilitation of neuronal responses and inverts inhibitory responses into excitatory (Populin, 2005). Therefore, differential variation of excitatory connections, under ketamine, may lead to differential variations of the neuronal activity resulting in reducing or potentiating post-adaptation shifts. It is also likely that the dual effect of ketamine depends on the cell's type. Actually, it was shown that in monocular visual cortex (layer 2/3), pyramidal cells and interneurons showed different behaviour following deprivation, since only excitatory neurons recover activity while inhibitory neurons show no recovery (Barnes et al., 2015).

Overall, our results challenge a fundamental tenet of plasticity (change of the intrinsic proprieties of the neuron that is the OS in this study) induced by ketamine. While the drug affects the E-I balance, it induces changes in the effect of the adaptor since the selectivity of the cell does not remain stable at the imposed orientation. This would suggest that ketamine leads to a new equilibrium of the synaptic inputs and therefore a reactivation of cortical plasticity. Several findings might explain how ketamine promotes visual cortical plasticity. It was shown that a single ketamine treatment leads to down-regulation of the neuregulin-1 (NRG1) expression in PV inhibitory cells. Subsequently, ketamine induces excitatory input loss to PV neurons which in turn reactivates plasticity in mouse visual cortex (Grieco et al., 2020). Hence, ketamine promotes neural plasticity via molecular mechanisms (Moda-Sava et al., 2019; Takei et al., 2004; Zhou et al., 2014). It seems that the time course of 10 min of ketamine application was enough to produce neuronal structural changes. Indeed, with strong stimuli, growth of dendritic spines with stabilisation of their volume was observed in a short time window of 5 min (Harvey et Svoboda, 2007). Such

structural changes may explain the slow recovery process and thus the long recovery time (180 min) reported in the present study.

4.3.2. Network dynamics following adaptation and adjustment of the synaptic connection of the functional network by ketamine

Visual processing is an occurrence that requires network formation. To investigate the relationship between orientation tuning plasticity and neuronal crosstalk, a comparison of the connectivity between the simultaneously recorded cells during experimental conditions was carried out. The results reported in this paper demonstrate modifications in the synaptic scheme of the V1 network-selectivity following adaptation. Since it was suggested that adaptation is a short version of orientation learning (Bachatene et al., 2013; Bachatène et al., 2015; Dragoi et al., 2000), we postulate that the reorganization of the connections' strengths between orientation-selective neurons is involved in perceptual learning (Bachatene, Bharmauria, Cattan, Rouat, et al., 2015; Bachatène et al., 2015; Gilbert et Li, 2012) which requires NMDAR activation (Frenkel et al., 2006). We next aimed at investigating the linkage dynamics between neuron-pairs following ketamine application to reveal if there are any changes in the post-adaptation neuronal connectivity. An emergence of a novel sub-network after drug administration was observed. This may mean that ketamine induces plasticity via unmasking pre-existing connections. Several mechanisms may be involved, such as changes in neuronal membrane excitability and physiological deletion of local inhibition. Moreover, several investigations suggest that reduced synaptic inhibition leads to excitatory reorganization (Chen et al., 2011; Keck et al., 2011; Kuhlman et al., 2013; van Versendaal et al., 2012). Although both adaptation (via the forceful presentation of a particular stimulus) and ketamine application might lead to similar results that alter the E-I balance, the involved pathways seem to be different. Indeed, contrary to adaptation where plasticity might be induced by the activation of NMDAR, ketamine blocks the latter and thus it involves different molecular paths. The results also raise a new question: Does the new equilibrium of the synaptic inputs promoted by the drug (and thus the emergence of the new selectivity) allow the functional modification of neuronal circuits (Jaffer et al., 2012) or do orientation tuning curves that are found physiologically change connection strengths in the microcircuits of V1(Ben-Yishai et al., 1995; Carandini et Ringach, 1997; Somers et al., 1995). Since it was shown that cortical networks generate orientation selectivity (Schummers et al., 2004),

we hypothesized that the changes in post-adaptation PO, specially for refractory neurons, after ketamine application might be the network effect after ketamine treatment.

It was suggested that ketamine binds the NMDAR only when it is open, inducing a modification of the channel conformational state. The trapped channels become blocked, thereby hindering Ca2+ and Na+ flow through the channels. It seems that the anesthetic, analgesic, and antidepressant effects of ketamine are due, but not solely, to this blockage (Dinis-Oliveira, 2017; Zanos et Gould, 2018). Moreover, the occlusion of Ca2+ alters neurotransmission, and produces an impairment in neuronal calcium homeostasis (Lisek et al., 2020). The drug-induced Ca2+ imbalance and therefore the change in synaptic transmission might revise neuronal networks and disrupt stimulus-selective connectivity between cells, thereby altering the encoding of stimuli. It is worth to signal that ketamine could binds to not only NMDAR, but also several other sites. There is little evidence that contrary to Dizocilpine (MK-801 [(+)-5-methyl-10,11-dihydro-5H-dibenzo [a,d] cyclohepten-5,10-imine maleate]), a non-competitive antagonist of NMDA receptors, ketamine at higher concentrations activates α6β2δ and α6β3δ receptors (subtypes of GABAA receptors) (Hevers et al., 2008). However, these GABAA receptor subtypes are expressed in cerebellar granule cells (Quirk et al., 1994) and so far are not found to be expressed in the cortex (Kurt et al., 2008). On the other hand, although the effect of ketamine on NMDAR is widely supported by the literature, we cannot exclude the hypothesis that, beyond ion channels in V1, there other systems which may be affected by ketamine especially cholinergic systems that could contribute to neural network changes (Sleigh et al., 2014).

4.3.3. Stability of synaptic weights and connection counts through conditions in mouse but not in cat's microcircuits

The sum connectivity volumes of the recorded assembly (total of all the individual contributions to the connectivity matrix) as well as the sums of all the functional connections were counted and the means were compared across conditions in mouse and cat. We report that within functionally connected cells, on average, the summed peaks' strengths and counts remained constant in all experimental conditions in mouse. In cat, on average, the total connectivity strength and counts remained unchanged following adaptation but increased following ketamine application. Indeed, in mouse and cat, adaptation fails to change the average strength (p) of connections across the population despite the modification of the links between cell-pairs. During adaptation-dependent

plasticity, neuronal circuits are subjected to two opposing mechanisms: the Hebbian mechanism that allows experience to change the properties of microcircuits and thus tends to destabilize the activity of neuronal networks by modifying both synapse number and strength, and another mechanism that stabilizes the total synaptic strength and number in the neuronal assemblies, which restores stability of their basic properties (Turrigiano et Nelson, 2000). It seems that a balance of the two forces is needed because the change following experience dependent-plasticity allows the microcircuits' refinement with stability to maintain responsiveness to inputs (Shatz, 1990; Turrigiano, 1999). These compensatory processes (strengthening of some links leads to weakening of others) probably leads to adjustment of synaptic efficacy in the network within a functional level. The homeostasis after adaptation occurs by synaptic scaling and appears to be independent of NMDAR activation (Turrigiano et Nelson, 2000), which may explain, in mouse, maintaining the total synaptic strength and numbers at a roughly constant range following the block of NMDAR by ketamine. Interestingly, in cat, results show a significant increase in the sum of connectivity strength following ketamine application. This could be explained by a spreading of functional connections between neurons belonging to distinct microcircuits. The parallel increase of the functional connection number following ketamine protocol may support this assumption.

4.3.4. Ketamine enhances neuronal synchrony in cat

We examined and compared the synchrony strengths and counts under different experimental conditions. Neuronal synchrony is generated when cells receive a common input from other neurons in the network (Denman et Contreras, 2014; Ghisovan et al., 2008; König et al., 1995). Our results revealed that ketamine induces, in cat but not in mouse, a higher probability of synchronizing inputs upon the recipient neurons compared to control and post-adaptation values. It has often been proposed that the basic outline of cortical information processing rests as much on the temporal patterns of spikes as on firing rates of cortical neurons (Decharms et Zador, 2000; Tiesinga et al., 2008). In addition, it was suggested that synchronous cortical inputs coordinate the activity of the recipient units with each other (Yu et Ferster, 2010). Indeed, cells receiving a common input, potentially fire synergistically and these correlated spikes should impact postsynaptic cells (Tiesinga et al., 2008). Accordingly, synchrony governs the activity in the primary visual cortex (Yu et Ferster, 2010), and increasing its strength by ketamine may lead to improved accuracy and reliability of the cortical processes. In addition, several arguments support

an association between neuronal synchrony and γ-oscillations in the visual cortices of cat and monkey (Engel et al., 1990; Siegel et König, 2003). It is worthwhile to indicate that in visual cortex, synchronization is due in part to specific horizontal connections between cortical domains having similar tuning properties (Gilbert et Wiesel, 1989; Malach et al., 1993). Previous work has also revealed that the increase in synchrony occurred for neurons with similar feature selectivity (Brosch et al., 1995; Eckhorn et al., 1988; Ts'o et al., 1986). For instance, synchrony was reported to be enhanced between neurons belonging to columns with iso-orientation preference. In addition, a growing number of studies performed on the cat visual cortex showed that neurons within a column discharge synchronously in response to oriented moving light bar. Thus, the state of highly synchronous activity is favored by the column organisation (Freiwald et al., 2001; Ghisovan et al., 2008; Gray, 1987; Gray et al., 1989; Gray et Singer, 1989). Therefore, the columnar arrangement may favor spike time coordination and thus synchrony between pairs sharing identical orientation tuning. Given the organisation of cells in radial columns according to their PO in cat and considering the apparent lack of columnar clustering in mouse, it becomes more likely to encounter close neurons with similar preferences in cat than in mouse where neighboring cells exhibit different selectivities. This could potentially explain why ketamine enhanced synchrony only in cat. However, it is worth to signal that the lack of increase in the synchronous activity in the mouse and its presence in cat, could not be related to the lack of column organisation in rodents given the fact that recordings were performed on only one cat which can imply a limitation of the results interpretation. Next, we expanded our analysis by computing for every CCG showing synchronous activity, the cumulative distribution of spikes. The cumulative sum (cs) graphs above histograms shows that all target neurons receive excitatory inputs in a window of 1 ms (examples of cs are shown in Fig. 4.5), which agrees with an increase of excitation in the network. Taken together, it seems that enhanced synchronous activity by ketamine yields cooperation between V1 cells which constitutes a supplementary path of information that may enhance the fine discrimination of orientation (Samonds et al., 2003; Samonds et Bonds, 2004). Thus, improving the neuronal processing and the feature encoding, that is, increasing information rate, is probably the advantage gained from the increase of synchrony (Wang et al., 2011). However, it must be underlined that other changes in the neural population (tuning width, tuning preference, dynamics) could well influence orientation discrimination.

Conclusion

In this paper, we examined the impact of ketamine on the maintenance of adaptation induced effects in terms of tuning proprieties and the microcircuit organisation of V1 cells. The most striking effects of ketamine are the abolition of adaptation effects and the imposition of new intrinsic properties of individual neurons as well as changes in the synaptic links between units. Although the tuning curve changes and the network recalibration were caused by both adaptation and drug application, the pathways involved in plasticity were different. From our own and previous results (Bachatene et al., 2013), it is tempting to suggest that push–pull mechanisms explaining adaptation effects are sensitive to antidepressant drugs. In cat, a supplementary effect of ketamine was found, that is, enhancement of the neuronal synchronization. Finally, the present study joins the classic antidepressant role of ketamine with the newer assumption of the trigger for neuroplasticity. Notably, the effects induced by locally applied ketamine are mimicked by systemically administered ketamine since it was revealed, in rat, that both cortical local application and systemic injections of ketamine lead to an increase in γ frequency (30–80 Hz) oscillations (Koulakov et Chklovskii, 2001). In addition, the local infusion of ketamine in rats was sufficient to quickly rescue the depression-like behaviours (Yang et al., 2018). Moreover, this study discloses how the microcircuits in V1 are set up and adjusted in response to different visual stimulation and protocols.

4.4. Experimental Procedure

4.4.1. Ethical approval

Nineteen CD-1 strain adult mice (weight: 28 – 31 g, 9 to 11 weeks) and one adult cat (weight: 2.0 – 3.0 kg, ~ 12 – 24 months) were supplied by the Division of Animal Resources of the University of Montreal. Animal anaesthesia, surgery and electrophysiological recordings were carried out following the guidelines of Canadian Council on Animal Care. The mouse and cat protocols were approved by the Institutional Animal Care and Use Committee of University of Montreal.

4.4.2. Animal preparation: anaesthesia and surgical procedures

Mice were anaesthetized with 10% urethane (1.5 g/kg) injected intraperitoneally. Lidocaine hydrochloride 2% (Xylocaine; AstraZeneca, Mississauga, ON, Canada), a local anesthetic, was administered subcutaneously at the surgical site and pressure sites. In the deeply anesthetized

animal, the brain was exposed and a dural flap was made (2.5 x 2.5 mm) over the visual cortex. General anaesthesia was assessed throughout the experiment by applying pinch reflexes. After the surgery, the mouse was fixed in a stereotaxic apparatus allowing visual stimulation of the entire contralateral visual field. Head movement was eliminated using a head holder. Within the period of recordings, acuity was improved by avoiding corneal desiccation of the stimulated eye using silicone oil applied in a thin layer. The unstimulated eye was closed.

The cat was prepared in conventional fashion. Briefly, it was sedated with a mixture of acepromazine maleate (Atravet; Wyeth-Ayerst, Guelph, ON, Canada; 1 mg/kg, i.m.) and atropine sulphate (ATRO-SA; Rafter, Calgary, AB, Canada; 0.04 mg/kg, i.m.), then anaesthetized with ketamine hydrochloride (Rogarsetic, Pfizer, Kirkland, QC, Canada; 25 mg/kg, i.m.). Lidocaine hydrochloride 2% was injected subcutaneously for local anaesthesia at the surgical site and xylocaine gel 5% (Astra Pharma, Mississauga, ON, Canada) was applied at the pressure sites. Craniotomy was carried out following the cat fixation in a stereotaxic apparatus. Duplocillin (0.1 mL/kg, i.m.; Intervet, Whitby, ON, Canada) and Tribrissen (30 mg/kg/day, s.c.; Schering-Plough, Point-Claire, QC, Canada) were injected to avoid bacterial infection. Muscle paralysis was induced with 40 mg gallamine triethiodide and maintained with 10 mg/kg/h gallamine triethiodide (Toronto Research Chemicals, ON, Canada) administered in 5% dextrose in lactated Ringer's nutritive solution. General anaesthesia was maintained by artificial ventilation with a mixture of N2O/O2 (70:30) supplemented with 0.5% isoflurane, and ensured throughout the experiment by electrocardiogram, electroencephalogram, end-tidal CO2 partial pressure (25 – 30 mmHg), and rectal temperature (using a heated pad to maintain a body temperature of 37.5 °C). Atropine sulfate (1%, Isopto-Atropine; Alcon, Mississauga, ON, Canada) was used to dilate pupils and phenylephrine hydrochloride (2.5%, Mydfrin; Alcon) was applied to retract the nictitating membranes. The loci of the area centrale were inferred from the position of the blind spots, which were ophthalmoscopically focused and projected onto a translucent screen. Corneal desiccation was prevented by fixing Plano lenses with artificial pupils (5 mm in diameter) allowing clear optical transmission. At the end of each experiment, the mouse was killed by intravenous injection of a lethal dose of 10% urethane (1.5 g/kg) and the cat via pentobarbital sodium (100 mg/kg, Somnotol; MTC Pharmaceuticals, Cambridge, ON, Canada).

4.4.3. Experimental steps

A schematic of the experimental setup is displayed in Fig. 4.1. Purple zone in mouse and cat illustrates V1. In Fig. 4.1A left (mouse), two glass electrodes filled with saline placed laterally at 1.2 mm between them were inserted in V1. The average cortical depth is less than 1mm. In cat (right), two 1.2 mm multisite electrodes (16 microsites for each electrode, inter-site 50 μm) were implanted in V1. Each electrode was lowered in V1 in a manner that eight microsites were placed at cortical depth of 500 μm, and eight microsites at 1000 μm. Fig. 4.1B illustrates experimental phases for both mouse and cat: control recordings were performed using eight orientations covering a span of 157.5° and equally spaced. The orientations were presented in a random order. Each orientation was applied in blocks of 25 trials. Each trial lasted 4.096 s. An interval of 1.0 - 3.0 s separated trials during which no stimulus was presented (dark screen). Control phase was followed by the adaptation period where an adapting stimulus (90°) was presented continuously for 12 minutes. During this adaptation period no recordings were performed. Immediately following the adaptation session, test orientations were presented. Once post-adaptation recordings were completed, drug was applied using a strip of filter paper (1 × 1 mm) impregnated with a racemic mixture, i.e. (R,S)-ketamine (10 mM) and placed over the animal's cortex next to the recording sites (yellow square). Ten minutes after ketamine application, test orientations were presented, and recordings were performed. To assure that the effect of the drug application on the post-adaptation orientation tuning curves was indeed due to ketamine and not to random fluctuation or to the solvent (0.9% NaCl), we placed simultaneously a filter paper soaked with only solvent over the mouse cortex at electrode e1 and with ketamine at electrode e2. Cells' responses were recorded simultaneously by e1 and e2 10 min after the solvent and ketamine application (Fig. 4.1C). This control experiment tested the spread of ketamine. In cat, recovery sessions followed the ketamine application in which four recordings were performed. The first recording was done 90 minutes following the post- ketamine phase. The other recordings were done every 30 minutes (Fig. 4.1D).

4.4.4. Visual stimulation and electrophysiological recording

Mouse

Monocular stimulation was applied with an eye screen-distance of 30 cm in mouse. Drifting sine wave gratings were generated with a VRG Volante 34020 graphic board (Vision Research Graphics, New Hampshire, USA). Gratings were presented on a 21-in. monitor (60 Hz refresh rate,

Mitsubishi FHS6115SLK Color Display Monitor, Tokyo, Japan) with 1024×512 pixels. Spatial frequency, temporal frequency, and velocity were fixed at 0.07 cycles/°, 2 Hz, and 4°/s, respectively. These parameters were set to evoke the best firing in mouse and were maintained constantly throughout the duration of the experiment. The center of the monitor was positioned at about 30.7° azimuth, 0° elevation. Since the mouse excitatory receptive field is rarely smaller than 10° (Mangini et Pearlman, 1980), no attempt was made to stimulate it. Two glass electrodes filled with 0.9% NaCl simultaneously recorded neuronal activities from V1 superficial layers (<1 mm). For the entire study and in all conditions, the signal from several recording sites (multi-unit activity) was band-pass filtered (300 Hz–3 kHz), amplified, displayed on an oscilloscope, and audio-monitored. Multi-unit activity was digitized and recorded with data acquisition software (Spike 2, Cambridge Electronic Design, CED Limited, Cambridge, England).

Cat

Pharmacology and modelling experiments shows that the mean plasma half-lives after ketamine anesthetic doses were 151 min (Clements et al., 1982). In cats, the anesthesia was initialized by systemic administration of ketamine, to be sure that NMDARs are not already blocked, at least partially, before the local application of ketamine, the initial ketamine application was carried out at the begging of the experiment to relax the animal, while tests in visual cortex were performed many hours later (at least eight hours).

Monocular stimulation (drifting sine wave gratings) was generated with a VSG 2/5 stimulation system (Cambridge Research Systems, Rochester, Kent, UK) and presented on a 21-in. monitor (60 Hz refresh rate, Mitsubishi FHS6115SLK Color Display Monitor, Tokyo, Japan) placed 57 cm from the cat's eyes, with 1024×768 pixels, running at 100Hz refresh (Sony GDM-F 520 Trinitron, Tokyo Japan). Maximal responses were evoked with the following parameters: mean luminance = 40 cd/m2, contrast = 80%, spatial frequency = 0.24 cycles/°, temporal frequency = 3 Hz, size = 7-10°. Gratings were placed in the cat receptive field that was characterised manually using an ophthalmoscope. Multiunit activity was recorded using depth electrodes. Electrodes were composed of 16 microsites equally spaced on a silicon linear array (A1x16-5mm-100–177-A16, Neuronexus, Ann Arbor, MI, USA; 1 – 2 MΩ at 1 kHz) and were manually lowered perpendicular to V1 using micromanipulators and allowing recordings from 0.4 - 0.5 mm (layer 2/3) and 0.8 - 1 mm (layer 5/6).

Multiunit signals were acquired with a Blackrock Cereplex system at 30,000 samples/sec, band-pass filtered (300 Hz–3 kHz), amplified, displayed on an oscilloscope and audio-monitored.

4.4.5. Data analysis

Cells were well isolated from multi-unit recordings (MUR) (Fig. 4.1E1) using the off-line spike sorting method which was based on cluster classification in reduced space. The action potentials fired by a neuron recorded in a given electrode have a particular shape. Hence, cell-separation and the stability of each cell's activity across conditions was verified qualitatively by visual control of spike-waveforms (Fig. 4.1E2). To further confirm that every sorted spike was unique, cluster-isolation using first principal components analyses (PCA) with K means index (k = 2.5) was used as feature extraction and dimensionality reduction method. PCA showed separation and no overlap between clusters of cells (Fig. 4.1E3). In addition, autocorrelograms (ACG) (Fig. 4.1E4) were computed and showed absence of events at 0 ms on the time-scale point indicating the absolute refractory period and suggesting no contamination from noise. Peri-stimulus time histograms (PSTH) (Fig. 4.1E5) and raster plots (RP) (Fig. 4.1E6) denote for each trial the cell's spontaneous activity and its response to the stimulus presentation. Orientation tuning curves were constructed from raw data. Because the interval between the stimulus orientations is relatively large, 22.5°, the raw tuning curves may be imperfect in determining the preferred orientation (PO). Therefore, van Mises tuning curves were constructed from raw data. Thus, we fitted our raw data with the von Mises function (Swindale, 1998)which is defined as:

$$M(\Theta) = A.e^{b[\cos(\Theta - c)]} + d$$

where A is the value of the function at the PO, c, and b is a width parameter. The parameter d represents the neuron's spontaneous firing rate (FR) (Kohn et Movshon, 2004; Mangini et Pearlman, 1980). The above calculation allowed us to determine with precision the PO of neurons and then measure shifts in orientation preference. The goodness of fit was verified by the R2 values in mouse and cat.

The shifts of tuning curve peaks between several conditions (adaptation, ketamine, and recovery) were calculated between pre- and post- condition using the following formula:

$$\textbf{Shift} = |XC \textbf{ post} - XC \textbf{ pre}|$$

where *Xc* is the central value derived from the Van Mises fit. In the present investigation, all the shifts inferior to 5° were considered not significant (Ghisovan et al., 2009; Jeyabalaratnam et al., 2013a). In this study, we fixed a threshold of 24° to specify whether the post-adaptation shift amplitude is small or big. Hence, shift amplitudes inferior to 24° were considered small. Then, we examined the ketamine effect on the PO of the two cell categories (cells displaying, following visual adaptation, small shifts, or cells showing big shifts). In order to compare the adaptation induced shifts (*Xc control – Xc post-adaptation*) to ketamine induced shifts (*Xc control – Xc post-ketamine*), a Wilcoxon paired test was performed with a significance level of 95%. In addition, to test potential correlation between the post-adaptation control shifts and post-ketamine control shifts, and since the "control shifts" are subtracted from both the post-adaptation and post-ketamine shifts, a permutation testing method for multiple linear regression was performed on R package to obtain p-values.

Orientation selectivity index (*OSI*) was calculated from data as the minimum firing rate (FR_m) divided by the firing rate for the preferred orientation (FR_{PO}), and subtracting the result from 1 (Liao et al., 2004b; Ramoa et al., 2001b) as follows:

$$OSI = 1 - (FR_m / FR_{PO})$$

FRm and FRpo were derived from the fitted tuning curve. The *OSI* value denotes the strength of the OS. The closer the *OSI* is to 1, thus a small baseline/PO ratio, the stronger the OS. The *OSI* threshold for tuned cells was fixed at 0.3. Therefore, cells with an *OSI* value inferior to our threshold were considered untuned. To verify if ketamine's impact on maintaining visual adaptation depends on the degree of the cell's tuning, the control *OSI* value was calculated.

4.4.6. Crosscorrelograms, shift predictor and confidence limits

In order to investigate the impact of adaptation on the strength of inter-neuronal relationships and to show if ketamine modifies the response correlation strength of cell-pairs established after adaptation, we performed crosscorrelograms (CCGs) between simultaneously recorded spike trains of neuron-pairs (in mouse and cat) at all the applied orientations and in all conditions (control, post-adaptation, post-ketamine, and post-recovery). In CCGs, one cell is set as reference and the second as target. Hence, the CCG is a histogram of the spike distribution of the target cell

in relation to the spikes of the reference cell within a determined time-frame. This correlation probability reveals the functional connections between cell-pairs.

In CCGs, the time axis is divided into bins of 1 ms. In each bin we measured maximum number of correlated events in a contiguous 1 ms interval on the right side of each CCG and divided this sum by the number of reference events. Hence, when multiplied by 100, the efficacy ratio is equivalent to the probability of a functional connection between two units (a reference and a target cell) in one particular bin. For each bin, the probability is significant when it exceeds the confidence limit. Therefore, the significance depends on the bin and the functional connection between two neurons is illustrated by a significant peak of at least one bin (Alloway et Roy, 2002) within a window of 5 ms offset from zero. The $\pm$ 1 ms significant bins around zero were classified as synchronous events (putative common afferent input to both cells). The statistical threshold for the significance peak was set at 95% and presented by the red line in Fig. 4.5. The *Y*-axis corresponds to the probability (*p*) of a neuron firing in the small bin of the size *b* considering the spike train is a Poisson process (Moshe Abeles, 1982) ; this probability *p* is calculated as follows:

$$p = F \times b$$

$$F = N / T$$

where *F* is the neuronal firing rate, *b* is the bin size of the calculated firing of the neuron, *T* is the total time interval, and *N* is the number of spikes in that interval. The expected bin count *C* for the histogram has a Poisson distribution and was calculated as follows:

$$C = p \times Nref$$

here *Nref* represents the number of the reference events (spikes of the reference cell, that is, at time zero in the CCG). The 95% confidence limit is calculated for *p* and *C* according to Abeles (1982) as follows:

$$Low\ Conf. = x\ such\ that\ Prob\ (S < x) = 0.005$$

$$High\ Conf. = y\ such\ that\ Prob\ (S > y) = 0.005$$

where S represents a random variable, which has a Poisson distribution with parameter *C*.

The raw CCGs were shift-corrected by subtracting a shift-predictor algorithm in order to eliminate the putative significant peaks due to the simultaneous stimulation of both cells during each trial (Perkel et al., 1967) .

For every CCG, the cumulative distribution of spikes was computed. This computation represents the modulation of the FR of the target neuron after the reference neuron fired a spike. The cumulative sum (cs) graphs above histograms are calculated for each bin *i* as:

$$Cs[i] = \sum_{(j=1)}^{i} bc[j] - A^i; i = 1, 2, ..., N$$

where *bc* is the bin counts (i.e., the number of spikes falling inside the histogram bin *j*) and *A* the average of all *bc*.

To perform matrices of connectivity, 346 neuron - pairs in mouse and 345 neuron – pairs in cat were used. In cat, contrary to mouse (Shapiro-Wilk normality test with 95% confidence interval: $p < 0.0001$, for control condition $W = 0.3598$; D'Agostino & Pearson omnibus normality test with 95% confidence interval: $K2 = 569.9$, $p < 0.0001$), data were sampled from a Von Mises distribution. Therefore, in cat, a Pearson coefficient was calculated to assess the significance of the difference between two matrices (post-adaptation and post-ketamine matrices) (Bachatene, Bharmauria, Cattan, Chanauria, et al., 2015; Cattan et al., 2014). In mouse, we used a non- Von Mises statistics (Spearman) to quantify correlation between data matrices.

A computation of the number of connections and the CCG magnitudes of all summed pairs was performed at all presented orientations and in all conditions (control, post-adaptation, and post-ketamine). A repeated measures ANOVA test was performed among three conditions (control, adaptation, and ketamine) with a significance level of 95% followed by Sidak's multiple comparisons as post hoc test (GraphPad Prism 9.3.1) to compare the mean of the number of connections (ΣC) as well as the sums (ΣP) of CCG magnitudes between conditions and cell pairs. Furthermore, in cats, pair-wise synchrony strengths (ΣPs) and the number of coupling (ΣPc) for the matrices were computed for all conditions and all presented orientations. Values of ΣPs and ΣPc were compared between conditions and cell pairs using a repeated measures ANOVA test with a significance level of 95% followed by Sidak's multiple comparisons as post hoc test (GraphPad Prism 9.3.1).

Acknowledgements:

We acknowledge the Conseil de Recherche en Sciences Naturelles et en Genie du Canada (CRSNG) to support the completion of this study, Steve Itaya for his comments on the early version of the manuscript and Pierre Legendre for his advice and support during statistical tests.

Funding information: NSERC

This work was supported by the Natural Sciences and Engineering Research Council of Canada (NSERC) [RGPIN/04813, 2017]

Conflict of Interest Statement:

Authors declare that they have no conflict of interest

5. Post-adaptation plasticity shapes cortical neuron tuning properties

Ouelhazi A, Lussiez R, Molotchnikoff. S (2022). Post-adaptation plasticity shapes cortical neuron tuning properties.

Soumis à **: Neuroscience Letters** (NSL-221239).

Numéro CDEA : **20-068**

Rôles des auteurs

Conceptualization, O.A. Methodology, O.A.; Software, O.A.; Validation, O.A.; Formal Analysis, O.A.; Investigation, O.A.; LR.; and M.S.; Resources, O.A; Data Curation, O.A.; Writing – Original Draft, O.A.; Writing – Review & Editing, O.A. and M.S; Visualization, O.A.; Supervision, M.S. and O.A.; Project, M.S; Funding Acquisition, M.S. and NSERC Canada.

Abstract

In mouse, whose V1 has no orientation map, neurons sharply tuned to orientation were observed. The degree of the orientation selectivity could be measured with the orientation selectivity index (OSI). The goal of this paper is to disclose the modification in the OSI of V1 cells after visual

adaptation (prolonged exposure to a non-preferred orientation), and if the modifications in the synaptic scheme of the V1 network after adaptation leads to changes in the OSI.

Electrophysiological analysis showed that adaptation mainly increases the OSI of tuned cells but doesn't affect the OSI of untuned cells. Cross-correlogram data processing demonstrates that, overall, adaptation promotes a reorganisation of V1 networks, since many individual cell-pairs exhibit changes in their response correlation. In addition, sharp OS emerges in networks showing new connectivities.

1) The mean OSI before and after adaptation remain similar

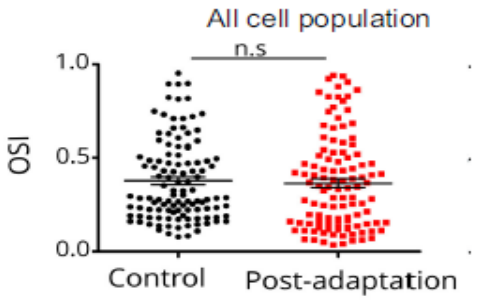

2) Post-adaptation emerged connections enhance the cell's tuning

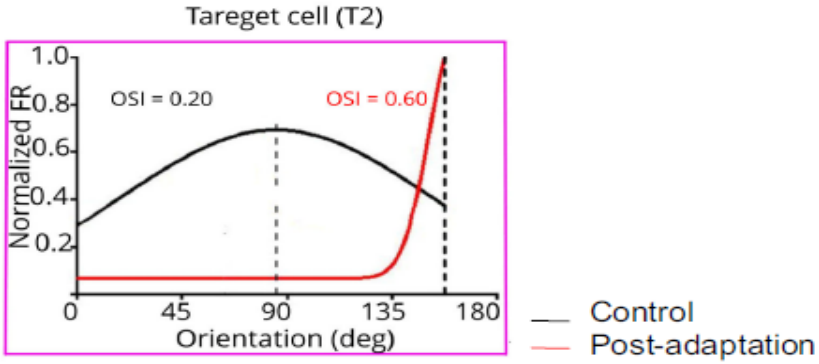

Control micricircuit

Post-adaptation microcircuit

5.1. Introduction

To encode visual inputs, cortical neurons, embedded in a microcircuit, must generate selective responses for distinct stimulus features. In the visual cortex, visual object representation arises from activation of functional domains in the cerebral cortex that encode feature specific information such as orientation, color, and motion direction (Hu et al., 2018; Li et al., 2013; Tanigawa et al., 2010). The selective responses of neurons to the orientation of edges has been extensively studied (Campbell et al., 1968; Carandini et Ferster, 2000; Chao-Yi et Creutzfeldt, 1984; Douglas et al., 1991; Hubel et Wiesel, 1959; Monier et al., 2003; Nowak et al., 2008; Schiller et al., 1976). Many studies have shown that sharp selectivity is observed even in species where V1 lacks an orientation map, such as rodents (Bonin et al., 2011; Metin et al., 1988; Niell et Stryker, 2010; Ohki et al., 2005; Regan et Beverley, 1985; Tan et al., 2011). In addition, the degree of orientation selectivity, measured by the orientation selectivity index (OSI), is highly heterogeneous across neurons. In mouse V1, strongly tuned neurons, showing highly selective responses to oriented stimuli, have neighboring neurons that do not necessarily show a similar degree of orientation discrimination. Such feature specific units have specific parallel networks (Roe et al., 2012) and therefore visual processing is based on the activation of multiple circuits. However, sensory systems need to process signals in a highly dynamic way in order to efficiently respond to variations in the animal's environment (Calhoun et al., 2019; Salay et al., 2018). Several studies showed that the visual system is subject to neuroplasticity since the neurons' firing changes according to stimulus properties. Other studies suggest that visual processing should be optimized and adapted to the properties of the stimulus. For instance, it is well known that orientation discrimination is subject to short term learning as shown in visual adaptation after the imposition of a non-preferred orientation for several minutes (Dragoi et al., 2000; Ghisovan et al., 2009). It was shown in mouse that adaptation shifts the peak of the neuron's tuning curve (Jeyabalaratnam et al., 2013b). However, is the emergence of a new selectivity following adaptation accompanied with a modification in the OSI? Moreover, since visual processing in V1 is constrained by the structure of cortico-cortical neural connections (D'Souza et Burkhalter, 2017; Douglas et Martin, 2004; Livingstone et Hubel, 1983; Vélez-Fort et al., 2014), it is unclear whether connectivity between cells in the network, following adaptation, influence the sharpness of the acquired selectivity. It is also still unknown if the dynamic information processing might be supported by a network reorganisation. Since adaptation affects orientation selectivity, it can be used to explore

cortical plasticity sustaining cortical map changes and connectivity reorganization. The goal of this paper is to investigate the effect of adaptation on the OSI of the cells in relation to the dynamics of the network connectivity; that is to investigate if neuron's inherent proprieties alteration might result in a change of correlated and uncorrelated neural activity through changes in firing rates. Electrophysiological comparisons of mouse monocular stimulation in control and post-adaptation groups showed that in all the recording cell populations, adaptation failed to modify the mean OSI. However, cross-correlation techniques, which disclose functional relationships between cells, showed that in networks where connections are not modified across protocols, the degree of selectivity remains unchanged through all conditions. However, the emergence of new connections in a microcircuit, following adaptation, enhanced a cell's tuning.

5.2. Materials and methods

The animal studies were approved by the Institutional Animal Care and Use Committee of the University of Montreal following the guidelines of the Canadian Council on Animal Care. Experiments (animal surgery procedures and electrophysiological recordings) were performed using nineteen CD-1 strain adult mice (weight: 28 – 31 g, 9 to 11 weeks). Animals were supplied by the Division of Animal Resources of the University of Montreal. Anesthetized mice were prepared for electrophysiological recordings in primary visual cortex as described below.

5.2.1 Animal preparation, visual stimulation, and electrophysiological recording

Mice were deeply anaesthetized with 10% urethane (1.5 g/kg), injected intraperitoneally. A local anesthetic (Lidocaine hydrochloride 2% (Xylocaine; AstraZeneca, Mississauga, ON, Canada)) was administered subcutaneously at the surgical site and pressure sites at the start of the surgery. An incision was made into the skin over the brain and a dural flap was made (2.5 x 2.5 mm) over the visual cortex. Mice were placed in a stereotactic frame allowing monocular visual stimulation of the entire contralateral visual field. The unstimulated eye was closed. Tungsten microelectrodes (2–10 MΩ at 1 kHz; Frederick Haer & Co, Bowdoinham, ME, USA) were inserted at a depth less than 1mm to record the signal. The latter was amplified, band-pass filtered (300 Hz–3 kHz), digitized and recorded with a data acquisition software (Spike 2, Cambridge Electronic Design, CED Limited, Cambridge, England).

Monocular stimulation (drifting sine wave gratings generated with a VRG Volante 34020 graphic board (Vision Research Graphics, New Hampshire, USA)) were presented, with an eye screen-distance of 30 cm, on a 21-in. monitor (60 Hz refresh rate, Mitsubishi FHS6115SLK Color Display Monitor, Tokyo, Japan) with 1024×512 pixels resolution. The center of the monitor was positioned at about 30.7° azimuth, 0° elevation. Spatial frequency, temporal frequency, and velocity were set to evoke optimal firing in mouse, and fixed at 0.07 cycles/°, 2 Hz, and 4°/s, respectively. Eight orientations covering a span of 157.5°, equally spaced and shown in a random order were presented in the control condition (Fig .5.1A). Each orientation was applied in blocks of 25 trials of 4.096 s each, separated by an interval of 1.0 - 3.0 s during which a dark screen was presented. An adaptation session followed the control phase where an adapting stimulus (90°) was presented continuously for 12 minutes. Test orientations were presented immediately following the adaptation period (Fig. 5.1A). Control and post-adaptation recordings were carried out, but no recordings were performed during adaptation session (Fig. 5.1B).

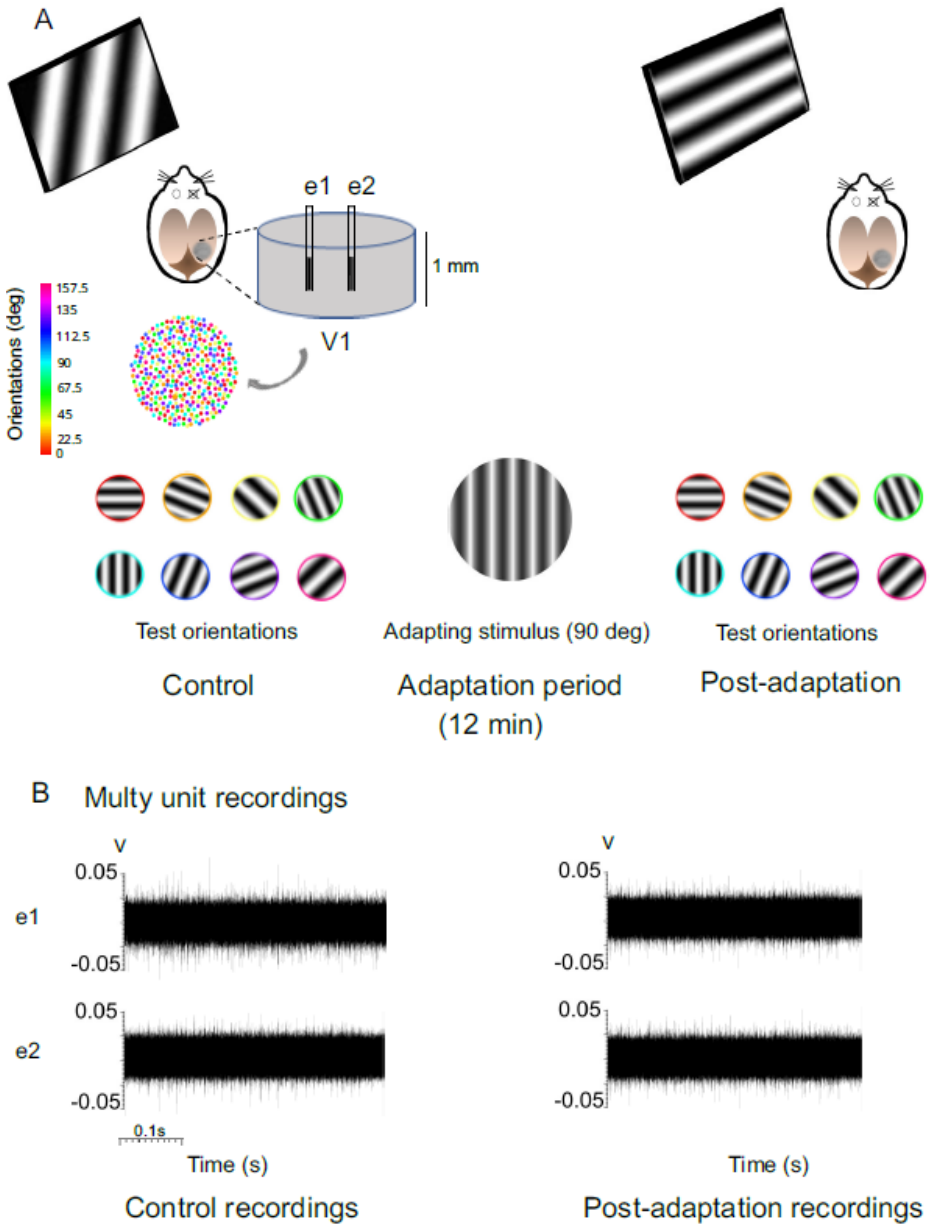

Fig 5.1. Experimental design. (A) Cartoon displaying visual stimulation on mouse striate cortex. Two multisite electrodes (e1 and e2) were inserted into V1 to record cells with different PO (preferred orientations), organised in salt and pepper fashion. (B) Experimental time course. (C) Test orientations were performed in the control condition, and after 12 min of uninterrupted presentation of an adaptor at 90°. All the orientations were randomly presented on the screen in 25 trials with arbitrary intervals (1-3 s).

Action potentials were sorted from the multi-unit signal using the spike sorting method based on cluster-isolation. First principal components analysis (PCA) with K means index (k = 2.5) were used to confirm no overlap between clusters of cells. The stability of each cell's response across

conditions was verified qualitatively by visual control of the cluster disposition and of the waveform shape. Auto-correlograms were systematically computed to ensure proper single-cell capture (absence of events at 0 ms). Then, orientation tuning curves were constructed from the raw data and fitted with the von Mises function (Swindale, 1998)allowing a precise determination of the neuron's preferred orientation (PO). The von Mises function is defined as:

$$M(\Theta) = A.e^{b[\cos(\Theta - c)]} + d$$

where A is the value of the function at the PO, c, and b is a width parameter. An additional parameter, d, represents the spontaneous firing rate of the cell (Kohn et Movshon, 2004; Swindale, 1998) . It was also necessary to determine the degree of tuning of each cell in our sample. To this end, an orientation selectivity index (OSI) was calculated for each cell from the fitted tuning curve and calculated as follow:

$$OSI = 1 - (FR_m / FR_{PO})$$

Where FRm is the minimum firing rate and FRPO is the firing rate for the PO.
The OSI value denotes the strength of the orientation selectivity (OS); hence, the closer the OSI is to 1, the stronger the tuning (Liao et al., 2004a; Ramoa et al., 2001a). In this study, an OSI threshold of 0.4 was fixed for tuned cells (T). Therefore, cells with an OSI value inferior to this threshold were considered untuned (UT). Paired two-tailed Student's tests with a significance level of 95% were carried out to compare the mean OSI between control and post-adaptation conditions.

Crosscorrelogram analysis, shift predictor and confidence limits

To examine the impact of the functional relationships established after adaptation between cell-pairs (a source and a target cell) on the OSI variation of the target cell, we measured correlations in the spike count between simultaneously recorded pairs of neurons for all presented gratings in control and post-adaptation conditions. The correlation probability is calculated for each bin (1 ms) within a window of 5 ms offset from zero. We reveal functional connections between cell-pairs if this probability is significant (it exceeds the confidence limit sets at 95%). In the CCG, the X-axis corresponds to the time and the Y-axis corresponds to the probability (p) of a neuron firing in the small bin of the size b considering the spike train is a Poisson process (Moshe Abeles, 1982); p is defined as follows:

$$p = F \times b$$

$$F = N / T$$

here F is the neuronal firing rate, b is the bin size of the calculated firing of the neuron, T is the total time interval, and N is the number of action potentials in that interval. The expected bin count C for the histogram has a Poisson distribution and was defined as follows:

$$C = p \times Nref$$

where Nref represents the number of the reference events, that is, the spikes of the source cell at time zero in the CCG. The 95% confidence limit is calculated for p and C according to Abeles (1982) as follows:

$$Low\ Conf. = x\ such\ that\ Prob\ (S < x) = 0.005$$

$$High\ Conf. = y\ such\ that\ Prob\ (S > y) = 0.005$$

Where S represents a random variable, which has a Poisson distribution with parameter C.
To eliminate the putative significant peaks due to the simultaneous stimulation of cell-pairs during each trial (Perkel et al., 1967), the raw CCGs were shift-corrected by subtracting a shift-predictor algorithm.

To validate that the found effects of adaptation are significantly above chance, statistical tests were used with an α criterion of 0.05. For data sampled from a gaussian population, paired t-test was used to compare the set of data between the two conditions (control and post-adaptation). However, non-gaussian statistics were performed for data that doesn't pass normality test (Shapiro-Wilk normality test). Wilcoxon paired tests and a Spearman correlation were carried out to compare data between the two conditions and divulge correlations, respectively (GraphPad Prism 9.3.1).

5.3. Results

To elucidate the effect of adaptation in relation with cortical microcircuit dynamics on the neurons' degree of selectivity, first we performed orientation tests before and after visual adaptation to determine the Gaussian orientation tuning curves in control and in post-adaptation conditions. Then we calculated the OSI from the fitted tuning curve of the recorded neurons in the two

conditions. The functional relationships between neuron-pairs were determined using CCG tool (see materials and methods). In this study, 114 cells were sorted and could be tracked in the two phases (control and post-adaptation) of recording sessions.

5.3.1. Effect of adaptation on the cells'OSI

Out of investigated 114 cells, 47 (41.23%) cells were tuned (T) to orientation in control condition, the remaining cells (n = 67, 58.77%) were untuned (U). Across the T population, 30 cells (63.2%) exhibited tuning after adaptation (OSI > 0.4); they were tuned in all conditions (T-T). However, 17 units (36.17%) were tuned in control but exhibited absence of OS post-adaptation (T-U). Out of the U population, most of cells (n = 52, 77.61%) displayed no PO prior and post-adaptation (U-U), but 22.39% of U neurons (n = 15) acquired a significant OS after adaptation (U-T) (Fig. 5.2A). Hence, following adaptation, similar proportions of T (n = 45, 39.47%) and U (n = 69, 60.52%) units were observed compared to control condition (T: n = 47, 41.23%; U: n = 67, 58.77%) (McNemar test, X2MN = 0.125, P = 0.752) (Fig. 5.2B). Globally, the comparison of the OSI of all sorted cells pre- (OSIpre) and post-adaptation (OSIpost) showed no significant effect of visual adaptation on the strength of the cells' selectivity (Wilcoxon paired test, P = 0.9589). To further understand this result, we compared the neuron's OSIpre and OSIpost in the two different populations: U and T units in Control (regardless to their tuning following adaptation). Results showed that both T and U cells did not exhibit a significant OSI variation between the two conditions (Wilcoxon paired test, P = 0.0843 for T units and p = 0.0677 for U units) (Fig. 5.2C). However, the effect of adaptation on OSI values was different depending on the sub-populations (U-U, T-T, T-U, or U-T). While the adaptation failed to change the OSI of U-U sub-population (Wilcoxon paired test, P = 0. 3099), the OSI increased significantly in the T-T sub-population (Paired t-test, P = 0.0090, t = 2.772, df =34) (Fig. 5.2D). For the T-U sub-population, adaptation significantly decreased the OSI by 26.52% (Paired t-test, P < 0.0001, t = 7.713, df =15). By contrast, following adaptation, the U-T sub-population showed a significant increase of their OSI by 48.7% (Paired t-test, P < 0.0001, t = 9.193, df =16) (Fig. 5.2E).

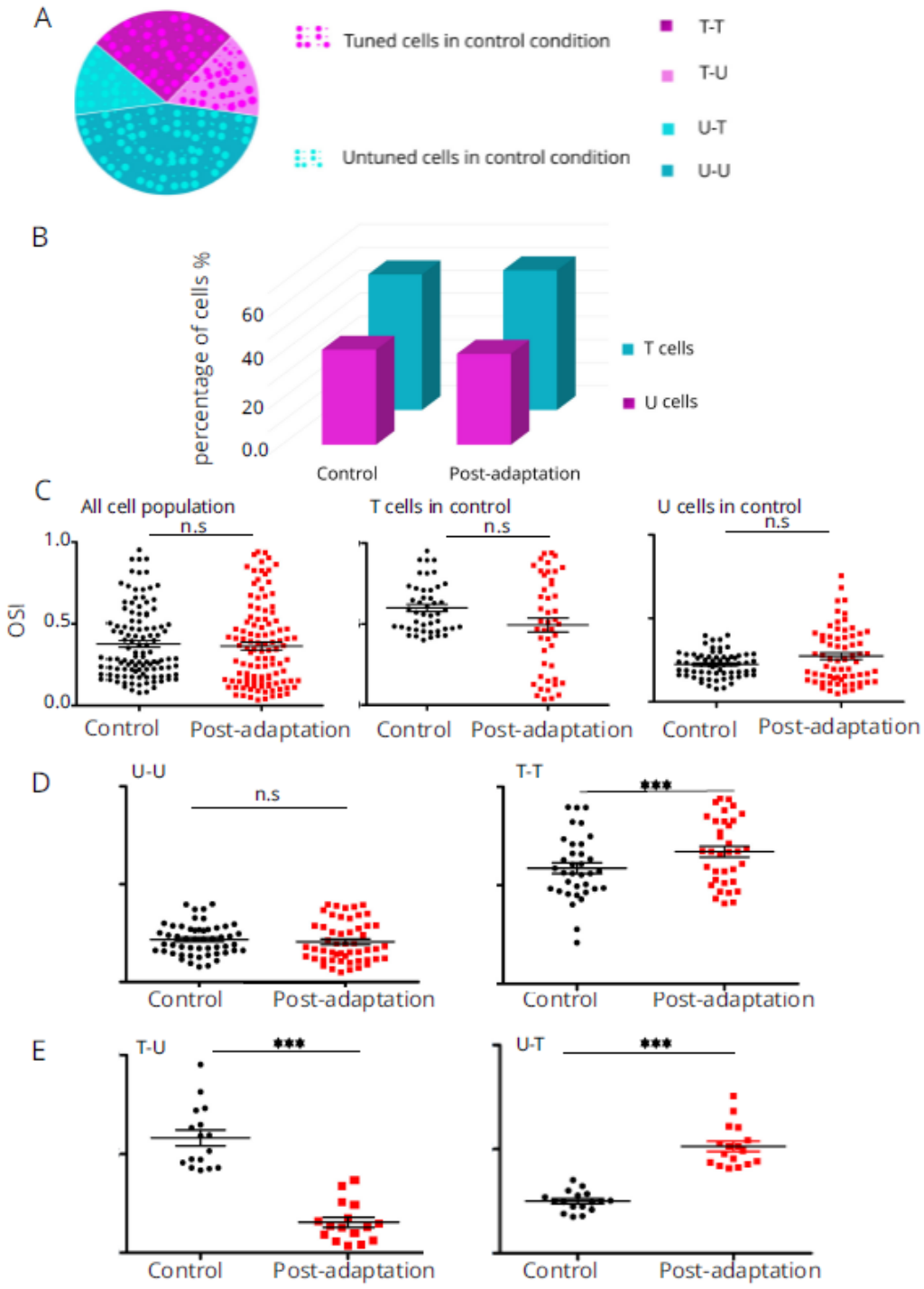

Fig 5.2 Percentage of tuned and untuned cells and the impact of adaptation on the OSI values. (A) Pie chart showing 41.23% tuned (T) cells and 58.77% untuned (U) cells in control condition. Across the T population, 63.2% were tuned in all conditions (T-T) and 36.17% were tuned in control but exhibited absence of OS post-adaptation (T-U). Out of the U population, 77.61% were

untuned in all conditions (U-U) and 22.39% acquired a significant OS after adaptation (U-T). (B) In control condition, the proportion of T units (41.23%) and U units (58.77%) were similar to the proportions of T units (39.47%) and U units (60.52%) following adaptation (McNemar test, X2MN = 0.125, P = 0.752). (C) There was no significant effect of visual adaptation on the OSI of all the cell populations (control OSI = 0.37±0.21 vs post-adaptation OSI = 0.36±0.25; Wilcoxon paired test, P = 0.9589). The OSI of T and U cells in control condition did not change after adaptation. For T cells, control OSI = 0.60±0.15, post-adaptation OSI = 0.49±0.29; Wilcoxon paired test, P = 0.0843. For U cells, control OSI = 0.22±0.07, post-adaptation OSI = 0.27±0.16; Wilcoxon paired test, P = 0.0677. (D) There was no significant variation between the OSI of the U-U sub-population in control and post-adaptation conditions (control OSI = 0.21±0.07 vs post-adaptation OSI = 0.20±0.10; Wilcoxon paired test, P = 0.3099). The OSI of the T-T sub-population increased significantly after adaptation (control OSI = 0.58±0.16 vs post-adaptation OSI = 0.67±0.16; paired t-test, P = 0.0090, t = 2.772, df =34). (E) Following adaptation, while the OSI of T-U sub-population decreased significantly by 26.52% (control OSI = 0.58±0.15 vs post-adaptation OSI = 0.15±0.10; paired t-test, P < 0.0001, t = 7.713, df =15), the OSI of the U-T sub-population increased significantly by 48.7% (control OSI = 0.25±0.04 vs post-adaptation OSI = 0.51±0.09; paired t-test, P < 0.0001, t = 9.193, df =16). The bars displayed around the average in C – E represent the standard deviation.

5.3.2. Role of dynamic neuronal connections in shaping cortical neuron tuning properties after adaptation

Following adaptation, some cortical functional connections in a microcircuit are modified by changing synaptic weights. Hence, in the network, new connections could emerge, whereas others could be preserved across conditions (Bachatène et al., 2015; Bachatene, Bharmauria et Molotchnikoff, 2012). As a neuron receives its inputs from many cells, it is unclear whether the preserved or the new links of the network influences its post-adaptation selective output. To this end, CCGs were computed between spike trains of neuron pairs for each recording at all blocks of applied orientations in control and post-adaptation conditions. Data allowed us to retrace all the inputs a cell is receiving, that is, the assembly connectivity pre- and post-adaptation. Then, the OSIpre and OSIpost of cells exhibiting the same connections across conditions were compared as well the OSIpre and OSIpost of cells receiving new connections following adaptation. Fig. 5.3A illustrates functional relationships between the same three cells before and after 12 min of adaptation. T1 is a target neuron which preserved its coupling with two sources (S1 and S2 units) across conditions and displayed OSIpre and OSIpost = 0.46. Hence, in a network exhibiting preserved connections through conditions, the degree of selectivity post-adaptation remains

unchanged compared with control condition (Wilcoxon paired test, P = 0.08, n = 180), even though cells exhibited a new PO following adaptation (Fig. 5.3A middle, the T1 PO was 67.54 deg in control condition and became 135.72 deg after adaptation). However, cells receiving new connections following adaptation varied their output tuning strength in ways that demonstrate sharper selectivity. Fig. 5.3B shows a typical example of a neuron (T2) displaying new connections with S1' and S2' after adaptation. The OSIpre and the OSIpost were 0.20 and 0.60 respectively. The comparison of OSIpre and OSIpost values for this group of target cells reveals a significant increase of their OSIpost compared with OSIpre (Wilcoxon paired test, P = 0.0018, n = 80). Therefore, within a microcircuit, new connections influence cells' output and contribute to improve its tuning curve. In addition, Spearman correlation revealed a strong correlation between the OSIpre and the OSIpost for this group of cells (r = 0.60, P = 0.0001). In summary, it seems that the OSI changes are related to the cell's functional relationship dynamics.

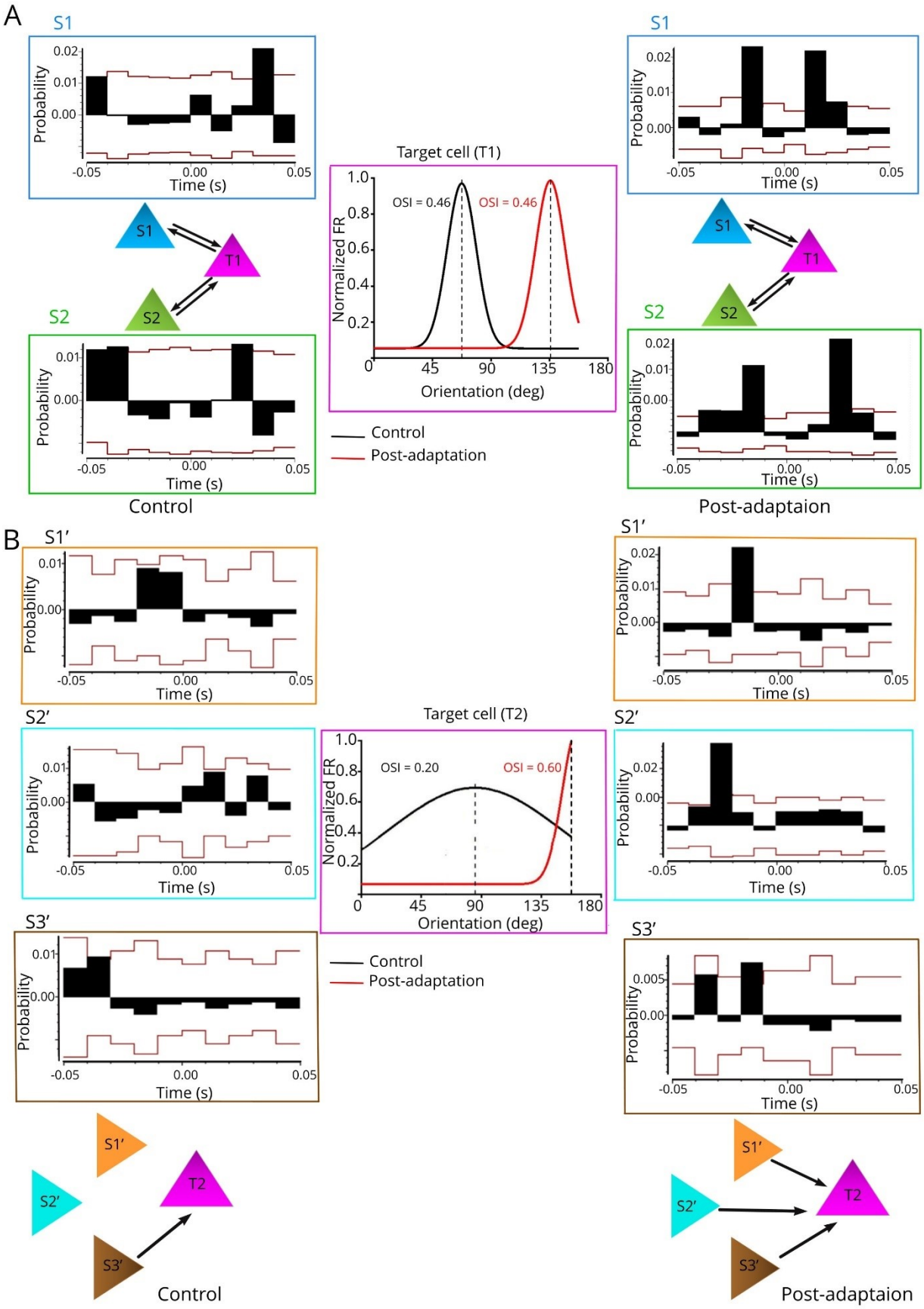
A
S1
Probability
Time (s)
S2
T1
Target cell (T1)
Normalized FR
OSI = 0.46
OSI = 0.46
Orientation (deg)
Control
Post-adaptation
Control
Post-adaptaion
B
S1′
S2′
S3′
T2
Target cell (T2)
OSI = 0.20
OSI = 0.60
Control
Post-adaptation
Control
Post-adaptaion

Fig 5.3 Typical examples of two target cells embedded or not in a conserved microcircuit. (A) The target cell T1 (magenta) participating in an unchanged microcircuit, that is, it showed the same bidirectional connections, revealed by CCGs, with two source cells S1 (blue) and S2 (green). In control condition, S1 and S2 connected T1 with the same strength of connection ($p = 0.012$). T1 projected on S1 and S2, with $p = 0.021$ and $p = 0.013$, respectively. Following adaptation, T1 received the same connections from S1 ($p = 0.022$) and S2 ($p = 0.020$) and projected to the same cells S1 and S2 with $p = 0.021$ and $p = 0.029$, respectively. T1 exhibited a shift of the peak of its tuning curve following adaptation from 67.54° to 135.72°, but it maintains the same OSI value (0.46) between control and post-adaptation conditions. (B) The target cell T2 (magenta) is embedded in a microcircuit showing new connections after adaptation. CCGs showed a unique connection between the source cell S3' and T2 ($p = 0.009$). After adaptation, two new connections with T2 were added in addition to the pre-existing connection ($p = 0.007$). S1' and S2' connected T2 with respective strengths of $p = 0.021$ and $p = 0.028$. The control and post-adaptation PO were 85.53 ° and 157.5, respectively. The control OSI of T2 increased from 0.20 to 0.60.

5.4. Discussion

In this study we investigate how, after visual adaptation, tuning properties vary in a cortical network with a salt-and-pepper organization, and whether dynamic connectivity contributes to this variation. We first show that post-adaptation selectivity strength is highly heterogeneous across neurons, with groups of cells exhibiting significant modification of their OSI following adaptation, whereas another group of neurons maintains their OSI through experimental conditions. Moreover, the analyses of correlations in the spikes count between pairs of neurons (CCGs) for drift gratings, revealed that the OSI increases significantly only in cells receiving new post-adaptation connections.

5.4.1. Adaptation increases the tuning of tuned cells but doesn't affect the tuning of untuned cells.

Modeling studies assume that in networks operating in a balanced regime, that is, excitation balances inhibition, the tuned component of the input is amplified while the untuned part is suppressed. Consequently, sharp OS, i.e.,almost half of units in this study, could emerge in a network even without feature-selective recurrent connectivity (Hansel et van Vreeswijk, 2012; Sadeh et Rotter, 2015). The large proportion of U cells described in this study is also not surprising since their participation in the sensory coding occurs in early visual cortex. It was reported that despite U cells having stimulus-independent spiking activity, they contribute to the sensory neural

code (Leavitt et al., 2017; Safaai et al., 2013). The T and U ratios as well as the average OSI were maintained after twelve minutes of adaptation. However, most T cells increased the strength of their selectivity following adaptation as well as a small group of U cells. It seems that, for this group of cells, adaptation enhances their OS responses leading to sharper tuning curves. This might occur because adaptation affects the excitatory-inhibitory (E-I) balance. Indeed, several cortical functions such as feature selectivity are affected by the two opposing forces (synaptic excitation and inhibition) (Anderson et al., 2000; Haider et McCormick, 2009). V1 pyramidal cells show stable E/I ratios since an increase of excitation through the increased recruitment of excitatory neurons induces a proportional increase of inhibition (Anderson et al., 2000; Haider et McCormick, 2009; Shu et al., 2003; Wehr et Zador, 2003). This balance can be disrupted by the prolonged viewing of a particular stimulus, the adapter. As the interaction of excitation and inhibition in the microcircuit determines the output selectivity, changes in E-I balance might induce a higher selective response in some networks. A computational study reported that a slightly reduced net recurrent cortical excitation could improve OS (Teich et Qian, 2003). In addition, it was revealed that adaptation can improve orientation discrimination at the adapted orientation (Regan et Beverley, 1985) and in MT, it affects synaptic inhibition (Qian et al., 1994; Snowden et al., 1991). Hence, we hypothesize that during the adaptation process, there is a small increase in the strength of recurrent inhibition to cells around the adapted orientation. Indeed, it was shown in cortical brain slices that repetitive drive leads to a synapse facilitation between pyramidal and some types of inhibitory neurons (Thomson et Deuchars, 1997). This inhibition could strengthen the degree of selectivity on the flank of the new preferred orientation after adaptation and favor its emergence. A small group of T cells showed a decrease of their OSI value. For this group, broadening of tuning curves after adaptation could be explained by a reduction of both net recurrent excitation and net recurrent inhibition. Indeed, it was demonstrated that, for cells tuned around the adapted orientation, the V1 orientation tuning curves after adaptation became broader (Dragoi et al., 2000)and this can be accounted for by appropriately scaling down both excitation and inhibition to cells around the adapted orientation (Teich et Qian, 2003). This finding strongly suggests that the adaptation process induced different changes to the slope of the orientation tuning curves (becoming sharper or broader), that could be explained by an active recalibration of E-I balance in different ways. This might depend on the direction of the shift, toward or away from the adapted orientation or to its amplitude that depends on the cell's PO in control condition

(Ghisovan et al., 2009). Most of U cells remain U post-adaptation since their OSI failed to reach statistical significance. Adaptation is predicted to induce changes in the slope of tuning curves; however, we found that it is not the case for most U cells. This discrepancy could be explained by different effects of adaptation which would depend on the cell's class. It was reported that the tuning curve changes found only occurred in complex cells, whereas simple cells showed no changes at all (Muller et al., 1999).

5.4.2. Post-adaptation emerged connections contribute to enhance orientation selectivity.

To reveal principles that relate cortical dynamic connectivity of a microcircuit to dynamic cells' OSI (modulation), we divide cells into two groups according to the cell's functional relationship after adaptation regardless to their OSI values in control and post-adaptation conditions. In the first group, we encountered cells exhibiting unchanged functional connections across protocols. In the second group new connections are added following adaptation protocol. Then we compared the OSI values pre- and post-adaptation of the two groups of cells. We found that, contrary to the insignificant change of OSI values in the first group of cells, the OSI of the second group showed a significant post-adaptation increase. Hence, it seems that acquiring new connections following adaptation enhanced the orientation discrimination of the cell at its post-adaptation PO. Conversely, stable (conserved) connections didn't contribute significantly to sharpen the cell's output. It was shown that adaptation generates new functional connectomes in cat, that is, the strength of inter-neuronal relationships was modified (Bachatène et al., 2015). It was also shown that the forceful presentation of a particular orientation results in emergence of new relationships between cells in cat (Bachatene, Bharmauria et Molotchnikoff, 2012). Here, we revealed dynamics of correlation in mouse after adaptation. Results demonstrate that the neuronal network was reorganised in the post-adaptation condition, with the appearance of new connections. It is worth noting that, in the microcircuit, some connections are preserved through conditions. In addition, it was reported that the specificity of synaptic connectivity in cortical networks relies on cortical functionality (Alonso et Martinez, 1998; Song et al., 2005). Consequently, in a microcircuit, when a single cell connects with the same interacting partners in pre-and post-adaptation process, it suggests similar patterns of the cell's activity which generate the same degree of selectivity of the output. However, in an assembly, modifications of the functional coupling, like joining a new neuron, may affect the cell's OSI. It was reported that within a cell-assembly, some connections

are flexible and can emerge in the network as the stimulus changes (Bharmauria et al., 2016). Because of the synaptic flexibility of these neuronal groups, a dynamic microcircuit is emerging after adaptation. The flexibility of the neuronal circuit keeps it ready to receive the input efficiently and hence the output is related to the assembly organisation. Accordingly, the unit output is the result of synaptic weights distributed over its dendritic tree and when a forceful presentation of a particular stimulus was applied, a given cell in a microcircuit may be activated by receiving new connections which in return could change not only its PO, but also its degree of selectivity. In the next section we display a proposed model to explain this result.

5.4.3 Proposed model

It is well known that orientation discrimination, like most other visual discrimination tasks, is highly sensitive to NMDAR mediated activity (Fox et al., 1989; Miller et al., 1989; Rivadulla et al., 2001). Moreover, it was reported that NMDAR plays a critical role in the formation of OS in V1, and that its blockade, using antagonists, abolished the patterning and weakened the amplitude of the orientation map .(Ramoa et al., 2001a; Yu et al., 2008) . Therefore, in our proposed model, we suggest that adaptation, via emergence of new connections, involves NMDA receptor activation and therefore induces a sharper tuning curve of the cell (Fig. 5.4). In control condition, despite the cell's PO at 22.5 deg (Fig. 5.4.1A), each single dendritic segment shows a wide range of orientation-selective spines (Wilson et al., 2016) (Fig. 5.4.1B). The involvement of metabotropic glutamate receptor (here NMDAR, Fig. 5.4.1C) is commonly believed (Fox et al., 1989; Rivadulla et al., 2001). The somatic orientation preference is predicted by the orientation preference of the summed spine inputs (Fig. 5.4.1D). The response properties (PO and strength of selectivity) of the visual neuron change after adaptation (Fig. 5.4.2A). The synaptic mechanism of adaptation results in the alteration of the orientation preferences of the dendritic segments (Fig. 5.4.2B) and the increase of the activation of NMDAR (Fig. 5.4.2C). Hence, when a cell receives new connections (cyan spines in Fig. 5.4.2D) due to a repetitive stimulation (here 90 deg), the increase of NMDAR activation (dark purple receptors) could lead to changes in calcium flux followed by signalling cascades and resulting in further sharpening the cell's response and re-centering its tuning around the prevailing stimulus, which is the adaptor (here 90 deg, Fig. 5.4.2D). Indeed, it was shown that metabotropic receptors are activated by repetitive activity (Kohn et Whitsel, 2002). Also, in mouse, repeated presentations of grating stimuli of a single orientation leads to a persistent improvement of a cell's response, which requires activation of NMDA

channels (Frenkel et al., 2006). Moreover, NMDAR are known to be heavily involved in many forms of perceptual learning (Beste et al., 2012; Dinse et al., 2003; Kang, 2015) and visual adaptation could be considered as a short version of visual learning (Bachatène et al., 2015; Dragoi et al., 2000). Through a process of synaptic reinforcement in the neuronal microcircuit under non-interrupted stimulation during twelve minutes by a non-preferred stimulus, synaptic connections might be subject to short and transient facilitation, commonly referred to as short-term plasticity. This facilitation is mediated by an increase of the transmitter release which regulates information transfer between interconnected neurons (Zucker et Regehr, 2002). Thus, adaptation results in short-term facilitation, implying NMDAR, which high-pass-filters orientation selective signals across the synapse (Abbott et Regehr, 2004; Schneggenburger et al., 2002), and higher selective output responses could be generated. This is in line with previous findings proposing that the pairwise interactions within a population can shape information representation (Averbeck et al., 2006; Dechery et MacLean, 2018; Ecker et al., 2011; Moreno-Bote et al., 2014).

All of the above findings underscore that adaptation might alter pyramidal cell activity which in turn redeploys the strength of projections between cells to restructure the entire wiring-dynamic of the neuronal assembly, and thus rebalance the E/I ratios since it was shown that the latter is activity-dependent (Xue et al., 2014). In addition, adaptation may lead to structural rearrangement of dendrites and spines coupled with functional synaptic modifications. Conclusively, it seems that OS is influenced by patterns of neural activity. First, the feedforward thalamo-cortical afferents are related to the establishment of OS (Markan et Bhaumik, 1999; Vidyasagar et al., 1996), then cortical connections play a key role in shaping cortical neuron tuning properties (Bosking et al., 1997; Ferster et Koch, 1987; Mayo et Smith, 2017). This may allow the visual system to support dynamic information processing thereby efficiently responding to variations of stimuli.

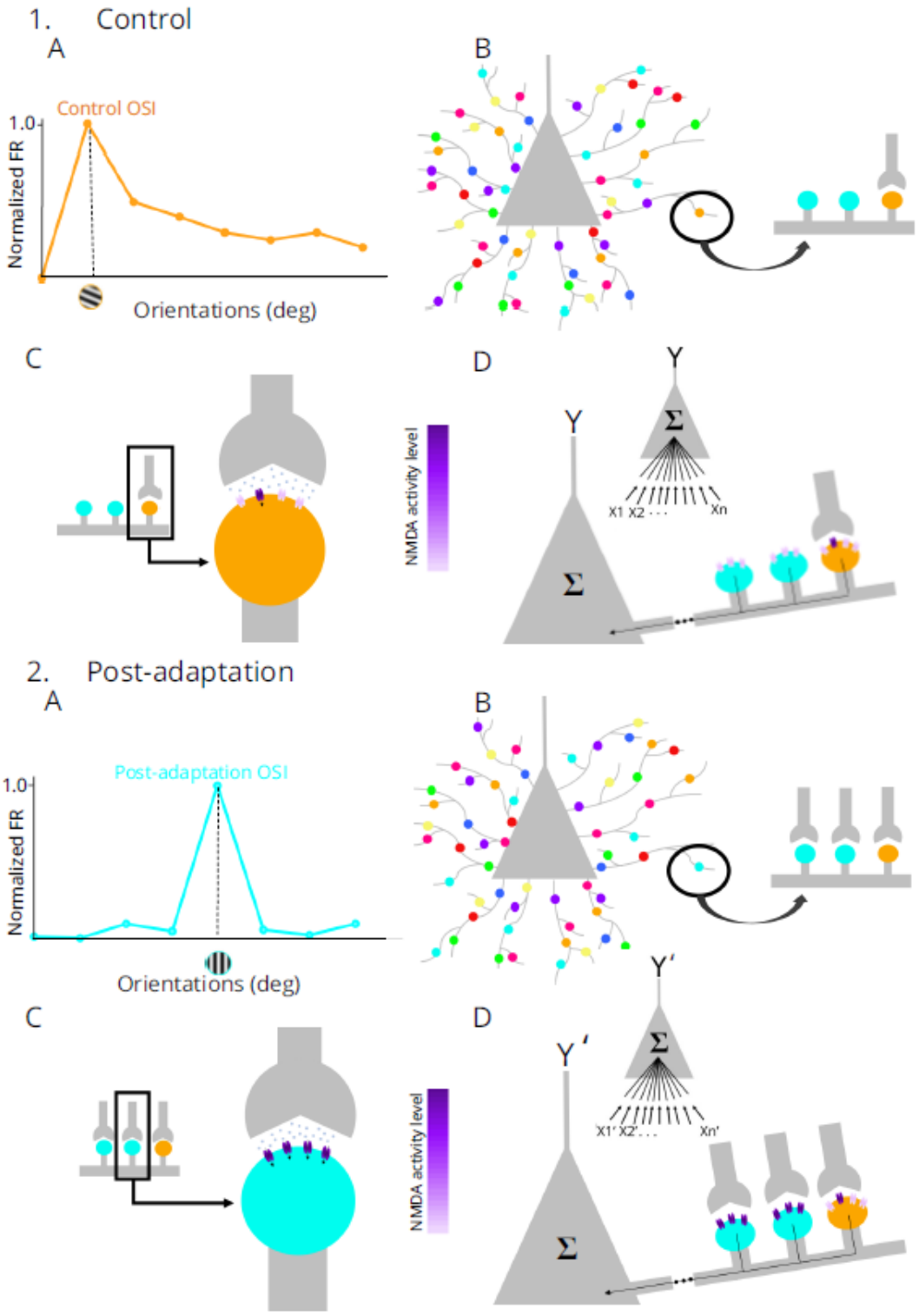

Fig 5.4. Proposed model for adaptation mechanisms on the OSI dynamics. (1A) Example of a tuning curve of a neuron in control condition (orange) showing a PO of 22,5°. (1B) The neuron receives a distribution spectrum of orientations between 0° and 180°. Colored circles represent all the POs for each dendritic domain which depend on the activation of its spines. (1C) The activation

of a given spine depends on the activation of the NMDAR. (1D) The cell's output (Y) depends on the integration of all the relative strengths of inputs (X1, X2, …, Xn). (2A) After adaptation, the tuning curve of the neuron shows a new PO (90°). (2B) The imposition of 90° for 12 min leads to rearrangement of functional relationships between synaptic contacts. (2C) The appearance of new connections, then new synaptic inputs, triggered by the adapter, leads to the activation of NMDAR via glutamate transmission which increases the driving force for synaptic events. (2D) The activation of NMDAR, via the new inputs provided by the adapter (X1', X2', …, Xn'), implies changes in Ca2+ flux followed by a signaling cascade and access of molecular effectors to the cell soma which in turn might modify the cell's output (Y') and increase the control OSI.

6. Discussion générale

Hubel et Wiesel ont découvert une caractéristique clé des réponses des neurones de V1, soit leur haute sélectivité à l'orientation (Hubel et Wiesel, I959). Les principaux résultats de la présente étude sont que, elle déprime la sélectivité à l'orientation et installe une certaine stabilité des réponses évoquées sans affecter l'activité spontanée. Dans les sections suivantes, nous discutons ces trois résultats majeurs plus en détail. Chez l'animal adulte, les propriétés sélectives de chaque cellule demeurent les mêmes tout au long de sa vie. Toutefois, les résultats de nos travaux ont montré qu' à la suite de certaines manipulations telles que l'imposition d'une orientation non préférée pendant douze minutes (adaptation visuelle) ou l'application locale de la kétamine, les cellules du V1 peuvent montrer des nouvelles préférences différentes de leur préférences initiales. La sélectivité est, donc, sujette à la plasticité. Le rôle des récepteurs glutamatergiques dans la plasticité visuelle est évident, et ce par les récepteurs ionotropes (AMPA et NMDA) qui assurent la régulation de la dépolarisation membranaire, et les niveaux de calcium intracellulaire ; et par les récepteurs métabotropiques (mGluR) qui assurent la régulation des événements de signalisation en aval (Purves et al., 2019). Les récepteurs AMPA (α-amino-3-hydroxy-5-methyl-4-isoxazolepropionic acid receptor) dans le cerveau sont principalement composés de GluR2 et des sous-unités GluR1 ou GluR3. Ils sont impliqués dans la plasticité puisque l'efficacité synaptique et la LTP (potentialisation à long terme) sont significativement déterminées par le nombre de récepteurs AMPA, leur composition et par la perméabilité au calcium qui à son tour dépend de ces récepteurs (Zanos et al., 2016). La composition des récepteurs NMDA (NR1 et les sous-unités NR2A ou NR2B) change avec l'âge et ce qui régule le potentiel plastique lié à l'expérience (Guo et al., 2017; Lepack et al., 2015).

Dans les sections suivantes, on va discuter les effets de l'adaptation et de la kétamine sur la sélectivité à l'orientation proposer des mécanismes potentiels permettant à ces deux manipulations d'induire la plasticité visuelle au niveau du V1.

6.1. Induction de la plasticité par l'adaptation visuelle

6.1.1. Effet de l'adaptation sur l'orientation préférée et sur les relations fonctionnelles entre les cellules

Chez la souris et le chat, après adaptation, la majorité des cellules ont montré un déplacement de pic de leur courbe d'accord à l'orientation, et ce en se rapprochant de l'orientation imposée (déplacement attractif) ou en s'éloignant de celle-ci (déplacement répulsif). Une minorité de cellules, appelée cellules réfractaires, n'ont pas montré un changement de leur sélectivité. Le modèle « push-pull » a été proposé pour expliquer le déplacement attractif. En effet, ce déplacement est le résultat de la facilitation des réponses à l'orientation adaptante (flanc adapté de la courbe d'accord) et de la dépression des réponses à l'orientation initiale (flanc opposée de la courbe d'accord) (Ghisovan et al. 2009). Le déplacement répulsif est le résultat d'une diminution de l'excitation sur le flanc adapté de la courbe d'accord (Bachatene et al. 2013). L'ampleur du déplacement varie aussi selon les cellules. Il est probable que les grandes amplitudes des shifts de l'OP sont dues au plus grand spectre de distribution d'orientation sur une branche dendritique particulière, alors que les cellules recevant une distribution étroite des orientations montrent de petits shifts de leur OP. Peu importe le sens et l'ampleur du déplacement, il était démontré que les réponses cellulaires se trouvent améliorées quand les cellules sont exposées d'une façon répétitive au même stimulus (Frenkel et al., 2006) : la réponse cellulaire acquise après adaptation se trouve facilitée par le mécanisme SRP (stimulus-selective response potentiation) qui nécessite l'activation des récepteurs NMDA. En effet, il a été démontré que le niveau d'activité des récepteurs métabotropiques augmente à la suite de leur sollicitation répétitive (Kohn et Whitsel, 2002). De plus, il était rapporté que, chez la souris, les présentations répétées de stimuli ont conduit à une amélioration persistante de la réponse cellulaire, et que ceci nécessite l'activation des canaux NMDA (Frenkel et al., 2006). En outre, les NMDAR sont connus pour être fortement impliqués dans de nombreuses formes d'apprentissage perceptif (Beste et al., 2012; Dinse et al., 2003; Kang, 2015) or l'adaptation visuelle pourrait être considérée comme un apprentissage visuel (Bachatène et al., 2015; Dragoi et al., 2000). L'intérêt physiologique du changeant de préférences cellulaires

initiales après adaptation pourrait être l'élargissement de la gamme perceptive (Krekelberg et al., 2006). En effet, il était suggéré que ces déplacements de pics permettent une meilleure discrimination des différentes orientations (Teich et Qian, 2003) ainsi qu'une meilleure détectabilité des stimuli (Clifford et al. 2001).

Afin d'étudier l'effet de l'adaptation sur les relations fonctionnelles chez la souris et le chat, la somme moyenne des poids synaptiques de toutes les connexions entre les paires cellulaires ainsi que le nombre moyen de toutes les connexions fonctionnelles ont été comptées et comparées entre les deux conditions (contrôle et adaptation) chez la souris et le chat. Nous rapportons qu'aucune différence significative de la force moyenne et du nombre moyen des connexions ne soit notée chez les deux espèces. De plus, pour examiner s'il existe une relation entre le changement de la sélectivité des cellules et la composition des réseaux neuronaux auxquels elles appartiennent, une comparaison de la connectivité entre les cellules enregistrées simultanément avant et après adaptation a été réalisée. Les résultats démontrent des modifications dans le schéma synaptique de la sélectivité du réseau V1 après l'adaptation. Lors de la plasticité induite par l'adaptation, les circuits neuronaux sont soumis à deux mécanismes opposés : le mécanisme Hebbian qui permet à l'expérience de modifier les propriétés des microcircuits et tend ainsi à déstabiliser l'activité des réseaux neuronaux en modifiant à la fois le nombre et la force des synapses et un autre mécanisme qui stabilise la force synaptique totale et le nombre dans les microcircuits, ce qui restaure la stabilité de leurs propriétés de base (Turrigiano et Nelson, 2000). Il semble qu'un équilibre entre les deux forces soit nécessaire pour que le codage neuronal soit efficace. La flexibilité du réseau neuronal, dont le résultat est le raffinement des microcircuits, assure des réponses mieux adaptées aux nouvelles expériences transitoires alors que la stabilité de ces microcircuits facilite le retour à l'état initial (récupération) quand les nouvelles conditions transitoires prennent fin (Shatz, 1990; Turrigiano, 1999). Les processus compensatoires (le renforcement de certains liens entraîne l'affaiblissement d'autres) conduisent probablement à un ajustement de l'efficacité synaptique dans le réseau et donc à l'homéostasie de ce dernier.

6.1.2. Effet de l'adaptation sur le degré de syntonisation des cellules

On a montré dans la section précédente que l'adaptation visuelle change les propriétés sélectives des neurones ainsi que l'organisation des connexions entre les cellules dans V1 de la souris et du chat. Dans cette section, on s'intéresse à étudier et discuter si la dynamique de la connectivité entre

les neurones après adaptation contribue à un changement du degré de sélectivité (OSI) des cellules chez la souris. On rapporte que l'effet de l'adaptation sur l'OSI est très hétérogène entre les neurones, avec des groupes de cellules présentant une modification significative de leur OSI après l'adaptation, tandis qu'un autre groupe de neurones maintient leur OSI à travers les conditions expérimentales. En moyenne, le nombre des cellules syntonisées et celui des cellules non syntonisées ainsi que l'OSI se sont maintenus similaires après douze minutes d'adaptation. Cependant, la plupart des cellules syntonisées ont augmenté la force de leur sélectivité à la suite de l'adaptation. Il semble que, pour ce groupe de cellules, l'adaptation améliore leurs réponses sélectives conduisant à des courbes d'accord plus affines. Cela peut se produire parce que l'adaptation affecte l'équilibre excitateur-inhibiteur (E-I). En effet, plusieurs fonctions corticales telles que la sélectivité à plusieurs attributs comme l'orientation sont affectées par les deux forces opposées (excitation et inhibition synaptiques) (Anderson et al., 2000; Haider et McCormick, 2009). Les cellules pyramidales du V1 présentent des ratios E/I stables puisqu'une augmentation de l'excitation par le recrutement accru de neurones excitateurs induit une augmentation proportionnelle de l'inhibition (Anderson et al., 2000; Haider et McCormick, 2009; Shu et al., 2003; Wehr et Zador, 2003). Cet équilibre peut être perturbé par la visualisation prolongée d'un stimulus particulier, l'adaptateur. Comme l'interaction de l'excitation et de l'inhibition dans le microcircuit détermine la réponse neuronale, les changements de l'équilibre E-I dans certains réseaux pourraient induire une réponse sélective plus élevée. Une étude computationnelle a rapporté qu'une légère réduction de l'excitation corticale nette pourrait améliorer la sélectivité à l'orientation (Teich et Qian, 2003). De plus, il a été révélé que l'adaptation peut améliorer la discrimination à l'orientation adaptante (Regan et Beverley, 1985) et dans l'aire MT, elle affecte l'inhibition synaptique (Qian et al., 1994; Snowden et al., 1991). Par conséquent, nous proposons qu'au cours du processus de l'adaptation, il se produise une petite augmentation de la force inhibitrice récurrente des cellules autour de l'orientation adaptante. En effet, il a été montré sur des tranches de cortex que la pulsion ou la décharge répétitive conduit à une facilitation des synapses entre les neurones pyramidaux et certains types de neurones inhibiteurs (Thomson et Deuchars, 1997). Cette inhibition pourrait par renforcement optimiser le degré de sélectivité de la nouvelle orientation préférée acquise après adaptation et favoriser son émergence.

Un petit groupe de cellules non syntonisées a montré une diminution de la valeur moyenne de l'OSI. Pour ce groupe, l'élargissement de la pente des courbes d'accord après adaptation pourrait

s'expliquer par une réduction à la fois de l'excitation et de l'inhibition récurrentes nettes. En effet, il a été démontré que pour les cellules syntonisées autour de l'orientation adaptante, les courbes d'accord à l'orientation deviennent plus larges (Dragoi et al., 2000). Ce même résultat est obtenu quand on réduit de manière appropriée l'excitation et l'inhibition dans les circuits neuronaux ce qui favorise l'émergence d'une orientation proche de l'adaptante (Teich et Qian, 2003). Cette découverte suggère fortement que le processus d'adaptation a induit des différents changements dans la pente des courbes d'accord d'orientation (devenant plus étroites ou plus larges) ce qui pourrait s'expliquer par une recalibration des deux forces excitatrice et inhibitrice, et ce de différentes manières. Cela peut dépendre du sens du déplacement, en se rapprochant ou en s'éloignant de l'orientation adaptante; ou de son amplitude, qui dépend de l'orientation préférée originale (dans la condition de contrôle) (Ghisovan et al., 2009). On a prévu que l'adaptation induira des changements dans la pente des courbes d'accord des cellules non syntonisées. Cependant, nous avons constaté que ce n'est pas le cas pour la plupart des cellules de cette catégorie qui restent toujours non syntonisées après l'adaptation. En effet, le changement de leur OSI n'a pas pu atteindre la signification statistique. Un petit nombre des cellules non syntonisées ont acquis une sélectivité après l'adaptation. Cette disparité pourrait s'expliquer par des effets d'adaptation différents selon la classe cellulaire. Ainsi, il a été rapporté que les modifications de la courbe d'accord observées ne se produisaient que dans les cellules complexes, alors que les cellules simples ne présentaient aucun changement (Muller et al., 1999).

Les connexions apparues après l'adaptation contribuent à améliorer la sélectivité de l'orientation.

Pour révéler les principes qui relient la dynamique de la connectivité corticale d'un microcircuit à l'OSI des cellules, nous avons divisé les cellules en deux groupes en fonction des relations fonctionnelles auxquelles ces cellules sont impliquées après adaptation, et ce indépendamment de la valeur de leur d'OSI. Dans le premier groupe, nous avons rencontré des cellules présentant des connexions fonctionnelles inchangées à travers les protocoles. Dans le deuxième groupe, les cellules ont reçu de nouvelles connexions qui sont donc ajoutées au réseau après le protocole d'adaptation. Ensuite, nous avons comparé les valeurs de l'OSI avant et après adaptation des deux groupes cellulaires. Nous avons constaté que, contrairement au changement insignifiant des valeurs OSI dans le premier groupe de cellules, l'OSI du deuxième groupe a montré une augmentation significative après adaptation. Par conséquent, il semble que l'acquisition de

nouvelles connexions améliore la discrimination de la cellule à son orientation préférée acquise après adaptation. À l'inverse, les connexions stables (conservées) n'ont pas contribué de manière significative à affiner la réponse sélective des cellules. Il a été démontré que l'adaptation génère de nouveaux connectomes fonctionnels chez le chat avec une modification au niveau des forces des connexions interneuronales (Bachatène et al., 2015). Il a été également démontré que la présentation prolongée d'une orientation particulière entraîne l'émergence de nouvelles connexions entre les cellules chez le chat (Bachatene, Bharmauria et Molotchnikoff, 2012). Ici, nous avons révélé la dynamique des corrélations chez la souris après adaptation. Les résultats démontrent qu'après un protocole d'adaptation, le réseau neuronal s'est réorganisé avec l'apparition de nouvelles connexions. Il convient de noter que, dans le microcircuit, certaines connexions sont préservées à travers les différents protocoles. De plus, il a été rapporté que la spécificité de la connectivité synaptique dans les réseaux corticaux assure la fonctionnalité corticale (Alonso et Martinez, 1998; Song et al., 2005). Par conséquent, dans un microcircuit, lorsqu'une cellule donnée se connecte avec les mêmes partenaires d'interaction avant et après adaptation, elle génère pour ces deux conditions des modèles d'activité similaires et donc des réponses avec des degrés de sélectivité similaires. Cependant, si des modifications au niveau du couplage fonctionnel entre les cellules se produisent comme la réception de nouvelles connexions par une cellule donnée, l'OSI de la ladite cellule serait modifié. Il a été rapporté qu'au sein d'un assemblé de cellules, certaines connexions sont flexibles et peuvent émerger dans le réseau en réponse au changement du stimulus (Bharmauria et al., 2016). Du fait de la flexibilité synaptique de ces groupes de neurones, un nouveau microcircuit émerge après adaptation. La flexibilité du circuit neuronal le maintien prêt à recevoir efficacement des nouvelles entrées. Il en découle l'émergence d'une nouvelle réponse cellulaire puisque celle-ci est le résultat des poids synaptiques répartis sur son arbre dendritique. L'application forcée d'une présentation prolongée d'un stimulus en particulier pourrait induire l'ajout de nouvelles connexions à la cellule, ce qui à son tour pourrait changer non seulement l'orientation préférée de la cellule en question, mais aussi son degré de sélectivité. Dans la section suivante, nous présentons un modèle proposé pour expliquer ce résultat.

Modèle proposé

Il est bien noté que la discrimination d'orientation est très sensible à l'activité médiée par NMDAR (Fox et al., 1989; Miller et al., 1989; Rivadulla et al., 2001). Par conséquent, dans notre modèle proposé, nous suggérons que l'adaptation, par l'émergence de nouvelles connexions, implique

l'activation des récepteurs NMDA et induit donc une courbe d'accord plus étroite. Dans la condition de contrôle, chaque segment dendritique présente une large gamme d'épines sélectives d'orientation, mais un biais fait qu'une unique orientation sera préférée par la cellule (Wilson et al., 2016) (Fig. 4.1B). L'implication du récepteur métabotropique (ici le NMDAR) dans l'émergence de cette sélectivité est communément admise (Fox et al., 1989; Miller et al., 1989; Rivadulla et al., 2001). La préférence d'une orientation déterminée au niveau somatique est prédite par les différentes préférences d'orientation des entrées reçues par le neurone au niveau de ses épines. Les propriétés de la réponse cellulaire changent après adaptation. Le mécanisme synaptique d'adaptation se traduit par l'altération des préférences d'orientation des entrées au niveau des segments dendritiques et par l'augmentation de l'activation des NMDARs. Ainsi, lorsqu'une cellule reçoit de nouvelles connexions en raison d'une stimulation répétitive (ici 90 degrés), l'augmentation de l'activation NMDAR pourrait entraîner des modifications du flux de calcium suivies de cascades de signalisation et ce qui a pour effet d'accentuer davantage la réponse de la cellule autour du stimulus dominant, qui est l'adaptateur. De plus, il a été rapporté que le NMDAR joue un rôle critique dans la génération de la sélectivité à l'orientation dans V1 et que son blocage par des antagonistes perturbe la carte d'orientation (Ramoa et al., 2001a; Yu et al., 2008). En effet, l'application de la kétamine a conduit à une diminution de l'OSI (Ouelhazi et al., 2019). Ce résultat pourrait témoigner l'implication de l'activation des récepteurs NMDA dans la syntonisation des cellules à l'orientation.

Après avoir étudier les différents effets de l'adaptation, la section suivante traite et discute les effets de la kétamine sur la plasticité corticale ce qui s'avère utile pour une meilleure compréhension du potentiel plastique de l'encodage neuronal dans le cerveau adulte de la souris et du chat.

6.2. Induction de la plasticité par la kétamine

6.2.1. Effet de la kétamine sur les orientations préférées originales et acquises après un protocole d' adaptation

Chez la souris et le chat, à la suite de l'application locale de la kétamine sur V1, nos résultats ont montré un changement de l'orientation optimale des neurones. De plus, après un protocole d'adaptation, les cellules, sous kétamine, ont changé leur sélectivité à l'orientation. La kétamine

est un antidépresseur qui bloque l'activité des récepteurs ionotropes NMDA en agissant comme un antagoniste non compétitif. Cela dit, la kétamine induit la plasticité visuelle (en modifiant l'orientation préférée initiale ou celle qui est acquise après adaptation) par une autre voie que celle glutamatergique. En effet, effet, plusieurs études récentes ont prouvé une augmentation de la signalisation synaptogénique de mTOR (mechanistic target of rapamycin), de BDNF (brain-derived neurotrophic factor), et de EEF2 (Eukaryotic Translation Elongation Factor 2) en réponse à l'application de la kétamine (Lepack et al., 2015; Zanos et Gould, 2018; Zanos et al., 2016). Le glissement des pics des courbes d'accord peut aussi être expliqué par des différences au niveau de la réactivité des neurones corticaux en réponse à l'application de la kétamine. En fait, le blocage des récepteurs NMDA pourrait diminuer la réactivité et la sensibilité du neurone à son orientation dominante, ce qui entraînerait l'émergence d'une réponse à une nouvelle orientation qui était initialement moins importante. Les mécanismes régissant cette nouvelle sélectivité peuvent être différents de ceux qui étaient décrits par Hubel et qui régissent la sélectivité qui se développe durant la période critique. En fait, en plus de la connectivité de LGN à V1, on pense que d'autres mécanismes sont impliqués y compris le seuil de potentiel d'action et la balance entre l'excitation et l'inhibition intracorticale (Atallah et al., 2012; Douglas et Martin, 2007; Katzner et al., 2011; Priebe et Ferster, 2008). De plus, il était démontré par une autre étude qui a annoncé que le blocage des récepteurs NMDAR modifie l'équilibre entre l'excitation et l'inhibition dans les circuits corticaux (Homayoun et Moghaddam, 2007). Or il est bien documenté à travers les espèces et à travers les sites d'enregistrement que le traitement des informations sensorielles est tributaire de l'équilibre entre l'excitation et l'inhibition (E-I). Ainsi, l'altération de cet équilibre par la kétamine induirait probablement des modifications de la réponse neuronale (Li et al., 2010; Populin, 2005; Zanos et al., 2016). Dès lors, la diminution de l'inhibition locale par la kétamine (Zhou et al., 2015) entraînerait l'activation d'un groupe de synapses alternatif (autre que celui qui était dominant) et ce qui pourrait expliquer le déplacement de l'orientation optimale, puisqu'un autre groupe synaptique prendrait « le relais » excitateur. En effet, le rôle des connexions synaptiques dans l'établissement de la sélectivité à l'orientation dans le cortex juvénile et adulte du furet est confirmé par une étude rapportée par Chapman (1993) (Chapman et Stryker, 1993). L'étude a démontré qu'au cours de la 7e semaine postnatale, la sélectivité à l'orientation arrive à maturité dans la couche corticale VI, ce qui peut refléter la maturation des connexions entre les couches supra et infragranulaires. Par conséquent, une modification synaptique due à l'application de kétamine

affaiblit les entrées initialement préférées, ce qui augmente la réponse dans un autre flanc de la courbe d'accord. Il semble que ce flanc ne soit pas acquis au hasard puisqu'il existe une corrélation significative entre l'orientation initialement préférée et l'orientation préférée après kétamine. Cette corrélation pourrait être due aux propriétés de la drogue utilisée et qui pourrait favoriser le changement de l'équilibre synaptique dans une fenêtre assez constante ou précise.

La dualité de l'effet de la kétamine après le protocole d'adaptation pourrait s'expliquer par les différents scénarios d'interactions possibles entre les neurones. En effet, ce sont les interactions neuronales qui déterminent la réponse que produit chaque neurone à une orientation présentée. Sachant que dans le cortex cérébral, l'inhibition corticale orchestre l'encodage sensoriel (Isaacson et Scanziani, 2011) et étant donné que les cellules inhibitrices exprimant la parvalbumine (PV) sont le locus initial sous-jacent aux effets de la kétamine (Grieco et al., 2020; Zhou et al., 2015), le résultat des interactions entre les neurones et la kétamine serait tributaire du phénotype cellulaire. En d'autres mots, sous l'effet de la kétamine, la réponse d'un neurone (une facilitation de la récupération ou une potentialisation du shift) dépend de la composition du réseau auquel il appartient. Alors que, dans certains réseaux, l'interaction entre cellules inhibitrices PV et cellules excitatrices pyramidales conduit à une excitation accrue due à la désactivation des PV par la kétamine (Browne et Lucki, 2013; Homayoun et Moghaddam, 2007), la dépression des interconnexions entre les cellules inhibitrices peut conduire à une désinhibition et donc une diminution de l'excitation dans d'autres microcircuits. En effet, plusieurs études ont décrit, en plus des connexions entre les cellules excitatrices et les cellules inhibitrices, des connexions entre les unités inhibitrices PV et d'autres unités inhibitrices (Avermann et al., 2012; Bachatene, Bharmauria, Rouat, et al., 2012; Dalezios et al., 2002; Pfeffer et al., 2013). Il était aussi montré que la désinhibition provoque une facilitation des réponses neuronales et inverse les réponses inhibitrices en excitatrices (Populin, 2005). Il est également probable que le double effet de la kétamine dépende du type cellulaire. En fait, il a été montré que dans les couches 2/3 du cortex visuel, les cellules pyramidales et les interneurones se comportent différemment en réponse à un protocole de privation oculaire, puisque seuls les neurones excitateurs retrouvent leur activité tandis que les neurones inhibiteurs ne montrent aucune récupération (Barnes et al., 2015). Puisqu'il a été démontré que les réseaux corticaux génèrent une sélectivité d'orientation (Schummers et al., 2004), on pense que les changements de l'OP acquise après adaptation sous l'effet de la kétamine,

en particulier pour les neurones réfractaires, pourraient être le résultat de la restructuration du réseau neuronal.

6.2.2. Effet de la kétamine sur l'organisation des microcircuits acquis après adaptation

Pour examiner s'il existe une relation entre le changement de la sélectivité des cellules et la composition des réseaux neuronaux auxquels elles appartiennent, une comparaison de la connectivité entre les cellules enregistrées simultanément dans les conditions d'adaptation et d'administration de kétamine a été faite. La dynamique de liaison entre les paires de neurones après l'application de kétamine a révélé des changements dans la connectivité neuronale acquis après adaptation. En effet, après l'administration de la substance, une émergence des nouveaux réseaux a été observée. Cela peut signifier que la kétamine induit la plasticité en démasquant les connexions préexistantes, et ce par une voie ou plusieurs voies autres que celle des NMDARs. Plusieurs mécanismes peuvent être impliqués, tels que des modifications de l'excitabilité de la membrane neuronale et la suppression physiologique de l'inhibition locale. De plus, plusieurs recherches suggèrent qu'une inhibition synaptique réduite conduit à une réorganisation excitatrice (Chen et al., 2011; Keck et al., 2011; Kuhlman et al., 2013; van Versendaal et al., 2012). Bien que l'adaptation (par la présentation forcée d'un stimulus particulier) et l'application de kétamine ont provoqué le déséquilibre entre E et I, les voies impliquées semblent être différentes. En effet, contrairement à l'adaptation où la plasticité pourrait être induite par l'activation du NMDAR, la kétamine bloque ce dernier et implique donc de différentes voies moléculaires.

Il convient de noter que la kétamine pourrait se lier non seulement au NMDAR, mais également à plusieurs autres sites. Contrairement à la Dizocilpine (MK-801 [(+) -5-methyl-10,11-dihydro-5H-dibenzo [a,d] cyclohepten-5,10-imine maléate]), un non- antagoniste compétitif des récepteurs NMDA, la kétamine à des concentrations plus élevées active les récepteurs α6β2δ et α6β3δ (sous-types de récepteurs GABAA) (Hevers et al., 2008). Cependant, ces sous-types de récepteurs GABAA sont exprimés dans les neurones granulaires cérébelleux (Quirk et al., 1994) et jusqu'à présent, on n'a pas noté leur expression au niveau du cortex (Kurt et al., 2008). En revanche, bien que l'effet de la kétamine sur le NMDAR soit largement étayé par la littérature, on ne peut exclure l'hypothèse qu'au-delà des canaux ioniques en V1, il existe d'autres systèmes susceptibles d'être affectés par la kétamine, notamment les systèmes cholinergiques qui pourraient contribuer également aux changements de l'organisation de réseaux (Sleigh et al., 2014).

Effet de la kétamine sur les poids synaptiques et le nombre de connexions chez la souris et le chat

La comparaison de la somme moyenne des poids synaptiques de toutes les connexions entre les paires cellulaires ainsi que le nombre moyen de toutes les connexions fonctionnelles ont a montré que, chez la souris, il n'y a aucune différence significative de ces deux facteurs entre les différentes conditions expérimentales (contrôle, adaptation et kétamine). Chez le chat, en moyenne, la force et le nombre de connectivités total ont augmenté seulement après l'application de la kétamine. Après adaptation, l'homéostasie qui se produit semble être indépendante de l'activation du NMDAR (Turrigiano, 1999), ce qui pourrait expliquer, chez la souris, que la force moyenne et le nombre des connexions synaptiques moyen ne soient pas différents à travers les conditions expérimentales, même après le blocage du NMDAR par la kétamine. Seulement chez le chat, les résultats montrent une augmentation significative de la somme moyenne des forces de connectivité après l'application de kétamine. Cela pourrait s'expliquer par un recrutement d'un plus grand nombre des connexions fonctionnelles entre les neurones dans les divers microcircuits. L'augmentation parallèle du nombre de connexions fonctionnelles après l'application de la kétamine, selon nos résultats, pourrait soutenir cette hypothèse.

La kétamine améliore la synchronisation neuronale chez le chat

Nous avons examiné et comparé la force moyenne et le nombre moyen de l'activité synchrone entre les différentes conditions expérimentales. La synchronie neuronale est générée lorsque deux cellules reçoivent une entrée commune provenant d'un autre neurone du réseau (Denman et Contreras, 2014; König et al., 1995). Nos résultats ont révélé que la kétamine induit, chez le chat mais pas chez la souris, une activité synchrone plus élevée en force et en nombre après kétamine. Il a été souvent proposé que le temps émis entre les potentiels d'action est crucial au traitement de l'information sensorielle (Decharms et Zador, 2000; Tiesinga et al., 2008). De plus, il a été suggéré que l'activité synchrone de plusieurs neurones procure un avantage à l'encodage des informations puisqu'elle assure une meilleure coordination de l'activité entre les unités réceptrices d'une entrée commune (Yu et Ferster, 2010). En effet, la décharge synchrone de ces cellules provoque une potentialisation de leur impact sur les cellules postsynaptiques due à une synergie de leurs potentiels d'action corrélés dans le temps (Tiesinga et al., 2008). Puisque la synchronie régit l'activité du cortex visuel primaire (Yu et Ferster, 2010), l'augmentation de sa force par la kétamine peut conduire à une meilleure précision et fiabilité de l'encodage neuronal. De plus, plusieurs

recherches soutiennent la relation entre la synchronie neuronale et les oscillations γ dans les cortex visuels du chat et du singe (Engel et al., 1990; Gray et Singer, 1989; Siegel et König, 2003). Il est intéressant d'indiquer que dans le cortex visuel, la synchronisation est due en partie à des connexions horizontales spécifiques entre des domaines corticaux ayant des propriétés sélectives similaires (Gilbert et Wiesel, 1989; Malach et al., 1993). Des travaux antérieurs ont également révélé que l'augmentation de la synchronie se produit entre les neurones qui partagent la même OP (Brosch et al., 1995; Eckhorn et al., 1988; Ts'o et al., 1986). Par exemple, il a été rapporté que la synchronie était améliorée entre les neurones appartenant à la même colonne d'orientation (Ghisovan et al., 2008). De plus, un nombre croissant d'études réalisées sur le cortex visuel du chat ont montré que les neurones d'une même colonne se déchargent de manière synchrone en réponse à une barre lumineuse mobile orientée. Ainsi, l'activité synchrone est favorisée par l'organisation corticale en colonne d'orientation (Freiwald et al., 2001; Gray, 1987; Gray et al., 1989; Gray et Singer, 1989). Par conséquent, la disposition en colonnes peut favoriser la coordination des potentiels d'action et donc la synchronisation entre les paires cellulaires partageant les mêmes préférences sélectives. Compte tenu de l'organisation des cellules en colonnes d'orientation chez le chat et compte tenu de l'absence apparente de cette organisation chez la souris, il devient plus probable de rencontrer des neurones proches avec des préférences similaires chez le chat que chez la souris où les cellules voisines présentent des sélectivités différentes. Cela pourrait potentiellement expliquer pourquoi la kétamine n'a amélioré l'activité synchrone que chez le chat. Pour mieux fonder notre résultat, une nouvelle analyse s'est ajoutée. Il s'agit de calculer pour chaque CCG présentant une activité synchrone, les distributions cumulées des pics. Les résultats montrent que tous les neurones cibles reçoivent des entrées excitatrices dans une fenêtre de 1 ms, ce qui correspond à une augmentation de l'excitation dans le réseau.

6.2.3 Effet de la kétamine sur l'OSI et le Fano facteur

Chez la souris, les neurones du V1 reçoivent des inputs correspondant à un large spectre d'orientations, et la préférence globale est déterminée par l'intégration de diverses entrées synaptiques (Jia et al., 2010). Pour évaluer le degré de la sélectivité à l'orientation et la variabilité des activités neuronales, nous avons comparé l'indice de sélectivité à l'orientation : OSI (Niell et Stryker, 2008) et le fan facteur F, une des mesures standards de la variabilité de décharge, et ce dans les conditions de contrôle et après kétamine. Un résultat intéressant tiré de cette étude est que

la sélectivité à l'orientation, mesurée par l'OSI moyen; à l'instar de la variabilité moyenne de la réponse évoquée, mesurée par le F moyen, était toujours plus faible après la kétamine que dans la condition du contrôle. Il semble que la diminution de l'OSI est due au fait qu'à l'échelle d'un seul neurone, il aurait une désinhibition au niveau des épines dendritiques, ce qui annule le biais préétabli pour une orientation particulière. Notre résultat est en accord avec une étude récente montrant que l'application chronique de la kétamine diminuait les valeurs de l'OSI, d'où une sélectivité à l'orientation réduite, conjointement entraînait une désinhibition des neurones et conduisait à des transitions calciques plus importantes (Hamm et al., 2017). De plus, la même étude montrait que, tout comme l'application aiguë de la kétamine, la suppression pharmacogénétique de l'interneurone inhibiteur exprimant la parvalbumine PV, était suffisante pour désinhiber l'activité neuronale à des niveaux similaires à ceux de la Kétamine chronique. Une autre éventualité qui pourrait expliquer la diminution de l'OSI est que la kétamine affecte les microcircuits (circuits locaux) impliqués dans la sélectivité à l'orientation. Cette hypothèse est supportée par une autre étude faite sur des souris recevant des doses chroniques de kétamine et qui a décelé des modifications dans les populations locales d'interneurones inhibiteurs. En effet, la kétamine a induit des altérations anatomiques des interneurones GABAergiques PV et des changements durables dans la stabilité des épines dendritique (Behrens et al., 2007; Featherstone et al., 2012; Hamm et al., 2017). Ces changements peuvent entraîner une désorganisation des ensembles neuronaux locaux (Hamm et al., 2017). La diminution de l'OSI moyen après- kétamine ne peut pas être due à une variation aléatoire puisqu'une forte corrélation entre OSI moyen en condition de contrôle et OSI moyen après- kétamine a été révélée. Dans l'ensemble, cela suggère que ces résultats sont vraisemblablement dus à l'effet de la kétamine puisqu'ils sont plus robustes que les fluctuations stochastiques ou de références des réponses. La diminution du F à la suite du protocole de l'application de la kétamine reflète une plus faible variabilité du taux de décharge en réponse à des inputs différents. Charles F. Stevens et Anthony M. Zador (1998) ont démontré que dans le néocortex des rats adultes anesthésiés, la forte variabilité des activités neuronales en réponse à des stimuli sensoriels constants résulte de grandes et rapides fluctuations des courants synaptiques, telles que la réception synchrone de l'élément post-synaptique de nombreux afflux indépendants. L'étude a été faite avec plusieurs essais qui montraient que la variabilité du taux de décharge des neurones a apparu d'un essai à un autre, contribuant à une variabilité globale de la réponse évoquée des cellules. En plus, la synchronie pourrait être importante dans l'encodage de

l'information visuelle en fournissant un langage pour coder des signaux avec une fidélité temporelle élevée sur une population de neurones et donc toute altération de cette synchronie, telle que l'injection des courants in vitro à des tranches de néocortex, mène à une diminution de la variabilité neuronale démontrée par des taux de décharge plus réguliers que ceux observés in vivo (Fujisawa et al., 2008). Aussi, il était révélé que l'application de la kétamine produit un renforcement ou un affaiblissement des corrélations fonctionnelles et des altérations au niveau du réseau neuronal (Hamm et al., 2017). Une évidence c'est que les modifications de la neurotransmission perturbent le patron préexistant du fonctionnement des ensembles neuronaux dans le cortex. Subséquemment, la kétamine en tant que bloqueur des récepteurs NMDA altèrent la neurotransmission à de divers niveaux.

Il est peu probable que la variabilité de la réponse évoquée à la suite de l'application de la kétamine, soit due à une activité aléatoire, puisqu'il a été montré que ce composé induit au niveau de V1 des anomalies de l'activité évoquée à l'échelle d'un seul neurone, de paires et de l'ensemble des neurones. De plus, et de manière déterminante, nos résultats ont démontré que le F moyen ne change pas significativement pour les activités spontanées avant et après l'application de kétamine, alors qu'il était affecté pour les activités évoquées, ce qui suggère que la kétamine agit au niveau de la neurotransmission. En plus, il est à signaler que le F des neurones corticaux in vivo ne fluctue pas. En effet, les neurones de V1, comme tous les neurones corticaux, ont une valeur systématiquement proche ou supérieure à 1(Buracas et al., 1998; Gershon et al., 1998). Par exemple, on rapporte que les neurones de la zone temporale moyenne des singes non anesthésiés ont un F de 1,3 (Buracas et al., 1998). Ainsi, la diminution du F après l'application de la kétamine ne peut pas être attribuée à une fluctuation arbitraire.

7. Conclusion

La présente thèse, par l'application de deux manipulations : adaptation et application de la kétamine, a contribué à approfondir les connaissances reliées à la plasticité neuronale en termes de sélectivité à l'orientation et de la dynamique des microcircuits dans V1. En effet, les découvertes ci-dessus soulignent que l'adaptation pourrait changer la sélectivité à l'orientation des cellules, ainsi que patron de connexions dans V1. De plus, les analyses des corrélations croisées entre les potentiels d'action des paires de neurones (CCG) ont révélé que l'OSI n'augmente

significativement que dans les cellules recevant de nouvelles connexions après adaptation. Le modèle de « push-pull » a été proposé pour expliquer l'acquisition de nouvelles préférences sélectives après l'adaptation (Bachatene et al., 2013). La modification des relations fonctionnelles entre les cellules, après adaptation, est le résultat de l'interaction de deux forces opposées : l'une assure la stabilité du réseau et l'autre permet sa flexibilité. Il semble que l'adaptation, en affectant l'activité cellulaire, affecte l'équilibre E/I puisqu'il a été montré que ce dernier est activité-dépendant (Xue et al., 2014). Grâce à un processus de renforcement synaptique dans le microcircuit neuronal dû à une stimulation ininterrompue pendant douze minutes par un stimulus non préféré, les connexions synaptiques pourraient être soumises à une facilitation courte et transitoire, communément appelée plasticité à court terme. Cette facilitation est médiée par une augmentation de la libération des neurotransmetteurs qui régulent le transfert d'informations entre les neurones interconnectés (Zucker et Regehr, 2002). Cela dit, l'adaptation entraîne une facilitation à court terme, impliquant les NMDAR, qui filtrent les signaux sélectifs à l'orientation à travers la synapse en potentialisant la nouvelle orientation dominante (Abbott et Regehr, 2004; Schneggenburger et al., 2002). Dans ce cas, des réponses sélectives différentes et plus fortes que les réponses originales pourraient être générées par les cellules. Cela pourrait expliquer pourquoi l'acquisition de nouvelles connexions après adaptation a conduit à une augmentation de l'OSI des cellules. Ceci est conforme avec d'autres investigations suggérant que les interactions entre les paires de cellules au sein d'une population peuvent façonner la représentation de l'information (Averbeck et al., 2006; Dechery et MacLean, 2018; Ecker et al., 2011; Moreno-Bote et al., 2014).

L'application de la kétamine a induit le déplacement de l'orientation préférée, a aboli les effets d'adaptation et a induit des changements au niveau des liens synaptiques entre les unités. La désinhibition des interneurones PV ainsi que la modification de leur phénotype, l'altération du réseau neuronal, les changements qui surviennent aux oscillations gamma, et la perturbation de l'équilibre entre E et I au niveau de V1 ainsi que plusieurs autres modulations moléculaires et de leurs cascades subséquentes sont des modifications qui pourraient être les mécanismes de la plasticité induite par la kétamine. Cependant, cette liste des effets et des mécanismes sous-jacents n'est pas exhaustive. En effet, il a été démontré que cette dernière affecte aussi l'encodage « top-down ». Tous ces effets entraîneraient une transformation de « l'input-output » et par le fait même une modification d'activité des voies non linéaires impliquées dans la vision (van Loon et al., 2016). Ici, on associe le rôle antidépresseur classique de la kétamine à l'hypothèse plus récente du

déclencheur de la neuroplasticité. Chez le chat, un effet supplémentaire de la kétamine a été démontré qui est l'amélioration de la synchronisation neuronale. Il semble qu'une activité synchrone accrue due à la présence de la kétamine entraîne une coopération entre les cellules du V1, ce qui à son tour constitue une voie d'information supplémentaire susceptible d'améliorer la discrimination fine des orientations (Samonds et al., 2003; Samonds et Bonds, 2004). Ainsi, l'amélioration du traitement neuronal et de l'encodage des informations est probablement l'avantage tiré de l'augmentation de l'activité synchrone (Wang et al., 2011). Il semble que la durée de 10 minutes d'application de la kétamine ait été suffisante pour produire des changements structurels neuronaux. En effet, avec de forts stimuli, une croissance des épines dendritiques avec stabilisation de leur volume a été observée dans une courte fenêtre temporelle de 5 min (Harvey et Svoboda, 2007). De tels changements structurels peuvent expliquer le processus de récupération lent et donc le long temps de récupération (180 min) rapporté dans la présente étude. En outre, la kétamine diminue le degré de la sélectivité à l'orientation, et ce en induisant une désinhibition des neurones. Elle diminue aussi la stabilité des réponses évoquées. Ceci pourrait être le résultat des modifications au niveau de la transmission synaptique et l'activité synchrone des cellules. Il est important de mentionner que ce résultat n'est pas global pour toutes les cellules. Une possibilité d'expliquer ceci est que le nombre et la composition de sous-unités NR1 et les sous-unités NR2A ou NR2B du récepteur NMDA sont variables dans les cellules corticales d'où, leur inhibition par la kétamine conduit à des effets différents (Sleigh et al., 2014). Cette idée est soutenue par une étude montrant que le seuil des changements synaptiques est régulé par le rapport NR2A NR2B (Chen et Bear, 2007; Sawtell et al., 2003; Tongiorgi et al., 2003).

En somme, l'apprentissage visuel ainsi que l'application locale de la kétamine affectent l'encodage des stimuli visuels par les cellules. Il en résulte de nouvelles réponses cellulaires et de nouvelles connexions sélectives. En somme, ces deux manipulations ont induit la plasticité dans V1.Il semble que la sélectivité à l'orientation soit influencée par les schémas des activités neuronales. En premier temps, les afférences thalamo-corticales assure la génération de la sélectivité à l'orientation (Markan et Bhaumik, 1999; Vidyasagar et al., 1996), puis les connexions corticales affinent ces propriétés sélectives des neurones corticaux (Bosking et al., 1997; Ferster et Koch, 1987; Mayo et Smith, 2017). Cela peut permettre au système visuel de prendre en charge le traitement dynamique de l'information, répondant ainsi efficacement aux variations des stimuli. Bien que cette thèse révèle comment les microcircuits de V1 sont configurés et ajustés en réponse

à différentes stimulations visuelles et aux divers protocoles appliqués (adaptation et kétamine), les voies impliquées dans la plasticité semblent être différentes. Cela dit, d'après nos résultats, ainsi que des preuves récentes découlant des études énoncées ci-dessus on suggère un rôle critique (si non principal) du verrouillage synaptique glutamatergique dans la diminution de la sélectivité d'orientation, la transformation du code « input-output » et la diminution de la variabilité des réponses. Toutefois, ce verrouillage n'empêche pas l'induction de la plasticité corticale qui pourrait être le résultat de l'implication de plusieurs mécanismes et pas uniquement la voie glutamatergique. Ce travail serait aussi une sérieuse contribution à l'avancement des connaissances sur certaines pathologies associées directement ou indirectement à la fonction visuelle. Ainsi une application de la kétamine, par exemple, pourrait potentiellement aider au traitement de certains troubles visuels, ce qui ferait apparaitre une lueur d'espoir face à de différentes situations cliniques malheureuses. En effet, il a été montré qu'un seul traitement à la kétamine entraîne une régulation à la baisse de l'expression de la neuréguline-1 (NRG1) dans les cellules inhibitrices du PV ce qui à son tour réactive la plasticité dans le cortex visuel de la souris (Grieco et al., 2020). En plus des mécanismes moléculaires, la kétamine favorise la plasticité neuronale par des modifications structurelles en permettant la régénération des épines perdues lors des traumatismes (Moda-Sava et al., 2019; Takei et al., 2004; Zhou et al., 2014). Ainsi, cette récupération des épines perdues par la kétamine pourrait contribuer à corriger certaines lésions corticales (V1 ou autres zones). Mais, pour le confirmer d'autres études pharmacologiques sont à suivre.

8. Bibliographie

Abbott, L. et Regehr, W. G. (2004). Synaptic computation. *Nature, 431*(7010), 796-803.

Abeles, M. (1982). Quantification, smoothing, and confidence limits for single-units' histograms. *Journal of neuroscience methods, 5*(4), 317-325.

Abeles, M. (1982). Quantification, smoothing, and confidence limits for single-units' histograms. *Journal of neuroscience methods, 5*(4), 317-325.

Afef, O., Rudy, L. et Stéphane, M. (2022). Ketamine promotes adaption-induced orientation plasticity and vigorous network changes. *Brain Research, 1797*, 148111.

Aleksandrova, L. R., Phillips, A. G., Wang, Y. T. et Neuroscience. (2017). Antidepressant effects of ketamine and the roles of AMPA glutamate receptors and other mechanisms beyond NMDA receptor antagonism. *Journal of Psychiatry, 42*(4), 222-229.

Alloway, K. et Roy, S. (2002). Conditional cross-correlation analysis of thalamocortical neurotransmission. *Behavioural brain research, 135*(1-2), 191-196.

Alonso, J.-M. et Martinez, L. M. (1998). Functional connectivity between simple cells and complex cells in cat striate cortex. *Nature neuroscience, 1*(5), 395-403.

Anderson, J. S., Carandini, M. et Ferster, D. (2000). Orientation tuning of input conductance, excitation, and inhibition in cat primary visual cortex. *Journal of neurophysiology, 84*(2), 909-926.

Atallah, B. V., Bruns, W., Carandini, M. et Scanziani, M. (2012). Parvalbumin-expressing interneurons linearly transform cortical responses to visual stimuli. *Neuron, 73*(1), 159-170.

Autry, A. E., Adachi, M., Nosyreva, E., Na, E. S., Los, M. F., Cheng, P.-f., Kavalali, E. T. et Monteggia, L. M. (2011). NMDA receptor blockade at rest triggers rapid behavioural antidepressant responses. *Nature, 475*(7354), 91-95.

Avenet, P., Léonardon, J., Besnard, F., Graham, D., Depoortere, H. et Scatton, B. (1997, 1997/02/21/). Antagonist properties of eliprodil and other NMDA receptor antagonists at rat NR1A/NR2A and NR1A/NR2B receptors expressed in Xenopus oocytes. *Neuroscience Letters, 223*(2), 133-136. https://doi.org/https://doi.org/10.1016/S0304-3940(97)13422-X

Averbeck, B. B., Latham, P. E. et Pouget, A. (2006). Neural correlations, population coding and computation. *Nature reviews neuroscience, 7*(5), 358-366.

Avermann, M., Tomm, C., Mateo, C., Gerstner, W. et Petersen, C. C. (2012). Microcircuits of excitatory and inhibitory neurons in layer 2/3 of mouse barrel cortex. *Journal of neurophysiology, 107*(11), 3116-3134.

Bachatene, L., Bharmauria, V., Cattan, S., Chanauria, N., Rouat, J. et Molotchnikoff, S. (2015). Summation of connectivity strengths in the visual cortex reveals stability of neuronal microcircuits after plasticity. *BMC neuroscience, 16*(1), 1-11.

Bachatene, L., Bharmauria, V., Cattan, S. et Molotchnikoff, S. (2013). Fluoxetine and serotonin facilitate attractive-adaptation-induced orientation plasticity in adult cat visual cortex. *European Journal of Neuroscience, 38*(1), 2065-2077.

Bachatene, L., Bharmauria, V., Cattan, S., Rouat, J. et Molotchnikoff, S. (2015). Reprogramming of orientation columns in visual cortex: a domino effect. *Scientific reports, 5*(1), 1-11.

Bachatène, L., Bharmauria, V., Cattan, S., Rouat, J. et Molotchnikoff, S. (2015). Modulation of functional connectivity following visual adaptation: homeostasis in V1. *Brain Research, 1594*, 136-153.

Bachatene, L., Bharmauria, V. et Molotchnikoff, S. (2012). Adaptation and neuronal network in visual cortex. *Visual Cortex-Current Status and Perspectives*.

Bachatene, L., Bharmauria, V., Rouat, J. et Molotchnikoff, S. (2012). Adaptation-induced plasticity and spike waveforms in cat visual cortex. *Neuroreport, 23*(2), 88-92.

Barnes, S. J., Sammons, R. P., Jacobsen, R. I., Mackie, J., Keller, G. B. et Keck, T. (2015). Subnetwork-specific homeostatic plasticity in mouse visual cortex in vivo. *Neuron, 86*(5), 1290-1303.

Barria, A. et Malinow, R. (2005, 2005/10/20/). NMDA Receptor Subunit Composition Controls Synaptic Plasticity by Regulating Binding to CaMKII. *Neuron, 48*(2), 289-301. https://doi.org/https://doi.org/10.1016/j.neuron.2005.08.034

Behrens, M. M., Ali, S. S., Dao, D. N., Lucero, J., Shekhtman, G., Quick, K. L. et Dugan, L. L. (2007). Ketamine-induced loss of phenotype of fast-spiking interneurons is mediated by NADPH-oxidase. *Science, 318*(5856), 1645-1647.

Ben-Yishai, R., Bar-Or, R. L. et Sompolinsky, H. (1995). Theory of orientation tuning in visual cortex. *Proceedings of the National Academy of Sciences, 92*(9), 3844-3848.

Benfield, P., Heel, R. C. et Lewis, S. P. (1986). Fluoxetine: a review of its pharmacodynamic and pharmacokinetic properties, and therapeutic efficacy in depressive illness. *Drugs, 32*, 481-508.

Berman, R. M., Cappiello, A., Anand, A., Oren, D. A., Heninger, G. R., Charney, D. S. et Krystal, J. H. (2000). Antidepressant effects of ketamine in depressed patients. *Biological psychiatry, 47*(4), 351-354.

Berson, D. M., Dunn, F. A. et Takao, M. (2002). Phototransduction by retinal ganglion cells that set the circadian clock. *Science, 295*(5557), 1070-1073.

Beste, C., Wascher, E., Dinse, H. R. et Saft, C. (2012). Faster perceptual learning through excitotoxic neurodegeneration. *Current biology, 22*(20), 1914-1917.

Bharmauria, V., Bachatene, L., Cattan, S., Brodeur, S., Chanauria, N., Rouat, J. et Molotchnikoff, S. (2016). Network-selectivity and stimulus-discrimination in the primary visual cortex: cell-assembly dynamics. *European Journal of Neuroscience, 43*(2), 204-219.

Binzegger, T., Douglas, R. J. et Martin, K. A. (2004). A quantitative map of the circuit of cat primary visual cortex. *Journal of Neuroscience, 24*(39), 8441-8453.

Bonhoeffer, T. et Grinvald, A. (1991). Iso-orientation domains in cat visual cortex are arranged in pinwheel-like patterns. *Nature, 353*(6343), 429-431.

Bonin, V., Histed, M. H., Yurgenson, S. et Reid, R. C. (2011). Local diversity and fine-scale organization of receptive fields in mouse visual cortex. *Journal of Neuroscience, 31*(50), 18506-18521.

Bosking, W. H., Zhang, Y., Schofield, B. et Fitzpatrick, D. (1997). Orientation selectivity and the arrangement of horizontal connections in tree shrew striate cortex. *Journal of Neuroscience, 17*(6), 2112-2127.

Bouchard, M., Gillet, P.-C., Shumikhina, S. et Molotchnikoff, S. (2008). Adaptation changes the spatial frequency tuning of adult cat visual cortex neurons. *Experimental brain research, 188*(2), 289-303.

Boynton, G. M. et Finney, E. M. (2003). Orientation-specific adaptation in human visual cortex. *Journal of Neuroscience, 23*(25), 8781-8787.

Brosch, M., Bauer, R. et Eckhorn, R. (1995). Synchronous High-frequency Oscillations in Cat Area 18. *European Journal of Neuroscience, 7*(1), 86-95.

Browne, C. A. et Lucki, I. (2013). Antidepressant effects of ketamine: mechanisms underlying fast-acting novel antidepressants. *Frontiers in pharmacology, 4*, 161.

Buracas, G. T., Zador, A. M., DeWeese, M. R. et Albright, T. D. (1998). Efficient discrimination of temporal patterns by motion-sensitive neurons in primate visual cortex. *Neuron, 20*(5), 959-969.

Bushdid, C., Magnasco, M. O., Vosshall, L. B. et Keller, A. (2014). Humans can discriminate more than 1 trillion olfactory stimuli. *Science, 343*(6177), 1370-1372.

Bussey, T. J., Saksida, L. M. et Rothblat, L. A. (2001). Discrimination of computer-graphic stimuli by mice: a method for the behavioral characterization of transgenic and gene-knockout models. *Behavioral neuroscience, 115*(4), 957.

Calderone, J. B. et Jacobs, G. H. (1995). Regional variations in the relative sensitivity to UV light in the mouse retina. *Visual neuroscience, 12*(3), 463-468.

Calhoun, A. J., Pillow, J. W. et Murthy, M. (2019). Unsupervised identification of the internal states that shape natural behavior. *Nature neuroscience, 22*(12), 2040-2049.

Campbell, F., Cleland, B., Cooper, G. et Enroth-Cugell, C. (1968). The angular selectivity of visual cortical cells to moving gratings. *The Journal of physiology, 198*(1), 237-250.

Carandini, M. et Ferster, D. (2000). Membrane potential and firing rate in cat primary visual cortex. *Journal of Neuroscience, 20*(1), 470-484.
Carandini, M. et Ringach, D. L. (1997). Predictions of a recurrent model of orientation selectivity. *Vision research, 37*(21), 3061-3071.
Cattan, S., Bachatene, L., Bharmauria, V., Jeyabalaratnam, J., Milleret, C. et Molotchnikoff, S. (2014). Comparative analysis of orientation maps in areas 17 and 18 of the cat primary visual cortex following adaptation. *European Journal of Neuroscience, 40*(3), 2554-2563.
Chao-Yi, L. et Creutzfeldt, O. (1984). The representation of contrast and other stimulus parameters by single neurons in area 17 of the cat. *Pflügers Archiv, 401*, 304-314.
Chapman, B. et Stryker, M. P. (1993). Development of orientation selectivity in ferret visual cortex and effects of deprivation. *Journal of Neuroscience, 13*(12), 5251-5262.
Chen, J. L., Lin, W. C., Cha, J. W., So, P. T., Kubota, Y. et Nedivi, E. (2011). Structural basis for the role of inhibition in facilitating adult brain plasticity. *Nature neuroscience, 14*(5), 587-594.
Chen, W. S. et Bear, M. F. (2007). Activity-dependent regulation of NR2B translation contributes to metaplasticity in mouse visual cortex. *Neuropharmacology, 52*(1), 200-214.
Church, J. (1990). N-methyl-D-aspartate (MNDA) antagonism is central to the actions of ketamine and other phencyclidine receptor ligands. *Status of ketamine in anesthesiology*, 501-519.
Clark, D. L. et Clark, R. A. (2016, 2016/12/01/). Neutral point testing of color vision in the domestic cat. *Experimental Eye Research, 153*, 23-26. https://doi.org/https://doi.org/10.1016/j.exer.2016.10.002
Clements, J., Nimmo, W. et Grant, I. (1982). Bioavailability, pharmacokinetics, and analgesic activity of ketamine in humans. *Journal of pharmaceutical sciences, 71*(5), 539-542.
Clifford, C. W., Wyatt, A. M., Arnold, D. H., Smith, S. T. et Wenderoth, P. (2001). Orthogonal adaptation improves orientation discrimination. *Vision research, 41*(2), 151-159.
Crowley, J. C. et Katz, L. C. (1999). Development of ocular dominance columns in the absence of retinal input. *Nature neuroscience, 2*(12), 1125-1130.
D'Souza, R. D. et Burkhalter, A. (2017). A laminar organization for selective cortico-cortical communication. *Frontiers in neuroanatomy, 11*, 71.
Dalezios, Y., Luján, R., Shigemoto, R., Roberts, J. D. B. et Somogyi, P. (2002). Enrichment of mGluR7a in the presynaptic active zones of GABAergic and non-GABAergic terminals on interneurons in the rat somatosensory cortex. *Cerebral cortex, 12*(9), 961-974.
Darian-Smith, C. et Gilbert, C. D. (1995). Topographic reorganization in the striate cortex of the adult cat and monkey is cortically mediated. *Journal of Neuroscience, 15*(3), 1631-1647.
De Monasterio, F. et Gouras, P. (1975). Functional properties of ganglion cells of the rhesus monkey retina. *The Journal of physiology, 251*(1), 167-195.
Deane, K. E., Brunk, M. G., Curran, A. W., Zempeltzi, M. M., Ma, J., Lin, X., Abela, F., Aksit, S., Deliano, M. et Ohl, F. W. (2020). Ketamine anaesthesia induces gain enhancement via recurrent excitation in granular input layers of the auditory cortex. *The Journal of physiology, 598*(13), 2741-2755.
Decharms, R. C. et Zador, A. (2000). Neural representation and the cortical code. *Annual review of neuroscience, 23*(1), 613-647.
Dechery, J. B. et MacLean, J. N. (2018). Functional triplet motifs underlie accurate predictions of single-trial responses in populations of tuned and untuned V1 neurons. *PLoS computational biology, 14*(5), e1006153.
Denman, D. J. et Contreras, D. (2014). The structure of pairwise correlation in mouse primary visual cortex reveals functional organization in the absence of an orientation map. *Cerebral cortex, 24*(10), 2707-2720.
Dinis-Oliveira, R. J. (2017). Metabolism and metabolomics of ketamine: a toxicological approach. *Forensic sciences research, 2*(1), 2-10.

Dinse, H. R., Ragert, P., Pleger, B., Schwenkreis, P. et Tegenthoff, M. (2003). Pharmacological modulation of perceptual learning and associated cortical reorganization. *Science, 301*(5629), 91-94.
Douglas, R. J., Martin, K. et Whitteridge, D. (1991). An intracellular analysis of the visual responses of neurones in cat visual cortex. *The Journal of physiology, 440*(1), 659-696.
Douglas, R. J. et Martin, K. A. (2004). Neuronal circuits of the neocortex. *Annu. Rev. Neurosci., 27*, 419-451.
Douglas, R. J. et Martin, K. A. (2007). Mapping the matrix: the ways of neocortex. *Neuron, 56*(2), 226-238.
Dräger, U. C. (1975). Receptive fields of single cells and topography in mouse visual cortex. *Journal of Comparative Neurology, 160*(3), 269-289.
Dragoi, V., Rivadulla, C. et Sur, M. (2001). Foci of orientation plasticity in visual cortex. *Nature, 411*(6833), 80-86.
Dragoi, V., Sharma, J. et Sur, M. (2000). Adaptation-induced plasticity of orientation tuning in adult visual cortex. *Neuron, 28*(1), 287-298.
Dragoi, V., Turcu, C. M. et Sur, M. (2001). Stability of cortical responses and the statistics of natural scenes. *Neuron, 32*(6), 1181-1192.
Duffy, K. R. et Mitchell, D. E. (2013). Darkness alters maturation of visual cortex and promotes fast recovery from monocular deprivation. *Current biology, 23*(5), 382-386.
Ecker, A., Berens, P., Tolias, A. et Bethge, M. (2011). The effect of noise correlations in populations of diversely tuned neurons. *Nature Precedings*, 1-1.
Ecker, J. L., Dumitrescu, O. N., Wong, K. Y., Alam, N. M., Chen, S.-K., LeGates, T., Renna, J. M., Prusky, G. T., Berson, D. M. et Hattar, S. (2010). Melanopsin-expressing retinal ganglion-cell photoreceptors: cellular diversity and role in pattern vision. *Neuron, 67*(1), 49-60.
Eckhorn, R., Bauer, R., Jordan, W., Brosch, M., Kruse, W., Munk, M. et Reitboeck, H. (1988). Coherent oscillations: A mechanism of feature linking in the visual cortex? *Biological cybernetics, 60*(2), 121-130.
Engel, A. K., König, P., Gray, C. M. et Singer, W. (1990). Stimulus-dependent neuronal oscillations in cat visual cortex: Inter-columnar interaction as determined by cross-correlation analysis. *European Journal of Neuroscience, 2*(7), 588-606.
Enroth-Cugell, C. et Robson, J. G. (1966). The contrast sensitivity of retinal ganglion cells of the cat. *The Journal of physiology, 187*(3), 517-552.
Featherstone, R. E., Liang, Y., Saunders, J. A., Tatard-Leitman, V. M., Ehrlichman, R. S. et Siegel, S. J. (2012). Subchronic ketamine treatment leads to permanent changes in EEG, cognition and the astrocytic glutamate transporter EAAT2 in mice. *Neurobiology of disease, 47*(3), 338-346.
Felleman, D. J. et Van Essen, D. C. (1991). Distributed hierarchical processing in the primate cerebral cortex. *Cerebral cortex (New York, NY: 1991), 1*(1), 1-47.
Ferster, D. (1988). Spatially opponent excitation and inhibition in simple cells of the cat visual cortex. *Journal of Neuroscience, 8*(4), 1172-1180.
Ferster, D. (1992). The synaptic inputs to simple cells of the cat visual cortex. *Progress in brain research, 90*, 423-441.
Ferster, D. et Koch, C. (1987). Neuronal connections underlying orientation selectivity in cat visual cortex. *Trends in neurosciences, 10*(12), 487-492.
Field, G. D. et Chichilnisky, E. (2007). Information processing in the primate retina: circuitry and coding. *Annual review of neuroscience, 30*(1), 1-30.
Fox, K., Sato, H. et Daw, N. (1989). The location and function of NMDA receptors in cat and kitten visual cortex. *Journal of Neuroscience, 9*(7), 2443-2454.
Freeman, R. D. (2003). Cortical columns: a multi-parameter examination. *Cerebral cortex, 13*(1), 70-72.
Freiwald, W. A., Kreiter, A. K. et Singer, W. (2001). Synchronization and assembly formation in the visual cortex. *Progress in brain research, 130*, 111-140.

Frenkel, M. Y., Sawtell, N. B., Diogo, A. C. M., Yoon, B., Neve, R. L. et Bear, M. F. (2006). Instructive effect of visual experience in mouse visual cortex. *Neuron, 51*(3), 339-349.

Fujisawa, S., Amarasingham, A., Harrison, M. T. et Buzsáki, G. (2008). Behavior-dependent short-term assembly dynamics in the medial prefrontal cortex. *Nature neuroscience, 11*(7), 823-833.

Fuller, R. W., Wong, D. T. et Robertson, D. W. (1991). Fluoxetine, a selective inhibitor of serotonin uptake. *Medicinal research reviews, 11*(1), 17-34.

Garey, L. et Powell, T. (1968). The projection of the retina in the cat. *Journal of Anatomy, 102*(Pt 2), 189.

Gawaskar, S., Schepmann, D., Bonifazi, A., Robaa, D., Sippl, W. et Wünsch, B. (2015, 2015/12/15/). Benzo[7]annulene-based GluN2B selective NMDA receptor antagonists: Surprising effect of a nitro group in 2-position. *Bioorganic & Medicinal Chemistry Letters, 25*(24), 5748-5751. https://doi.org/https://doi.org/10.1016/j.bmcl.2015.10.076

Gershon, E. D., Wiener, M. C., Latham, P. E. et Richmond, B. J. (1998). Coding strategies in monkey V1 and inferior temporal cortices. *Journal of neurophysiology, 79*(3), 1135-1144.

Ghisovan, N., Nemri, A., Shumikhina, S. et Molotchnikoff, S. (2008). Visual cells remember earlier applied target: plasticity of orientation selectivity. *PloS one, 3*(11), e3689.

Ghisovan, N., Nemri, A., Shumikhina, S. et Molotchnikoff, S. (2009). Long adaptation reveals mostly attractive shifts of orientation tuning in cat primary visual cortex. *Neuroscience, 164*(3), 1274-1283.

Gilbert, C. D. et Li, W. (2012). Adult visual cortical plasticity. *Neuron, 75*(2), 250-264.

Gilbert, C. D. et Wiesel, T. N. (1989). Columnar specificity of intrinsic horizontal and corticocortical connections in cat visual cortex. *Journal of Neuroscience, 9*(7), 2432-2442.

Goel, A. et Lee, H.-K. (2007). Persistence of experience-induced homeostatic synaptic plasticity through adulthood in superficial layers of mouse visual cortex. *Journal of Neuroscience, 27*(25), 6692-6700.

Gray, C. M. (1987). Stimulus-specific neuronal oscillations in the cat visual cortex: A cortical functional unit. Dans. Society of Neuroscience Abstracts.

Gray, C. M., König, P., Engel, A. K. et Singer, W. (1989). Oscillatory responses in cat visual cortex exhibit inter-columnar synchronization which reflects global stimulus properties. *Nature, 338*(6213), 334-337.

Gray, C. M. et Singer, W. (1989). Stimulus-specific neuronal oscillations in orientation columns of cat visual cortex. *Proceedings of the National Academy of Sciences, 86*(5), 1698-1702.

Grieco, S. F., Qiao, X., Zheng, X., Liu, Y., Chen, L., Zhang, H., Yu, Z., Gavornik, J. P., Lai, C. et Gandhi, S. P. (2020). Subanesthetic ketamine reactivates adult cortical plasticity to restore vision from amblyopia. *Current biology, 30*(18), 3591-3603. e3598.

Grubb, M. S. et Thompson, I. D. (2003). Quantitative characterization of visual response properties in the mouse dorsal lateral geniculate nucleus. *Journal of neurophysiology, 90*(6), 3594-3607.

Guo, H., Camargo, L. M., Yeboah, F., Digan, M. E., Niu, H., Pan, Y., Reiling, S., Soler-Llavina, G., Weihofen, W. A. et Wang, H.-R. (2017). A NMDA-receptor calcium influx assay sensitive to stimulation by glutamate and glycine/D-serine. *Scientific reports, 7*(1), 11608.

Haider, B. et McCormick, D. A. (2009). Rapid neocortical dynamics: cellular and network mechanisms. *Neuron, 62*(2), 171-189.

Hamm, J. P., Peterka, D. S., Gogos, J. A. et Yuste, R. (2017). Altered cortical ensembles in mouse models of schizophrenia. *Neuron, 94*(1), 153-167. e158.

Hansel, D. et van Vreeswijk, C. (2012). The mechanism of orientation selectivity in primary visual cortex without a functional map. *Journal of Neuroscience, 32*(12), 4049-4064.

Harvey, C. D. et Svoboda, K. (2007). Locally dynamic synaptic learning rules in pyramidal neuron dendrites. *Nature, 450*(7173), 1195-1200.

Haverkamp, S., Wässle, H., Duebel, J., Kuner, T., Augustine, G. J., Feng, G. et Euler, T. (2005). The primordial, blue-cone color system of the mouse retina. *Journal of Neuroscience, 25*(22), 5438-5445.

Hensch, T. K. (2005). Critical period plasticity in local cortical circuits. *Nature reviews neuroscience, 6*(11), 877-888.
Hevers, W., Hadley, S. H., Lüddens, H. et Amin, J. (2008). Ketamine, but not phencyclidine, selectively modulates cerebellar GABAA receptors containing α6 and δ subunits. *Journal of Neuroscience, 28*(20), 5383-5393.
Hofer, S. B., Mrsic-Flogel, T. D., Bonhoeffer, T. et Hübener, M. (2006). Lifelong learning: ocular dominance plasticity in mouse visual cortex. *Current opinion in neurobiology, 16*(4), 451-459.
Homayoun, H. et Moghaddam, B. (2007). NMDA receptor hypofunction produces opposite effects on prefrontal cortex interneurons and pyramidal neurons. *Journal of Neuroscience, 27*(43), 11496-11500.
Horton, J. C. et Adams, D. L. (2005). The cortical column: a structure without a function. *Philosophical Transactions of the Royal Society B: Biological Sciences, 360*(1456), 837-862.
Hu, J., Ma, H., Zhu, S., Li, P., Xu, H., Fang, Y., Chen, M., Han, C., Fang, C., Cai, X., Yan, K. et Lu, H. D. (2018, 2018/10/02/). Visual Motion Processing in Macaque V2. *Cell Reports, 25*(1), 157-167.e155. https://doi.org/https://doi.org/10.1016/j.celrep.2018.09.014
Hubel, D. et Wiesel, T. (1969). Anatomical demonstration of columns in the monkey striate cortex. *Nature, 221*(5182), 747-750.
Hubel, D. H. et Wiesel, T. N. (1959). Receptive fields of single neurones in the cat's striate cortex. *The Journal of physiology, 148*(3), 574.
Hubel, D. H. et Wiesel, T. N. (1962). Receptive fields, binocular interaction and functional architecture in the cat's visual cortex. *The Journal of physiology, 160*(1), 106.
Hubel, D. H. et Wiesel, T. N. (1968). Receptive fields and functional architecture of monkey striate cortex. *The Journal of physiology, 195*(1), 215-243.
Hubel, D. H. et Wiesel, T. N. (1974). Sequence regularity and geometry of orientation columns in the monkey striate cortex. *Journal of Comparative Neurology, 158*(3), 267-293.
Hubel, D. H. et Wiesel, T. N. (I959). Receptive fields of single neurones in the cat's striate cortex. *J. Physiol, 148*(3), 574-559I.
Hübener, M. et Bonhoeffer, T. (2014, 2014/11/06/). Neuronal Plasticity: Beyond the Critical Period. *Cell, 159*(4), 727-737. https://doi.org/https://doi.org/10.1016/j.cell.2014.10.035
Huberman, A. D., Manu, M., Koch, S. M., Susman, M. W., Lutz, A. B., Ullian, E. M., Baccus, S. A. et Barres, B. A. (2008). Architecture and activity-mediated refinement of axonal projections from a mosaic of genetically identified retinal ganglion cells. *Neuron, 59*(3), 425-438.
Huberman, A. D. et Niell, C. M. (2011). What can mice tell us about how vision works? *Trends in neurosciences, 34*(9), 464-473.
Isaacson, J. S. et Scanziani, M. (2011). How inhibition shapes cortical activity. *Neuron, 72*(2), 231-243.
Jacobs, G. H., Williams, G. A., Cahill, H. et Nathans, J. (2007). Emergence of novel color vision in mice engineered to express a human cone photopigment. *Science, 315*(5819), 1723-1725.
Jaffer, S., Vorobyov, V., Kind, P. C. et Sengpiel, F. (2012). Experience-dependent regulation of functional maps and synaptic protein expression in the cat visual cortex. *European Journal of Neuroscience, 35*(8), 1281-1294.
Jeon, C.-J., Strettoi, E. et Masland, R. H. (1998). The major cell populations of the mouse retina. *Journal of Neuroscience, 18*(21), 8936-8946.
Jeyabalaratnam, J., Bharmauria, V., Bachatene, L., Cattan, S., Angers, A. et Molotchnikoff, S. (2013a). Adaptation shifts preferred orientation of tuning curve in the mouse visual cortex. *PloS one, 8*(5).
Jeyabalaratnam, J., Bharmauria, V., Bachatene, L., Cattan, S., Angers, A. et Molotchnikoff, S. (2013b). Adaptation shifts preferred orientation of tuning curve in the mouse visual cortex. *PloS one, 8*(5), e64294.

Jia, H., Rochefort, N. L., Chen, X. et Konnerth, A. (2010). Dendritic organization of sensory input to cortical neurons in vivo. *Nature, 464*(7293), 1307-1312.
Jin, D. Z., Dragoi, V., Sur, M. et Seung, H. S. (2005). Tilt aftereffect and adaptation-induced changes in orientation tuning in visual cortex. *Journal of neurophysiology, 94*(6), 4038-4050.
Kalatsky, V. A. et Stryker, M. P. (2003). New paradigm for optical imaging: temporally encoded maps of intrinsic signal. *Neuron, 38*(4), 529-545.
Kandel, E. R., Schwartz, J. H., Jessell, T. M., Siegelbaum, S., Hudspeth, A. J. et Mack, S. (2000). *Principles of neural science* (vol. 4). McGraw-hill New York.
Kang, J.-I. (2015). Cholinergic enhancement of perceptual learning: behavioral, physiological, and neuro-pharmacological study in the rat primary visual cortex.
Katzner, S., Busse, L. et Carandini, M. (2011). GABAA inhibition controls response gain in visual cortex. *Journal of Neuroscience, 31*(16), 5931-5941.
Keck, T., Scheuss, V., Jacobsen, R. I., Wierenga, C. J., Eysel, U. T., Bonhoeffer, T. et Hübener, M. (2011). Loss of sensory input causes rapid structural changes of inhibitory neurons in adult mouse visual cortex. *Neuron, 71*(5), 869-882.
Kisvarday, Z. (2000). Functional organisation of lateral connections in the primary visual cortex of the cat. Dans. Journal of Physiology-London.
Ko, H., Cossell, L., Baragli, C., Antolik, J., Clopath, C., Hofer, S. B. et Mrsic-Flogel, T. D. (2013). The emergence of functional microcircuits in visual cortex. *Nature, 496*(7443), 96-100.
Kocsis, B. (2012, 2012/06/01/). Differential Role of NR2A and NR2B Subunits in N-Methyl-D-Aspartate Receptor Antagonist-Induced Aberrant Cortical Gamma Oscillations. *Biological psychiatry, 71*(11), 987-995. https://doi.org/https://doi.org/10.1016/j.biopsych.2011.10.002
Kohn, A. et Movshon, J. A. (2004). Adaptation changes the direction tuning of macaque MT neurons. *Nature neuroscience, 7*(7), 764-772.
Kohn, A. et Whitsel, B. L. (2002). Sensory cortical dynamics. *Behavioural brain research, 135*(1-2), 119-126.
Kohn, A. J. J. o. n. (2007). Visual adaptation: physiology, mechanisms, and functional benefits. *97*(5), 3155-3164.
König, P., Engel, A. K., Roelfsema, P. R. et Singer, W. (1995). How precise is neuronal synchronization? *Neural Computation, 7*(3), 469-485.
Koulakov, A. A. et Chklovskii, D. B. (2001). Orientation preference patterns in mammalian visual cortex: a wire length minimization approach. *Neuron, 29*(2), 519-527.
Krekelberg, B., Van Wezel, R. J. et Albright, T. D. (2006). Adaptation in macaque MT reduces perceived speed and improves speed discrimination. *Journal of neurophysiology, 95*(1), 255-270.
Kuhlman, S. J., Olivas, N. D., Tring, E., Ikrar, T., Xu, X. et Trachtenberg, J. T. (2013). A disinhibitory microcircuit initiates critical-period plasticity in the visual cortex. *Nature, 501*(7468), 543-546.
Kurt, S., Moeller, C. K., Jeschke, M. et Schulze, H. (2008). Differential effects of iontophoretic application of the GABAA-antagonists bicuculline and gabazine on tone-evoked local field potentials in primary auditory cortex: interaction with ketamine anesthesia. *Brain Research, 1220*, 58-69.
Leavitt, M. L., Pieper, F., Sachs, A. J. et Martinez-Trujillo, J. C. (2017). Correlated variability modifies working memory fidelity in primate prefrontal neuronal ensembles. *Proceedings of the National Academy of Sciences, 114*(12), E2494-E2503.
Leong, D. A. (2002). *Ketamine disrupts synaptic transmission by interacting at AMPA/Kainate receptor channels in neocortical neurons* [University of British Columbia].
Lepack, A. E., Fuchikami, M., Dwyer, J. M., Banasr, M. et Duman, R. S. (2015). BDNF release is required for the behavioral actions of ketamine. *International Journal of Neuropsychopharmacology, 18*(1), pyu033.
Levick, W., Oyster, C. et Takahashi, E. (1969). Rabbit lateral geniculate nucleus: sharpener of directional information. *Science, 165*(3894), 712-714.

Li, N., Lee, B., Liu, R.-J., Banasr, M., Dwyer, J. M., Iwata, M., Li, X.-Y., Aghajanian, G. et Duman, R. S. (2010). mTOR-dependent synapse formation underlies the rapid antidepressant effects of NMDA antagonists. *Science, 329*(5994), 959-964.

Li, P., Zhu, S., Chen, M., Han, C., Xu, H., Hu, J., Fang, Y. et Lu, Haidong D. (2013, 2013/04/24/). A Motion Direction Preference Map in Monkey V4. *Neuron, 78*(2), 376-388. https://doi.org/https://doi.org/10.1016/j.neuron.2013.02.024

Li, X., Frye, M. A. et Shelton, R. C. (2012). Review of pharmacological treatment in mood disorders and future directions for drug development. *Neuropsychopharmacology, 37*(1), 77-101.

Li, Y., Lu, H., Cheng, P.-l., Ge, S., Xu, H., Shi, S.-H. et Dan, Y. (2012). Clonally related visual cortical neurons show similar stimulus feature selectivity. *Nature, 486*(7401), 118-121.

Liao, D. S., Krahe, T. E., Prusky, G. T., Medina, A. E. et Ramoa, A. S. (2004a). Recovery of cortical binocularity and orientation selectivity after the critical period for ocular dominance plasticity. *Journal of neurophysiology, 92*(4), 2113-2121.

Liao, D. S., Krahe, T. E., Prusky, G. T., Medina, A. E. et Ramoa, A. S. J. J. o. n. (2004b). Recovery of cortical binocularity and orientation selectivity after the critical period for ocular dominance plasticity. *92*(4), 2113-2121.

Lindquist, K. A. et Barrett, L. F. (2012). A functional architecture of the human brain: emerging insights from the science of emotion. *Trends in cognitive sciences, 16*(11), 533-540.

Ling, C., Schneider, G. E. et Jhaveri, S. (1998). Target-specific morphology of retinal axon arbors in the adult hamster. *Visual neuroscience, 15*(3), 559-579.

Lisek, M., Zylinska, L. et Boczek, T. (2020). Ketamine and calcium signaling—A crosstalk for neuronal physiology and pathology. *International Journal of Molecular Sciences21*(21), 8410.

Livingstone, M. S. et Hubel, D. H. (1983). Specificity of cortico-cortical connections in monkey visual system. *Nature, 304*(5926), 531-534.

Lovejoy, L. P. et Krauzlis, R. J. (2010). Inactivation of primate superior colliculus impairs covert selection of signals for perceptual judgments. *Nature neuroscience, 13*(2), 261-266.

Lussiez, R., Chanauria, N., Ouelhazi, A. et Molotchnikoff, S. (2021). Effects of visual adaptation on orientation selectivity in cat secondary visual cortex. *European Journal of Neuroscience, 53*(2), 588-600.

Malach, R., Amir, Y., Harel, M. et Grinvald, A. (1993). Relationship between intrinsic connections and functional architecture revealed by optical imaging and in vivo targeted biocytin injections in primate striate cortex. *Proceedings of the National Academy of Sciences, 90*(22), 10469-10473.

Malenka, R. C. et Bear, M. F. (2004, 2004/09/30/). LTP and LTD: An Embarrassment of Riches. *Neuron, 44*(1), 5-21. https://doi.org/https://doi.org/10.1016/j.neuron.2004.09.012

Mangini, N. J. et Pearlman, A. L. (1980). Laminar distribution of receptive field properties in the primary visual cortex of the mouse. *Journal of Comparative Neurology, 193*(1), 203-222.

Markan, C. M. et Bhaumik, B. (1999). Diffusive Hebbian model for orientation map formation. Dans. IJCNN'99. International Joint Conference on Neural Networks. Proceedings (Cat. No. 99CH36339).

Markram, H., Toledo-Rodriguez, M., Wang, Y., Gupta, A., Silberberg, G. et Wu, C. (2004). Interneurons of the neocortical inhibitory system. *Nature reviews neuroscience, 5*(10), 793-807.

Marshansky, S., Shumikhina, S. et Molotchnikoff, S. (2011). Repetitive adaptation induces plasticity of spatial frequency tuning in cat primary visual cortex. *Neuroscience, 172*, 355-365.

Masland, R. H. (2001). The fundamental plan of the retina. *Nature neuroscience, 4*(9), 877-886.

Maya Vetencourt, J. F., Sale, A., Viegi, A., Baroncelli, L., De Pasquale, R., O'Leary, O. F., Castren, E. et Maffei, L. (2008). The antidepressant fluoxetine restores plasticity in the adult visual cortex. *Science*.

Mayo, J. P. et Smith, M. A. (2017). Neuronal adaptation: tired neurons or wired networks? *Trends in neurosciences, 40*(3), 127-128.

McCoy, P. A., Huang, H.-S. et Philpot, B. D. (2009). Advances in understanding visual cortex plasticity. *Current opinion in neurobiology, 19*(3), 298-304.
McNally, J., McCarley, R. et Brown, R. (2013, 2013-September-17). Chronic Ketamine Reduces the Peak Frequency of Gamma Oscillations in Mouse Prefrontal Cortex Ex vivo [Original Research]. *Front. Psychiatry, 4*. https://doi.org/10.3389/fpsyt.2013.00106
McNally, J. M., McCarley, R. W. et Brown, R. E. (2013). Chronic ketamine reduces the peak frequency of gamma oscillations in mouse prefrontal cortex ex vivo. *Frontiers in psychiatry, 4*, 106.
Metin, C., Godement, P. et Imbert, M. (1988). The primary visual cortex in the mouse: receptive field properties and functional organization. *Experimental brain research, 69*, 594-612.
Michalski, A., Gerstein, G., Czarkowska, J. et Tarnecki, R. (1983). Interactions between cat striate cortex neurons. *Experimental brain research, 51*, 97-107.
Miller, K., Chapman, B. et Stryker, M. (1989). Visual responses in adult cat visual cortex depend on N-methyl-D-aspartate receptors. *Proceedings of the National Academy of Sciences, 86*(13), 5183-5187.
Moda-Sava, R., Murdock, M., Parekh, P., Fetcho, R., Huang, B., Huynh, T., Witztum, J., Shaver, D., Rosenthal, D. et Alway, E. (2019). Sustained rescue of prefrontal circuit dysfunction by antidepressant-induced spine formation. *Science, 364*(6436), eaat8078.
Monier, C., Chavane, F., Baudot, P., Graham, L. J. et Frégnac, Y. (2003, 2003/02/20/). Orientation and Direction Selectivity of Synaptic Inputs in Visual Cortical Neurons: A Diversity of Combinations Produces Spike Tuning. *Neuron, 37*(4), 663-680. https://doi.org/https://doi.org/10.1016/S0896-6273(03)00064-3
Moreno-Bote, R., Beck, J., Kanitscheider, I., Pitkow, X., Latham, P. et Pouget, A. (2014). Information-limiting correlations. *Nature neuroscience, 17*(10), 1410-1417.
Mountcastle, V. B. (1957). Modality and topographic properties of single neurons of cat's somatic sensory cortex. *Journal of neurophysiology, 20*(4), 408-434.
Mountcastle, V. B. (1997). The columnar organization of the neocortex. *Brain: a journal of neurology, 120*(4), 701-722.
Movshon, J. A., Thompson, I. D. et Tolhurst, D. J. (1978). Receptive field organization of complex cells in the cat's striate cortex. *The Journal of physiology, 283*(1), 79-99.
Muller, J. R., Metha, A. B., Krauskopf, J. et Lennie, P. (1999). Rapid adaptation in visual cortex to the structure of images. *Science, 285*(5432), 1405-1408.
Münch, T. A., Da Silveira, R. A., Siegert, S., Viney, T. J., Awatramani, G. B. et Roska, B. (2009). Approach sensitivity in the retina processed by a multifunctional neural circuit. *Nature neuroscience, 12*(10), 1308-1316.
Naarendorp, F., Esdaille, T. M., Banden, S. M., Andrews-Labenski, J., Gross, O. P. et Pugh, E. N. (2010). Dark light, rod saturation, and the absolute and incremental sensitivity of mouse cone vision. *Journal of Neuroscience, 30*(37), 12495-12507.
Nassi, J. J. et Callaway, E. M. (2009). Parallel processing strategies of the primate visual system. *Nature reviews neuroscience, 10*(5), 360-372.
Nemri, A., Ghisovan, N., Shumikhina, S. et Molotchnikoff, S. (2009). Adaptive behavior of neighboring neurons during adaptation-induced plasticity of orientation tuning in V1. *BMC neuroscience, 10*(1), 1-9.
Niell, C. M. et Stryker, M. P. (2008). Highly selective receptive fields in mouse visual cortex. *Journal of Neuroscience, 28*(30), 7520-7536.
Niell, C. M. et Stryker, M. P. (2010). Modulation of visual responses by behavioral state in mouse visual cortex. *Neuron, 65*(4), 472-479.

Normann, C., Schmitz, D., Fürmaier, A., Döing, C. et Bach, M. (2007, 2007/09/01/). Long-Term Plasticity of Visually Evoked Potentials in Humans is Altered in Major Depression. *Biological psychiatry, 62*(5), 373-380. https://doi.org/https://doi.org/10.1016/j.biopsych.2006.10.006

Nowak, L. G., Sanchez-Vives, M. V. et McCormick, D. A. (2008). Lack of orientation and direction selectivity in a subgroup of fast-spiking inhibitory interneurons: cellular and synaptic mechanisms and comparison with other electrophysiological cell types. *Cerebral cortex, 18*(5), 1058-1078.

Ohki, K., Chung, S., Ch'ng, Y. H., Kara, P. et Reid, R. C. (2005). Functional imaging with cellular resolution reveals precise micro-architecture in visual cortex. *Nature, 433*(7026), 597-603.

Orban, G. A. (2008). Higher order visual processing in macaque extrastriate cortex. *Physiological reviews*.

Ouelhazi, A., Bharmauria, V., Chanauria, N., Bachatene, L., Lussiez, R. et Molotchnikoff, S. (2019). Effects of ketamine on orientation selectivity and variability of neuronal responses in primary visual cortex. *Brain Research, 1725*, 146462.

Palmer, L. A. et Davis, T. L. (1981). Receptive-field structure in cat striate cortex. *Journal of neurophysiology, 46*(2), 260-276.

Park, M., Niciu, M. J. et Zarate, C. A. (2015). Novel glutamatergic treatments for severe mood disorders. *Current behavioral neuroscience reports, 2*, 198-208.

Perkel, D. H., Gerstein, G. L. et Moore, G. P. (1967). Neuronal spike trains and stochastic point processes: I. The single spike train. *Biophysical journal, 7*(4), 391-418.

Perry, V. H. et Cowey, A. (1985). The ganglion cell and cone distributions in the monkey's retina: implications for central magnification factors. *Vision research, 25*(12), 1795-1810.

Pfeffer, C. K., Xue, M., He, M., Huang, Z. J. et Scanziani, M. (2013). Inhibition of inhibition in visual cortex: the logic of connections between molecularly distinct interneurons. *Nature neuroscience, 16*(8), 1068-1076.

Poggio, G. et Fischer, B. (1977). Binocular interaction and depth sensitivity in striate and prestriate cortex of behaving rhesus monkey. *Journal of neurophysiology, 40*(6), 1392-1405.

Populin, L. C. (2005). Anesthetics change the excitation/inhibition balance that governs sensory processing in the cat superior colliculus. *Journal of Neuroscience, 25*(25), 5903-5914.

Priebe, N. J. et Ferster, D. (2008). Inhibition, spike threshold, and stimulus selectivity in primary visual cortex. *Neuron, 57*(4), 482-497.

Prusky, G. et Douglas, R. (2004). Characterization of mouse cortical spatial vision. *Vision research, 44*(28), 3411-3418.

Purves , D., Augustine , G., Fitzpatrick , D., Hall , W., LaMantia , A., McNamara , J. et Williams , S. (2004). *Neuroscience*. Sinauer Associates, Inc. Publishers, Sunderland, Massachusetts U.S.A.

Purves, D., Augustine, G. J., Fitzpatrick, D., Hall, W., LaMantia, A.-S. et White, L. (2019). *Neurosciences*. De Boeck Supérieur.

Qian, N., Andersen, R. A. et Adelson, E. H. (1994). Transparent motion perception as detection of unbalanced motion signals. I. Psychophysics. *Journal of Neuroscience, 14*(12), 7357-7366.

Quirk, K., Gillard, N. P., Ragan, C. I., Whiting, P. J. et McKernan, R. M. (1994). Model of subunit composition of gamma-aminobutyric acid A receptor subtypes expressed in rat cerebellum with respect to their alpha and gamma/delta subunits. *Journal of Biological Chemistry, 269*(23), 16020-16028.

Ramoa, A. S., Mower, A. F., Liao, D. et Jafri, S. I. (2001a). Suppression of cortical NMDA receptor function prevents development of orientation selectivity in the primary visual cortex. *Journal of Neuroscience, 21*(12), 4299-4309.

Ramoa, A. S., Mower, A. F., Liao, D. et Jafri, S. I. J. J. o. N. (2001b). Suppression of cortical NMDA receptor function prevents development of orientation selectivity in the primary visual cortex. *21*(12), 4299-4309.

Regan, D. et Beverley, K. (1985). Postadaptation orientation discrimination. *JOSA A, 2*(2), 147-155.

Reynolds, J., Baskys, A. et Carlen, P. (1988). The effects of serotonin on N-methyl-D-aspartate and synaptically evoked depolarizations in rat neocortical neurons. *Brain Research, 456*(2), 286-292.

Ringach, D. L., Shapley, R. M. et Hawken, M. J. (2002). Orientation selectivity in macaque V1: diversity and laminar dependence. *Journal of Neuroscience, 22*(13), 5639-5651.

Rivadulla, C., Sharma, J. et Sur, M. (2001). Specific roles of NMDA and AMPA receptors in direction-selective and spatial phase-selective responses in visual cortex. *Journal of Neuroscience, 21*(5), 1710-1719.

Roe, Anna W., Chelazzi, L., Connor, Charles E., Conway, Bevil R., Fujita, I., Gallant, Jack L., Lu, H. et Vanduffel, W. (2012, 2012/04/12/). Toward a Unified Theory of Visual Area V4. *Neuron, 74*(1), 12-29. https://doi.org/https://doi.org/10.1016/j.neuron.2012.03.011

Rolls, E. T. et Treves, A. (2011, 2011/11/01/). The neuronal encoding of information in the brain. *Progress in Neurobiology, 95*(3), 448-490. https://doi.org/https://doi.org/10.1016/j.pneurobio.2011.08.002

Sadeh, S. et Rotter, S. (2015). Orientation selectivity in inhibition-dominated networks of spiking neurons: effect of single neuron properties and network dynamics. *PLoS computational biology, 11*(1), e1004045.

Safaai, H., von Heimendahl, M., Sorando, J. M., Diamond, M. E. et Maravall, M. (2013). Coordinated population activity underlying texture discrimination in rat barrel cortex. *Journal of Neuroscience, 33*(13), 5843-5855.

Salay, L. D., Ishiko, N. et Huberman, A. D. J. N. (2018). A midline thalamic circuit determines reactions to visual threat. *Nature, 557*(7704), 183-189.

Samonds, J. M., Allison, J. D., Brown, H. A. et Bonds, A. (2003). Cooperation between area 17 neuron pairs enhances fine discrimination of orientation. *Journal of Neuroscience, 23*(6), 2416-2425.

Samonds, J. M. et Bonds, A. (2004). From another angle: differences in cortical coding between fine and coarse discrimination of orientation. *Journal of neurophysiology, 91*(3), 1193-1202.

Sato, M. et Stryker, M. (2008). Distinctive features of adult ocular dominance plasticity. *Journal of Neuroscience, 28*(41), 10278-10286.

Sawtell, N. B., Frenkel, M. Y., Philpot, B. D., Nakazawa, K., Tonegawa, S. et Bear, M. F. (2003). NMDA receptor-dependent ocular dominance plasticity in adult visual cortex. *Neuron, 38*(6), 977-985.

Schiller, P. H., Finlay, B. L. et Volman, S. F. (1976). Quantitative studies of single-cell properties in monkey striate cortex. II. Orientation specificity and ocular dominance. *Journal of neurophysiology, 39*(6), 1320-1333.

Schneggenburger, R., Sakaba, T. et Neher, E. (2002). Vesicle pools and short-term synaptic depression: lessons from a large synapse. *Trends in neurosciences, 25*(4), 206-212.

Schummers, J., Marino, J. et Sur, M. (2004). Local networks in visual cortex and their influence on neuronal responses and dynamics. *Journal of Physiology-Paris, 98*(4-6), 429-441.

Shadlen, M. N. et Newsome, W. T. (1998). The variable discharge of cortical neurons: implications for connectivity, computation, and information coding. *Journal of neuroscience, 18*(10), 3870-3896.

Shapley, R., Hawken, M. et Ringach, D. L. (2003, 2003/06/05/). Dynamics of Orientation Selectivity in the Primary Visual Cortex and the Importance of Cortical Inhibition. *Neuron, 38*(5), 689-699. https://doi.org/https://doi.org/10.1016/S0896-6273(03)00332-5

Sharma, J., Angelucci, A. et Sur, M. (2000). Induction of visual orientation modules in auditory cortex. *Nature, 404*(6780), 841-847.

Shatz, C. J. (1990). Impulse activity and the patterning of connections during CNS development. *Neuron, 5*(6), 745-756.

Shen, K., Bezgin, G., Hutchison, R. M., Gati, J. S., Menon, R. S., Everling, S. et McIntosh, A. R. (2012). Information processing architecture of functionally defined clusters in the macaque cortex. *Journal of Neuroscience, 32*(48), 17465-17476.

Shu, Y., Hasenstaub, A. et McCormick, D. A. (2003). Turning on and off recurrent balanced cortical activity. *Nature, 423*(6937), 288-293.

Siegel, M. et König, P. (2003). A functional gamma-band defined by stimulus-dependent synchronization in area 18 of awake behaving cats. *Journal of Neuroscience, 23*(10), 4251-4260.

Skottun, B. C., De Valois, R. L., Grosof, D. H., Movshon, J. A., Albrecht, D. G. et Bonds, A. (1991). Classifying simple and complex cells on the basis of response modulation. *Vision research, 31*(7-8), 1078-1086.

Sleigh, J., Harvey, M., Voss, L. et Denny, B. (2014). Ketamine–More mechanisms of action than just NMDA blockade. *Trends in anaesthesia and critical care, 4*(2-3), 76-81.

Snowden, R. J., Treue, S., Erickson, R. G. et Andersen, R. A. (1991). The response of area MT and V1 neurons to transparent motion. *Journal of Neuroscience, 11*(9), 2768-2785.

Sobczyk, A., Scheuss, V. et Svoboda, K. (2005). NMDA receptor subunit-dependent [Ca2+] signaling in individual hippocampal dendritic spines. *Journal of Neuroscience, 25*(26), 6037-6046.

Somers, D. C., Nelson, S. B. et Sur, M. (1995). An emergent model of orientation selectivity in cat visual cortical simple cells. *Journal of Neuroscience, 15*(8), 5448-5465.

Sompolinsky, H. et Shapley, R. (1997). New perspectives on the mechanisms for orientation selectivity. *Current opinion in neurobiology, 7*(4), 514-522.

Song, S., Sjöström, P. J., Reigl, M., Nelson, S. et Chklovskii, D. B. (2005). Highly nonrandom features of synaptic connectivity in local cortical circuits. *PLoS biology, 3*(3), e68.

Srihasam, K., Vincent, J. L. et Livingstone, M. S. (2014). Novel domain formation reveals proto-architecture in inferotemporal cortex. *Nature neuroscience, 17*(12), 1776-1783.

Steinzeig, A., Cannarozzo, C. et Castrén, E. (2019). Fluoxetine-induced plasticity in the visual cortex outlasts the duration of the naturally occurring critical period. *European Journal of Neuroscience, 50*(10), 3663-3673.

Stepanyants, A., Hirsch, J. A., Martinez, L. M., Kisvárday, Z. F., Ferecskó, A. S. et Chklovskii, D. B. (2008). Local potential connectivity in cat primary visual cortex. *Cerebral cortex, 18*(1), 13-28.

Stevens, C. F. et Zador, A. M. (1998). Input synchrony and the irregular firing of cortical neurons. *Nature neuroscience, 1*(3), 210-217.

Stiles, W. (1949). Increment thresholds & the mechanisms of colour vision. *Documenta ophthalmologica, 3*(1), 138-165.

Swindale, N. V. (1998). Orientation tuning curves: empirical description and estimation of parameters. *Biological cybernetics, 78*, 45-56.

Takei, N., Inamura, N., Kawamura, M., Namba, H., Hara, K., Yonezawa, K. et Nawa, H. (2004). Brain-derived neurotrophic factor induces mammalian target of rapamycin-dependent local activation of translation machinery and protein synthesis in neuronal dendrites. *Journal of Neuroscience, 24*(44), 9760-9769.

Tan, A. Y., Brown, B. D., Scholl, B., Mohanty, D. et Priebe, N. J. (2011). Orientation selectivity of synaptic input to neurons in mouse and cat primary visual cortex. *Journal of Neuroscience, 31*(34), 12339-12350.

Tanigawa, H., Lu, H. D. et Roe, A. W. (2010). Functional organization for color and orientation in macaque V4. *Nature neuroscience, 13*(12), 1542-1548.

Teich, A. F. et Qian, N. (2003). Learning and adaptation in a recurrent model of V1 orientation selectivity. *Journal of neurophysiology, 89*(4), 2086-2100.

Thompson, K. G., Leventhal, A. G., Zhou, Y. et Liu, D. (1994). Stimulus dependence of orientation and direction sensitivity of cat LGNd relay cells without cortical inputs: a comparison with area 17 cells. *Visual neuroscience, 11*(5), 939-951.

Thomson, A. M. et Deuchars, J. (1997). Synaptic interactions in neocortical local circuits: dual intracellular recordings in vitro. *Cerebral cortex (New York, NY: 1991), 7*(6), 510-522.

Tiesinga, P., Fellous, J.-M. et Sejnowski, T. J. (2008). Regulation of spike timing in visual cortical circuits. *Nature reviews neuroscience, 9*(2), 97-107.
Tolhurst, D. et Dean, A. (1990). The effects of contrast on the linearity of spatial summation of simple cells in the cat's striate cortex. *Experimental brain research, 79*, 582-588.
Tongiorgi, E., Ferrero, F., Cattaneo, A. et Domenici, L. (2003). Dark-rearing decreases NR2A N-methyl-D-aspartate receptor subunit in all visual cortical layers. *Neuroscience, 119*(4), 1013-1022.
Tropea, D., Van Wart, A. et Sur, M. (2009). Molecular mechanisms of experience-dependent plasticity in visual cortex. *Philosophical Transactions of the Royal Society B: Biological Sciences, 364*(1515), 341-355.
Troy, J. B. et Enroth-Cugell, C. (1993). X and Y ganglion cells inform the cat's brain about contrast in the retinal image. *Experimental brain research, 93*(3), 383-390.
Troyer, T. W., Krukowski, A. E., Priebe, N. J. et Miller, K. D. (1998). Contrast-invariant orientation tuning in cat visual cortex: thalamocortical input tuning and correlation-based intracortical connectivity. *Journal of Neuroscience, 18*(15), 5908-5927.
Ts'o, D. Y., Gilbert, C. D. et Wiesel, T. N. (1986). Relationships between horizontal interactions and functional architecture in cat striate cortex as revealed by cross-correlation analysis. *Journal of Neuroscience, 6*(4), 1160-1170.
Turrigiano, G. G. (1999). Homeostatic plasticity in neuronal networks: the more things change, the more they stay the same. *Trends in neurosciences, 22*(5), 221-227.
Turrigiano, G. G. et Nelson, S. B. (2000). Hebb and homeostasis in neuronal plasticity. *Current opinion in neurobiology, 10*(3), 358-364.
Ungerleider, L. G. et Haxby, J. V. (1994). 'What'and 'where'in the human brain. *Current opinion in neurobiology, 4*(2), 157-165.
Van Hooser, S. D. (2007). Similarity and diversity in visual cortex: is there a unifying theory of cortical computation? *The Neuroscientist, 13*(6), 639-656.
Van Hooser, S. D., Heimel, J. A. F., Chung, S., Nelson, S. B. et Toth, L. J. (2005). Orientation selectivity without orientation maps in visual cortex of a highly visual mammal. *Journal of Neuroscience, 25*(1), 19-28.
van Loon, A. M., Fahrenfort, J. J., van der Velde, B., Lirk, P. B., Vulink, N. C., Hollmann, M. W., Steven Scholte, H. et Lamme, V. A. (2016). NMDA receptor antagonist ketamine distorts object recognition by reducing feedback to early visual cortex. *Cerebral cortex, 26*(5), 1986-1996.
van Loon, A. M., Scholte, H. S., Fahrenfort, J. J., van der Velde, B., Lirk, P. B., Vulink, N. C., Hollmann, M. W. et Lamme, V. A. (2013). Ketamine changes the neural representation of object recognition in early visual cortex. *Journal of Vision, 13*(9), 129-129.
van Versendaal, D., Rajendran, R., Saiepour, M. H., Klooster, J., Smit-Rigter, L., Sommeijer, J.-P., De Zeeuw, C. I., Hofer, S. B., Heimel, J. A. et Levelt, C. N. (2012). Elimination of inhibitory synapses is a major component of adult ocular dominance plasticity. *Neuron, 74*(2), 374-383.
Vélez-Fort, M., Rousseau, Charly V., Niedworok, Christian J., Wickersham, Ian R., Rancz, Ede A., Brown, Alexander P. Y., Strom, M. et Margrie, Troy W. (2014, 2014/09/17/). The Stimulus Selectivity and Connectivity of Layer Six Principal Cells Reveals Cortical Microcircuits Underlying Visual Processing. *Neuron, 83*(6), 1431-1443. https://doi.org/https://doi.org/10.1016/j.neuron.2014.08.001
Vidyasagar, T., Pei, X. et Volgushev, M. (1996). Multiple mechanisms underlying the orientation selectivity of visual cortical neurones. *Trends in neurosciences, 19*(7), 272-277.
Völgyi, B., Chheda, S. et Bloomfield, S. A. (2009). Tracer coupling patterns of the ganglion cell subtypes in the mouse retina. *Journal of Comparative Neurology, 512*(5), 664-687.
Wagor, E., Mangini, N. J. et Pearlman, A. L. (1980). Retinotopic organization of striate and extrastriate visual cortex in the mouse. *Journal of Comparative Neurology, 193*(1), 187-202.

Wandell, B. A. et Smirnakis, S. M. (2009). Plasticity and stability of visual field maps in adult primary visual cortex. *Nature reviews neuroscience, 10*(12), 873-884.
Wang, J., Ni, Z., Jin, A., Yu, T. et Yu, H. (2019). Ocular dominance plasticity of areas 17 and 21a in the cat. *Frontiers in Neuroscience, 13*, 1039.
Wang, L., Sarnaik, R., Rangarajan, K., Liu, X. et Cang, J. (2010). Visual receptive field properties of neurons in the superficial superior colliculus of the mouse. *Journal of Neuroscience, 30*(49), 16573-16584.
Wang, Q. et Burkhalter, A. (2007). Area map of mouse visual cortex. *Journal of Comparative Neurology, 502*(3), 339-357.
Wang, Q., Gao, E. et Burkhalter, A. (2011). Gateways of ventral and dorsal streams in mouse visual cortex. *Journal of Neuroscience, 31*(5), 1905-1918.
Wehr, M. et Zador, A. M. (2003). Balanced inhibition underlies tuning and sharpens spike timing in auditory cortex. *Nature, 426*(6965), 442-446.
Wilson, D. E., Whitney, D. E., Scholl, B. et Fitzpatrick, D. (2016). Orientation selectivity and the functional clustering of synaptic inputs in primary visual cortex. *Nature neuroscience, 19*(8), 1003-1009.
Wise, A. K., Cerminara, N. L., Marple-Horvat, D. E. et Apps, R. (2010). Mechanisms of synchronous activity in cerebellar Purkinje cells. *The Journal of physiology, 588*(13), 2373-2390.
Xue, M., Atallah, B. V. et Scanziani, M. (2014). Equalizing excitation–inhibition ratios across visual cortical neurons. *Nature, 511*(7511), 596-600.
Yang, Y., Cui, Y., Sang, K., Dong, Y., Ni, Z., Ma, S. et Hu, H. (2018). Ketamine blocks bursting in the lateral habenula to rapidly relieve depression. *Nature, 554*(7692), 317-322.
Yu, H., Chen, X., Sun, C. et Shou, T. (2008). Global evaluation of contributions of GABAA, AMPA and NMDA receptors to orientation maps in cat's visual cortex. *Neuroimage, 40*(2), 776-787.
Yu, J. et Ferster, D. (2010). Membrane potential synchrony in primary visual cortex during sensory stimulation. *Neuron, 68*(6), 1187-1201.
Zanos, P. et Gould, T. (2018). Mechanisms of ketamine action as an antidepressant. *Molecular psychiatry, 23*(4), 801-811.
Zanos, P., Moaddel, R., Morris, P. J., Georgiou, P., Fischell, J., Elmer, G. I., Alkondon, M., Yuan, P., Pribut, H. J. et Singh, N. S. (2016). NMDAR inhibition-independent antidepressant actions of ketamine metabolites. *Nature, 533*(7604), 481-486.
Zhou, W., Wang, N., Yang, C., Li, X.-M., Zhou, Z.-Q. et Yang, J.-J. (2014). Ketamine-induced antidepressant effects are associated with AMPA receptors-mediated upregulation of mTOR and BDNF in rat hippocampus and prefrontal cortex. *European Psychiatry, 29*(7), 419-423.
Zhou, Z., Zhang, G., Li, X., Liu, X., Wang, N., Qiu, L., Liu, W., Zuo, Z. et Yang, J. (2015). Loss of phenotype of parvalbumin interneurons in rat prefrontal cortex is involved in antidepressant-and propsychotic-like behaviors following acute and repeated ketamine administration. *Molecular neurobiology, 51*(2), 808-819.
Zucker, R. S. et Regehr, W. G. (2002). Short-term synaptic plasticity. *Annual review of physiology, 64*(1), 355-405.